“The role of the WASP family proteins in cellular migration and invasion in prostate cancer”

MD Thesis
by

Candidate: Muhammad Moazzam
Supervisors: Professor Wen G Jiang and Professor Howard Kynaston

Declaration

This work has not previously been accepted in substance for any degree and is not concurrently submitted in candidature for any degree.

Signed …… (candidate) Date……

Statement 1

This thesis is being submitted in partial fulfilment of the requirements for the degree of MD.

Signed …… (candidate) Date……

Statement 2

This thesis is the result of my own independent work/investigation. Other sources are acknowledged by explicit references.

Signed …… (candidate) Date……

Statement 3

I hereby give consent for my thesis, if accepted, to be available for photocopying and for inter-library loan, and for the title and summary to be made available to outside organisations.

Signed …… (candidate) Date……

Statement 4 - bar on access approved

I hereby give consent for my thesis, if accepted, to be available for photocopying and for inter-library loans after expiry of a bar on access approved by the Graduate Development**.**

Committee.

Signed …… (candidate) Date……

Acknowledgements

I would like to express my deep gratitude to Professor Kynaston and Professor Jiang, my research supervisors, for their excellent support, guidance and mentoring throughout my project. They gave me open and generous access to their guidance and compassionate help. I was granted with all the time and help needed to complete this thesis. It has been an honour to study under two world-renowned experts in their appropriate fields. They gave me the opportunity to complete this MD in a interesting and fascinating topic, namely the role of WASP proteins in prostate cancer which will add to understanding the mechanism of cellular movement and prostate cancer metastasis.

I would also like to express my great appreciation for Dr Lin Ye, who has been a keen laboratory mentor for me and helped me in every fashion to complete the laboratory work, preparation of presentations and completion of this thesis. I am also very thankful to Andy Sanders who has also provided exceptional support in the laboratory.

And finally, the biggest thanks go to my wife Dr Farah Afgan Chouhdry, whose love, support and encouragement throughout this project, has given me the opportunity to complete this thesis.

Summary:

Prostate cancer metastasis is a complex process, involving multiple pathways in its orchestration. Malignant cells are influenced by different growth factors from the extracellular environment which promote or inhibit cell movement and metastasis. HGF has been implicated in progression and metastasis of prostate cancer. A cell interacts with the environment through surface molecules like integrins. These interactions are further translated in to different responses through various intracellular machineries. Furthermore organization of the actin cytoskeleton is vital for many cellular functions. WAVEs are member of WASP family of proteins, which have important role in regulation of actin dynamics through regulation of actin related protein (ARP 2/3). The role of individual members of WASP family has been investigated in development and progression of different cancers. We documented the expression of different WAVE family members in various prostate cancer cell lines. Expression of WAVE-3 was effectively knocked down with the use of hammer head ribozymes. Loss of WAVE-3 expression resulted in reduced cell movement and invasion in the PC-3 cell line. These cells failed to show any significant increase in cellular movement and invasive potential following treatment with HGF. Further experiments to investigate the underlying mechanism of this phenotypic change revealed that optimum levels of phosphorylated paxillin play an important role in this change. Our study also indicates that reduced potential of invasive capability following WAVE-3 knock down, may be related to reduced availability of MMP-2 in the cellular environment.

National and international presentations:

June 2011 WAVE-3 knock-down results in reduced invasion and motility in prostate cancer cells via reduced MMP-2 expression.

Moazzam M, Ye L, Kynaston H, Mansel RE, Jiang WG.

BAUS Annual Meeting, Liverpool, UK.

March 2010 WAVE-3 knock-down results in reduced invasion and motility in prostate cancer cells via reduced phosphorylation of paxillin.

Muhammad Moazzam, Lin Yee, Howard Kynaston, W. G. Jiang

Annual European Association of Cancer Research (EACR) Conference, Oslo, Norway (June 2010)

Jan 2010 WAVE-3 is imperative for hepatocyte growth factor (HGF) induced migration and invasion of prostate cancer cells in vitro.

Moazzam Muhammad, Lin Ye, Howard Kynaston, Robert E. Mansel and Wen G. Jiang

BAUS section of Academic Urology, Royale Free Hospital, London.

Dec 2009 Aberrant Expression of ARP2/3 in Breast Cancer and the Association with Disease Progression.

Moazzam Muhammad, Lin Ye, Howard Kynaston, Robert E. Mansel and Wen G. Jiang

San Antonio Breast Cancer Symposium, Henry B. Gonzalez Convention Center, Texas, USA.

Oct 2009 Role of WAVE-3 in prostate cancer

Muhammad Moazzam, Lin Ye, Howard Kynaston, W. G. Jiang

Welsh Urology Biannual Meeting, Village Hotel, Swansea.

Published abstracts:

1. Moazzam M, Ye L, Kynaston H, Mansel RE, Jiang WG. WAVE-3 knock-down results in reduced invasion and motility in prostate cancer cells via reduced MMP-2 expression. BJU 108: Supplement 1: 31 (18-60).

2. Moazzam M, Ye L, Kynaston H, Mansel RE, Jiang WG: WAVE-3 is imperative for hepatocyte growth factor (HGF) induced migration and invasion of prostate cancer cells in vitro. BJS: e-publication

3. Moazzam M, Ye L, Kynaston H, Mansel RE, Jiang WG: Aberrant expression of ARP2/3 in breast cancer and the association with disease progression. Cancer Research 2009 Dec;69(24):878.

Table of Contents

List of Figures

Chapter: 2

Chapter: 3

Chapter: 4

Chapter: 5

Chapter: 6

Chapter: 7

List of Tables

List of Graphs

Chapter: 4

Chapter: 5

Chapter: 6

Abbreviation

3D-CRT	Three-dimensional conformal radiotherapy
cPSA	Complexed PSA
proPSA	precursor or zymogen form of PSA
BPSA	a cleaved form of PSA found in the transition zone of the prostate
iPSA	intact PSA
aa	amino acid
Ab	antibody
ADP	Adenosine di-phosphate
ADT	androgen-deprivation therapy
Ag	antigen
AJCC	American Joint Committee for Cancer
ALK	alkaline phosphatase
ALL	Acute lymphocytic leukaemia
ARP	actin related protein
Ash	absent, small, or homeotic discs
ATCC	American Type Culture Collection
ATP	Adenosine tri-phosphate
bp	base pair
BPH	benign prostatic hyperplasia
BPSA	bound prostate specific antigen
BRCA2	breast cancer type 2 susceptibility protein
BSA	bovine serum albumin
BSS	Balanced salt solution

Cdc42	Cell division control protein 42
Cdk5	cyclin-dependent kinase 5
CHEK2	Check point homolog
cm	centimeter
CO^2	carbon dioxide
CrkII	v-crk sarcoma virus CT10 oncogene homolog
CT	computerized tomography
CYP3A4	cytochrome P450, family 3, subfamily A, polypeptide 4
DES	diethyl stilbisterol
DHT	dihydrotestosterone
DMEM	Dulbecco's modified Eagle’s medium
DMSO	dimethyl sulphoxide
DNA	deoxyribonucleic acid
DRE	digital rectal examination
DRF	Diaphanous related formins
E. coli	Esherichia coli
ECACC	European Collection of Animal Cell Culture
ECL	enhanced chemiluminescence
ECM	extracellular matrix
EDTA	ethylene diaminetetraacetic acid
ELAC2	alternate name to HPC2 (human prostate cancer-2 gene)
ELMO	engulfment and cell motility
EMMPRIN	extracellular matrix metalloproteinase inducer
EMT	Epithelial to mesenchymal transition
Ena/VASP	Ena-vasodilator stimulated phosphoprotein

ERK	Extracellular signal-regulated kinases
ETS	E-twenty six (family of transcription factors)
EVH1	enabled/VASP homology 1 domain
FAK	Focal adhesion kinase
FCS	foetal calf serum
FGF	fibroblast growth factor
GAPs	GTPases activating proteins
GDP	guanosine di-phosphate
GEFs	guanine-nucleotide exchange factors
GIT	G-protien-coupled receptor kinase interacting protein
Grb2	growth factor receptor-bound protein 2
GTP	guanosine tri-phosphatase
H_2O_2	hydrogen peroxide
HEPES	N-hydroxyethylpiperazine-N'-2-ethansulphoxide
HGF/SF	hepatocyte growth factor/scatter factor
HPC	hereditary prostate cancer
HUIV26	cryptic site in collagen type IV
ICAM	Intercellular Adhesion Molecule
IF	immunofluorescence
IFN	interferon
IG	immunoglobulin
IGF	insulin-like growth factor
IMRT	Intensity modulated radiotherapy
ITP	idiopathic thrombocytopenia
JNK	Jun N-terminal kinases

kb	kilo-base
kDa	kilo-dalton
LB	Luria-Bertani
LD	homeobox protein
LHRH	Leutenising hormone releasing hormone
LIM	lipophilic protein
m	meter
M	molar
mA	milli-amp
mAb	monoclonal antibody
MAPK	mitogen activated protein kinase
mg	milligram
min	minute
ml	milli litre
MLCK	myosin light chain kinase
MMP	metalloproteases
MRI	magnetic resonance imaging
MSR1	macrophage scavenger receptor 1
MW	molecular weight
NaCl	sodium chloride
NaN_3	sodium azide
NaOH	sodium hydroxide
NCK	non-catalytic region of tyrosine kinase adaptor protein
ng	nano-gram
nM	nano molar

nm	nanometre
NMDA	N-methyl-D-aspartate
NO	nitric oxide
NSAID	nonsteroidal anti-inflammatory drug
N-WASP	Neural Wiskott-Aldrich Syndrome Protein
PAGE	polyacrylamide gel electrophoresis
PAK	p21-activated serine/threonine kinase
PBS	phosphate buffered saline
PCR	polymerase chain reaction
PDGF	platelet-derived growth factor
PF	platelet factor
PI3K	phosphoinositide 3-kinase
PIP	phosphatidylinositol phosphates
PIX	PAK-interacting exchange factor
PSA	prostate specific antigen
PSMA	phosphoinositide 3-kinase
Rac	Ras-related C3 botulinum toxin substrate
RASA	RAS p21 protein activator (GTPase activating protein) 1
Rb	retinoblastoma
Rho	ρ (17th letter of the Greek alphabet)
RNA	ribonucleic acid
RNAse	ribonuclease
ROCK	Rho-associated protein kinase
rpm	revolutions per minute
RT	reverse transcription

SCID	Severe Combined Immunodeficiency
SD	standard deviation
SDF-1	stromal-cell derived factor-1
SDS	sodium dodecyl sulphate
sec	second
siRNA	small interfering RNA
SPARC	secreted protein, acidic and rich in cysteine
Src	sarcoma
TBE	Tris/Borate/EDTA electrophoresis buffer
TBS	Tris-buffered saline
TE	Tris/EDTA buffer
TEMED	N,N,N',N'-tetramethylethylenediamine
TGF	Transforming growth factor
TGF-β	Transforming growth factor-β
TIMP	tissue inhibitors of metaloprotienases
TNF-α	tumour necrosis factor-alpha
TNM	tumour, node and metastasis
tPA	tissue plasminogen activator
Tris	Tris-(hydoxymethyl)-aminomethane
TRITC	Tetra-Rhodamine Isothiocyanate
TRUS	transrectal ultrasonography
UICC	International Union against Cancer
uPA	urokinase plasminogen activator
UV	ultraviolet
V	volt

VCA	verprolin homology motif (V), cofilin homology motif (C), acidic motif (A)
VEGF	Vascular endothelial growth factor
WASP	Wiskott-Aldrich Syndrome Protein
WAVE	WASP verpolin homologous
WIP	WASP-interacting protein
WT	wild type
µg	microgram
µl	microlitre
µm	micro meter
µM	micro molar

Chapter 1
Prostate cancer

1.1: Incidence and mortality:

Prostate cancer is the fourth most common male malignant neoplasm worldwide. The incidence is highly variable among different countries and ethnic populations. The highest incidence is noted in North America, especially in African Americans and the lowest in Asia. Prostate cancer is responsible for 15% of all cancers in developed countries compared with under developed countries where it accounts for only 4% of all diagnosed cancers (Parkin et al. 2001). The mortality of prostate cancer also varies widely among countries, being highest in Sweden and lowest in Asia. In Europe, prostate cancer is the most common solid neoplasm in males, with an incidence rate of 214 cases per 1000 men (Boyle et al. 2005).

1.2: Epidemiology:

1.2.1: Racial differences:

Environmental factors seem to play important role in prostate cancer risk around the world. Japanese and Chinese men in the United States have a higher risk of dying from the disease compared to their relatives living in Japan and China. However, Asian-Americans have the lowest prostate cancer incidence indicating the role of genetics as well (Muir et al. 1991; Landis et al. 1999).

1.2.2: Age at diagnosis:

Prostate cancer is rare in men below 50 years of age and accounts for less than 0.1% of all diagnosed prostate cancers. The cumulative risk of clinically diagnosed prostate

cancer at 85 years of age ranges from 0.5% to 20% worldwide. However, there is evidence from autopsy series that 30% of men in their fourth decade, 50% in their sixth decade and more than 75% of men older than 85 years can have microscopic evidence of prostate cancer (Sakr et al. 1993). This effect is clearly shown by PSA-based screening and its role in age migration effect (Bartsch et al. 2001).

1.2.3: Stage at diagnosis:

The introduction of PSA testing has increased the incidence of localised disease along with the decrease in metastatic disease, at presentation. There is also a downward migration of the pathological stage with an increasing incidence of organ confined disease in radical prostatectomy specimens (Jhaveri et al. 1999). This improvement has been noted in clinical stages T1 to T3. Due to earlier diagnosis, 5 and 10 year survival rates have also improved. This may be due to lead time bias but there is ongoing debate over this effect which may be answered from ongoing trials in United States and Europe (Pinsky et al. 2012; Schroder et al. 2012).

1.3: Risk factors

1.3.1: Familial and genetic influences:

Prostate cancer can be divided into three phenotypes: sporadic, familial and hereditary. Familial prostate cancer is defined as, occuring in men with one or more affected relatives. While hereditary prostate cancer is a subset of familial cancer with three or

more affected members, with prostate cancer in three successive generations or two affected individuals before the age of 55 years. Fortunately hereditary prostate cancers are responsible for only 15% of all prostate cancers. Cancers usually arise from individual cells that have acquired one or more mutations resulting in malignant transformation followed by clonal expansion. Most of these mutations affect genes involved in signaling for cell proliferation, cell cycle control, cell death, and DNA repair.

There have been at least eight well established prostate cancer susceptibility genes reported in the literature, including RNase, Hereditary prostate cancer-1 (HPC1) (Goode et al. 2001), Hereditary prostate cancer-2 (HPC2) (Smith et al. 2004), the macrophage scavenger receptor 1 gene (SR-A/MSR1) (Platt et al.2001), Check point homolog-2 (CHEK2) (Dong et al. 2003), Breast cancer type-2 (BRCA2) (Edwards et al. 2003), Serum paraoxonase/arylesterase 1 (PON1) (Marchesani et al. 2003) and 8-Oxoguanine glycosylase (OGG1) (Boiteux et al. 2000). Despite of the fact that there is a long list of susceptibility genes, prostate cancer appears to be polygenic in origin. However, out of the most common cancers, prostate cancer is the only malignancy for which a highly penetrant allele has not yet been identified. Importantly, we might be able to exploit these findings to develop more sensitive tools for early diagnosis of prostate cancer and for better treatment of this dreadful disease.

1.3.2: Role of prostatic inflamation:

Chronic inflammation associated with cellular proliferation is a well known factor in the

development of infection associated cancers appearing in the oesophagus, stomach, bladder and liver (Coussens and Werb, 2002; Platz and De Marzo, 2004). Two previous meta-analyses comprising 34 case-control studies have reported a statistically significant association of prostate cancer with a previous history of sexually transmitted infection or prostatitis (Dennis et al. 2002). Proliferative inflammation in atrophy is a well-documented lesion and is characterized by epithelial atrophy, low apoptotic index and increased proliferative index (Putzi and De Marzo, 2000). Inflammation produces oxidative stress which can lead to DNA damage and mutations. If the cellular defence is compromised it can contribute to the development of prostate cancer. There is enough evidence to support the above-mentioned theory (Coussens and Werb, 2002):

(1): Defects in genes like HPC1 / RNase L are known to predispose knockout mice to infections

(2): Chronic inflammation is known to produce oxidative stress

(3): Inflammatory lesions associated with proliferative inflammatory atrophy are found in abundance in histopathological specimens from prostate

(4): Defects in antioxidant enzymes permit oxidative damage to DNA

(5): Defects in genes like SR-A/MSR1 can allow uncontrolled inflammatory response.

(6): Defects in RNase L allow mutated cells to escape apoptosis which can result in colonal expansion of malignant cells.

1.4: Molecular epidemiology

1.4.1: Androgens:

Androgens are responsible for development, maturation and maintenance of the prostate gland and there is little doubt about the role of androgens in prostate cancer development. Long-term absence of androgen exposure appears protective against prostate cancer, however whether the normal range of androgen concentration can increase the risk remains unclear. Androgen receptor abnormalities resulting in a longer response have also been implicated in development of hormone refractory disease. Genes involved in biosynthesis of androgens like cytochrome P450c17 have been found mutated. Polymorphism of CYP3A4, an enzyme responsible for oxidative degradation of testosterone has been found in locally advanced and poorly differentiated tumors (Rebbeck et al. 2000).

1.4.2: Oestrogens:

Oestrogens are known to be protective against prostate cancer by inhibiting epithelial cell growth and alternatively increasing the risk by producing inflammation in combination with androgens (Naslund et al. 1988). Studies on mice lacking estrogen receptor-β have demonstrated prostatic epithelial cell hyperplasia characterized by arrested cellular differentiation, which provide an ideal environment for the development of epithelial cancer (Imamov et al. 2004). There have been mixed conclusions regarding serum oestrogen level and prostate cancer risk due to interpretation of serum levels and the fact that estradiol can be produced from testosterone by intraprostatic aromatase (Risbridger et al. 2003).

1.5: Diagnosis:

1.5.1: DRE, PSA and TRUS:

The most commonly used primary diagnostic tools for prostate cancer are digital rectal examination (DRE), prostate specific antigen (PSA) and transrectal ultrasonography (TRUS). Due to peripheral localization, DRE can be positive when tumour volume is around 0.2ml or more, in the form of palpable nodule. However it can be variable depending opon the location and experience of the examiner. Digital rectal examination is only positive in 18% of patients diagnosed with prostate cancer (Richie J et al. 1993).

Prostate-specific antigen (PSA) is a kallikrein-like serine protease produced by the epithelial cells of the prostate, but it is organ-specific not cancer-specific. Serum levels may be elevated in the presence of benign prostatic hypertrophy (BPH), prostatitis and other non-malignant conditions. However PSA as an independent variable is a better predictor of cancer than suspicious findings on DRE or TRUS (Catalona et al. 1994). There is no specific cut off normal value for prostate cancer but higher values indicate more likely presence of cancer. Several modifications of serum PSA value have been described, which may improve the specificity of PSA in the early detection of prostate cancer. They include: PSA density, PSA density of the transition zone, age-specific reference ranges and PSA molecular forms. However, these derivatives and certain PSA isoforms (cPSA, proPSA, BPSA, iPSA) have limited usefulness in the routine clinical setting (Djavan et al. 2000; Mikolajczyk et al. 2001; Nurmikko et al. 2000; Partin et al. 2003).

1.5.2: Transrectal ultrasonography (TRUS) and biopsy:

TRUS may be able to demonstrate the classical picture of a prostatic nodule in the peripheral zone but this may not be the case in every patient. However, it provides an invaluable way to sample prostatic tissue by site directed biopsy from the peripheral zone of the prostate gland. It is usual practice to take 8 cores (4 from each lobe) and additional biopsies can be taken from suspicious areas like nodules. More than 12 cores are not significantly more conclusive (Eichler et al. 2006). The British Prostate Testing for Cancer and Treatment Study has recommended 10-core biopsies (Donovan et al. 2003).

1.6: Staging classification of prostate cancer:

Two main classification systems for clinical staging exist today: the Whitmore-Jewett (Jewett 1956; Whitmore 1956) and the tumor, node, metastases (TNM) classification systems. TNM classification has been widely used and accepted internationally and recognized. It was first adapted by the American Joint Committee for Cancer Staging and End Results Reporting (AJCC) in 1975. It was modified in 1992 and adopted by International Union against Cancer (UICC) as well.

1.7: Grading of prostate cancer

Multiple systems exist for grading of prostatic adenocarcinoma but the Gleason grading system (Gleason and Mellinger, 1974) is widely accepted. The Gleason score can be assessed using biopsy material from core biopsy and operative specimens. Cytological

features have no role but it is based on the differentiation of a glandular pattern and a score between 1-5 is assigned to most prevalent and second most prevalent pattern. The prognostic importance of Gleason grading is well established. The 15-year risk of dying from prostate cancer, in relation to Gleason score of 2-4 is 8% as compared to 93% for Gleason score of 8-10 (Albertsen et al. 1998).

1.8: Staging investigations for prostate cancer

1.8.1: T-Stage:

Distinction between intracapsular (T1-T2) and extracapsular (T3-T4) disease has the most profound impact on treatment decisions. Extensive examinations for adequate T-staging are only recommended when curative treatment is an option. Both CT and MRI are used for local T staging but they may not be sufficiently reliable for local tumor extension. However endorectal MRI can elicit more precise zonal anatomy of the prostate as compared to external MRI (Heijmink et al. 2007).

1.8.1: N-Stage:

N-staging is performed in patients for whom potentially curative treatments are planned. Higher PSA value, T2-T3 stage, high Gleason score and perineural invasion are associated with higher risk of nodal metastasis (Pisansky et al. 1996; Stone et al. 1998; Partin et al. 2001). As compared to MRI, CT appears to be a slightly better tool for investigation of lymph node enlargement (Hoivels et al. 2008). Commonly used criteria for enlarged lymph nodes are 1cm for rounded nodes and 2cm for oval nodes.

1.8.2: M-Stage:

Bone metastases are present in 85% of patients dying from prostate cancer (Whitmore et al. 1984). Elevated skeletal alkaline phosphatase levels are found in 70% of affected patients (Lorente et al. 1996). Early detection of bone metastases is important to prevent any complications related to skeletal destruction. Bone scintigraphy is highly valuable for assessing bone metastases which is found superior to clinical evaluation, bone radiographs and serum markers like alkaline phosphatase (McGregor et al. 1978). Technetium diphosphates are most commonly used compounds with high bone to soft tissue ratio (Buell et al. 1982).

In addition to bone, prostate cancer can metastasize to any organ but most commonly affected organs include distant lymph nodes, lung, liver, brain and skin. Further investigations to rule out metastases to these sites are performed only if clinically indicated. Serum PSA levels prior to the treatment can reliably indicate the possibility of bone metastases and the requirement for a bone scan. A bone scan is not usually indicated if the serum PSA level is less than 20 ng/ml in asymptomatic patients with well or moderately differentiated tumours. However, in patients with poorly differentiated tumours and clinically locally advanced disease, a staging bone scan is indicated irrespective of the serum PSA value (Rana et al. 1992).

TNM staging for prostate cancer (Sobin et al. 2002):

T - Primary tumor

Tx	Primary tumor cannot be assessed	
T0	No evidence of primary tumor	
T1	Clinically inapparent tumor not palpable or visible by imaging	**T1a:** Tumor incidental histological finding in 5% or less of tissue resected
		T1b: Tumor incidental histological finding in more than 5% of tissue resected
		T1c: Tumor identified by needle biopsy (e.g. because of elevated prostate-specific antigen (PSA) level
T2	Tumor confined within the prostate[1]	**T2a:** Tumor involves one half of one lobe or less
		T2b: Tumor involves more than half of one lobe, but not both lobes
		T2c: Tumor involves both lobes
T3	Tumor extends through the prostatic capsule[2]	**T3a**: Extracapsular extension (unilateral or bilateral)
		T3b: Tumor invades seminal vesicle(s)
T4	Tumor is fixed or invades adjacent structures other than seminal vesicles: bladder neck, external sphincter, rectum, levator muscles, or pelvic wall	

Table 1.1: TNM staging of prostate cancer

1: Tumor found in one or both lobes by needle biopsy, but not palpable or visible by imaging, is classified as T1c.

2: Invasion into the prostatic apex, or into (but not beyond) the prostate capsule, is not classified as T3, but as T2.

N - Regional lymph nodes[3]

Nx	Regional lymph nodes cannot be assessed
N0	No regional lymph node metastasis
N1	Regional lymph node metastasis

M - Distant metastasis[4]

Mx	Distant metastasis cannot be assessed	
M0	No distant metastasis	
M1	Distant metastasis	M1a: Non-regional lymph node(s)
		M1b: Bone(s)
		M1c: Other site(s)

Table 1.1(continued)**:** TNM staging of prostate cancer

3: Metastasis no larger than 0.2 cm can be designated pN1mi.

4: When more than one site of metastasis is present, the most advanced category should be used.

1.9: Treatment:

Prostate cancer is diagnosed in 15 to 20% of all men during their lifetime but the risk of death is only 3%, as the primary cause. Several autopsy studies of people dying from different causes have shown the presence of prostate cancer ranging from 60 to 70%, depending upon the age group (Haas et al. 2008).

1.9.1: Conservative management

Due to their low risk of death in low-grade well differentiated tumours and reducing the risk of treatment, there are two conservative management strategies proposed in the literature:

Watchful waiting: This is also known as deferred treatment or symptom guided treatment and refers to conservative treatment of prostate cancer until the element of local or distant symptoms appear. Broadly it means that a patient could be offered palliative treatment in the form of transurethral resection of the prostate and hormonal treatment or radiotherapy for palliation of symptoms. However, deferred treatment for locally advanced or metastatic disease is not indicated. Watchful waiting can be considered as a viable option in patients with well differentiated localized prostate cancer with limited life expectancy or asymptomatic older patients with medical co-morbidities.

Active surveillance: This is also known as active monitoring which includes a decision not to treat the patient immediately but to follow him with active monitoring. Active monitoring is performed at predefined intervals and includes clinical evaluation, measurement of serum markers like PSA and if indicated prostate biopsy along with repeat staging of disease. If the cancer shows any progression according to predefined parameters, treatment is undertaken provided the patient agrees to the potential benefits and risks of complications. In contrast to watchful waiting, active surveillance aims to reduce the ratio of overtreatment in patients with a low-risk prostate cancer without giving up option of radical treatment. Patients with clinically confined prostate cancer (T1-T2), Gleason score less than or equal to 7 and PSA <10 ng/ml are suitable candidates for this strategy.

1.9.2: Radical prostatectomy (RP):

Radical prostatectomy aims at complete eradication of disease and involves surgical removal of the prostate gland along with seminal vesicles and terminal parts of the vas deferens. Radical prostatectomy is indicated in patients with low and intermediate risk localized prostate cancer (cT1b-T2 and Gleason score 2-7 and PSA < 20) and a life expectancy > 10 years. Pelvic lymph node dissection is usually performed to rule out any pelvic lymph node metastasis. Most clinicians rely on nomograms (Partin tables), based upon the preoperative biochemical markers and biopsy results, to decide about the pelvic lymph node dissection (Makarov et al. 2007). Patients with low PSA (less than 10) and low Gleason score (7 or less) have a very low potential for the lymph node

metastases and may be spared from lymph node dissection (Makarov et al. 2007). There are multiple surgical approaches for radical prostatectomy including open, laparoscopic and perineal approaches. Laparoscopic and robotic prostatectomy are gaining popularity due to shorter convalescence and the results are comparable in short term follow-up (Chan et al. 2008). A perineal approach lacks the feasibility of direct access to pelvic lymph nodes and a slightly higher risk of rectal injury (Bishoff et al. 1998). RP is the only treatment which has demonstrated the improved overall survival and cancer specific survival, in one prospective randomised trial. When compared with conservative management, RP demonstrated a relative reduction of all cause mortality and prostate cancer-specific mortality (Bill-Axelson et al. 2011).

1.9.3: Radiotherapy:

There are no randomized studies comparing radical prostatectomy with either external beam therapy or brachytherapy for localized prostate cancer. Three-dimensional conformal radiotherapy (3D-CRT) is the gold standard, however intensity modulated radiotherapy (IMRT) which is an optimized form of 3D-CRT, is gradually gaining popularity in centres of excellence.

A recent systematic review from multiple studies was able to demonstrate that radiotherapy continues to be an important and valid alternative to surgery (Grimm et al. 2012). In localized prostate cancer T1c-T2c N0 M0, 3D-CRT with or without IMRT is recommended even for young patients who refuse surgical intervention. There is fairly strong evidence that intermediate and high-risk patients benefit from dose escalation

(Zietman et al. 2010; Kuban et al. 2011). For patients in the high-risk group, short-term ADT prior to and during radiotherapy results in increased overall survival (Bolla et al. 2010). Transperineal interstitial brachytherapy with permanent implants is an option for patients with cT1-T2a, Gleason score < 7 (or 3 + 4), PSA ≤ 10 ng/mL, prostate volume below 50 mL, without a previous TURP and significant lower urinary tract symptoms (Salembier et al. 2007).

1.9.4: Hormonal therapy:

Androgen-suppressing strategies have become the mainstay of the management of advanced prostate cancer. It may be effective in relieving symptoms of metastatic disease but has not proven to be of any significant survival benefit (McLeod, 2003). In advanced prostate cancer, all forms of castration as monotherapy (e.g. orchiectomy, LHRH agonist and diethyl stilbisterol DES) have equivalent therapeutic efficacy. Intermittent androgen-deprivation therapy is a viable option (Irani et al. 2008), even though long-term data from prospective randomized clinical trials are still awaited. In advanced prostate cancer, immediate androgen-deprivation therapy (given at diagnosis) significantly reduces disease progression as well as the complication rate due to progression itself compared with deferred androgen-deprivation therapy, delivered at symptomatic progression (Nair et al. 2002).

Chapter 2
Cancer metastasis and role of cell movement

Although surgery, chemotherapy and radiation therapy effectively control many cancers at the primary site, the development of metastatic disease always leads to a poor prognosis. In an ideal world, elimination of metastases would make almost all of the cancers curable. Most metastatic lesions are not treated by surgery, as the presence of one lesion often indicates wider systemic dissemination. Chemotherapy, hormonal therapy and radiation serve palliative purposes in the metastatic setting, and may offer a modest but statistically significant extension of survival. In spite of these facts, most deaths from cancer are due to metastases that are resistant to conventional therapies (Chambers et al. 2002). Morbidity and mortality arising from metastatic disease can result from direct organ damage by the growing lesions, paraneoplastic syndromes, or from the complications of treatment. The major problem during the treatment of metastasis is the biological heterogeneity of cancer cells in the primary and metastatic sites. This heterogeneity is exhibited in the form of specific biological characteristics such as expression of cell receptors, enzymes and growth properties. Expression or suppression of these biological characteristics can make these tumours susceptible or resistant to certain treatments (Ramaswamy et al. 2003).

Tumour metastasis is not a random process but consists of a series of discrete biological processes, when the tumour cells disseminate from the primary neoplasm to a distant location. It involves not only possession of certain characteristics by the tumour cells but also depends on host response and favourable properties of the secondary site. Tumour cells must invade the tissue surrounding the primary tumour, enter either the lymphatics or the bloodstream, survive and eventually arrest in the circulation, extravasate into a tissue and grow at the new site (Ramaswamy et al. 2003).

This seemingly simple process involves expression of certain essential genes at critical timing, enabling the cancer cell to complete the whole process (Wang et al. 2005).

2.1: Metastatic cascade:

Cancer cells must use their cytoskeletons to adapt and survive in a variety of hostile environments to successfully metastasise. Firstly, they must leave the site of the primary tumour and enter the blood or lymphatic system. They are often aided by angiogenesis in and around the tumour and also by stromal cells such as fibroblasts and macrophages that both remodel the extracellular matrix and provide signals to the tumour cells for migration. One of the key cellular processes that triggers the beginning of an invasive or metastatic programme in many cancers is the de-differentiation of epithelial cells toward a primitive mesenchymal state. This process is referred to as epithelial to mesenchymal transition (EMT). Having undergone EMT, cells become more fibroblast like (Lee et al. 2006). This fibroblastic morphology allows polarised assembly of the actin cytoskeleton into protrusive and invasive structures that help the cell to travel through the extracellular matrix (ECM). EMT was origionally identified in embryonic development studies (Nieto, 2001). This transition is marked by reduced expression of E-cadherins, cytokeratins and occludins along with upregulation of MMPs (Lee et al. 2006). These cells also alter their gene expression to acquire an amoeboid phenotype. This phenotype is characterized by lack of polarity and crawling type of cellular movement (Friedl, 2004). EMT also helps invasive cells to break away from the rest of tumour population and thus change from collective to individual metastatic activity (Gupta and Massague 2006). The cancer cell, having entered the blood or

lymph system, then has to survive in the circulation and is transported to distant sites in the body (Schmidt-Kittler et al. 2003; Pantel et al. 2006).

2.2: Physiological and pathological role of cellular motility:

A variety of cellular motility processes are essential throughout the life cycle of cells. From the early stages of development, cell movement is essential for the generation of the entire organism. Primary muscle cells migrate to places where limbs are formed, endothelial cells form the blood vessel walls, neurons migrate to their proper positions and send out axons and dendrites to find their target cells (Dormann, 2003). Also in adult organisms cell motility is crucial as a response to a pathological situation. Vertebrate immune cells invade into infected tissue to eliminate infectious agents. Fibroblasts, surrounding a wound, migrate towards each other during wound healing. Not surprisingly, many pathologic events arise from aberrant motility such as inappropriate immune responses and migration leading to chronic inflammatory diseases or malignancy.

Basic concepts in cellular motility were introduced by Abercrombie. He identified the thin layers of cytoplasm which protrude beyond the migrating cell surface. This structure was described as “leading lamella” or “lamellipodium”, when parallel to substrate and reffered as “ruffle”; when it curled upwards (Abercrombie, 1980). Subsequent studies revealed the presence of concentrated layers of actin filaments in lamellipodia and demonstrated that protrusion was based on actin polymerization (Heath and Holifield, 1993). Filopodia are plasma membrane protrusions which have been described as

“finger-like”. They are formed by tightly packed parallel actin filaments (Mattila and Lappalainen, 2008). Cells are thought to use these structures as probes to detect the cues in extracellular environment (Gupton and Gertler, 2007).

Cells move in response to signals from their environment. These are sensed by transmembrane receptors by which signaling cascades are initiated and ultimately affect cytoskeletal and adhesive structures of the cell. Several actin rich cellular structures have been defined (Small, 1994; Kaverina et al. 2002). There is a close interplay between the different intracellular cytoskeletal systems (especially actin and microtubule containing structures) and these systems also interact with the cell–substratum and cell–cell adhesive machinery. Nevertheless, the actin microfilament system is still considered to be the engine of cellular migration. The temporally and spatially controlled turnover of specific actin structures drives protrusion. In recent years, many regulatory actin binding proteins have been characterised. In addition, some of the molecular components and relevant signaling cascades from the plasma membrane to the actin cytoskeleton have been identified yielding key roles to phosphoinositides (and enzymes involved in their metabolism), small GTPases, kinases and a variety of focal adhesion components.

There is sufficient evidence to suggest that invasive cancer cells acquire a migratory phenotype which is associated with an increased expression of several genes involved in cell motility (Wang et al. 2005). Migration of metastatic cells through tissues and endothelial barriers is complex and comprises a highly regulated cycle of cell shape changes including protrusion, retraction, adhesion and detachment. Cancer cells

respond to mitogenic stumuli through formation of numerous cell surface projections (Chambers et al. 2003).

2.3: Role of integrins and focal adhesion complexes in cell motility:

For a cell to translocate (i.e. to move from one place to another), the cell needs to attach at a new site and retract its rear end (Small et al. 1999). The new attachment sites or focal contacts, that constitute a physical link between the substrate and the actin cytoskeleton, are formed behind the leading edge (Lauffenburger et al. 1996). The cell attaches to the ECM through surface proteins like integrins. Integrins are attached to the actin cytoskeleton through multiple adaptor proteins (Figure: 2.1). Integrins are heterodimers containing two chains, the α (alpha) and β (beta) subunits. There are 19 alpha and 8 beta subunits which have been described. Various combinations have been found during characterization of different integrins (Eble et al. 2002; Berrier, 2007). Integrin mediated focal contacts are used by cells for firm attachment to substrate. Smaller adhesion sites known as focal complexes are utilized by motile cells for advancing movement. Integrins like αvβ3 are found to be upregulated in neovascularisation and invasive tumors (Mattern et al. 2005). Many integrin related accessory proteins interact with small guanosine tri-phosphatases (GTPase) like Rho, which causes suppression of myosin light chain phosphatase through its effect on ROCK (Jaffe, 2005). The Rho-ROCK mediated inhibition of myosin light chain phosphatase allows myosin light chain kinase (MLCK) to phosphorylate myosin light

chain, leading to activation of myosin-II (non muscle myosin) (Riento, 2003). The active myosin-II binds with actin filaments to generate the traction force which retracts the tail end of cell.

With the advancement in knowledge of integrins it was revealed that they are not merely serving as attachment sites for cells to extracellular matrix. They also act as two way transmitter of signals between intracellular machinery and the external environment. Cytoplasmic extensions of integrins do not possess any enzymatic activity so they need to recruit a variety of proteins before focal adhesion complexes can act as a conduit for transmission of signals (Berrier, 2007).

Paxillin was first identified as a 68 KDa protien which showed increased tyrosine phosphorylation following the transformation of chick embryonic fibroblasts by the Src-expressing Rous sarcoma virus (Glenney et al. 1989). The subsequent analysis of fibroblasts derived from paxillin deficient embryos has indicated defects in cell migration, responsible for severe developmental phenotype (Hagel et al. 2002). From prior studies it became evident that paxillin act as nexus for the function of Rho family of GTPases thus controlling essential regulators responsible for actin and adhesion dynamics (Turner et al. 1990).

Studies on molecular structure and peptide sequence analysis have revealed multiple protein binding modules leading to the belief that paxillin is a molecular adapter or scaffold protein (Turner et al. 1990). The C terminal of paxillin contains four LIM domains, which are double zinc finger motifs that mediate protein to protein interaction (Perez-Alvarado et al. 1994). It has been established that phosphorylation of these

domains contributes to the regulation of focal adhesion targeting by paxillin. The LIM domain of paxillin also serves as a binding site for several structural and regulatory proteins including tubulin and tyrosine phosphatase (Brown, 1998). The N terminal of paxillin controls most of its signaling activity. It consists of five leucine and aspartate rich LD motifs which are capable of interaction with multiple proteins (Tumbarello et al. 2002). The N-terminal also contains a proline rich region which interacts with vinculin binding protein, ponsin and this combination is important for formation of costameres (sites of actin-membrane interactions) in cardiac muscle cells (Zhang et al. 2006).

Multiple tyrosine, serine and threonine phosphorylation sites are present in the paxillin molecule, which are targeted by different kinds of kinases in response to adhesion stimuli and growth factors. The polarised cell migration require regulation of RHO family of small GTPases which includes Cdc42, Rac1 and Rho A. Cdc42 is required for cell polarisation and formation of filopodia, whereas Rac1 induces the formation of broad sheet like extensions or lamellipodia. Cdc42 and Rac1 are also involved in the assembly of early adhesion complexes at the leading edge and disassembly at the rear end (Ridley, 2001). These GTPases are essential for controlling the actin cytoskeleton and actin associated adhesions during cellular movement.

All the members of this family functions as molecular switches by cycling between an inactive (GDP- bound) and active state (GTP- bound). This cycling is controlled by a large group of guanine-nucleotide exchange factors (GEFs), which catalyse the exchange of GDP for GTP and by GTPase activating proteins (GAPs), which promote the hydrolysis of GTP to GDP. Paxillin contributes to the coordination of their downstream signals by indirectly recruiting various GEFs, GAPs and effector proteins.

For example, upon the ligation of an integrin to either a fibronectin or collagen substrate, paxillin becomes tyrosine phosphorylated, primarily on tyrosine residues 31 and 118 (Y31 and Y118, respectively) (Burridge et al. 1992; Bellis et al. 1997; Petit et al. 2000) in a FAK and Src-dependent manner (Schaller and Parsons, 1995). The CrkII-DOCK180-ELMO complex, which regulates Rac1 signaling (Grimsley et al. 2004), can interact with the phosphorylated Y31 and Y118 residues of paxillin via the SH2 domain of CrkII (Birge et al. 1993; Valles et al. 2004) and, by means of the unconventional Rac1- and Cdc42-GEF activity of DOCK180 (Brugnera et al. 2002), activates Rac1 to promote cell migration. Interestingly, the phosphorylation of Y31 and Y118 has also been shown to regulate RhoA activity. Phosphorylated paxillin binds directly to p120RasGAP (RASA1), which diminishes the interaction of p120RasGAP with p190RhoGAP (ARHGAP5) at the plasma membrane; this culminates in the suppression of localised RhoA activity by p190RhoGAP (Tsubouchi et al. 2002). Therefore, paxillin that is phosphorylated at Y31 and Y118 can indirectly activate Rac1 and inhibit RhoA, and both of these activities are necessary for efficient leading-edge protrusion during cell migration.

The LD4 motif of paxillin plays a particularly important role in its activity to control Rho GTPases activity and focal adhesion turnover. This motif is responsible for recruiting a molecular complex comprising of G-protien-coupled receptor kinase interacting protein (GIT1 or GIT2, p21-activated serine/threonine kinase (PAK), PAK-interacting exchange factor (PIX) and NCK. Fibroblasts expressing a mutant form of paxillin lacking the LD motif cannot recruit GIT1/2–PIX-PAK-NCK complex to focal adhesion sites and therefore exhibit abnormal membrane protrusion dynamics (West et al. 2001). These cells are also deficient in polarised cell movement (Brown et al. 2002).

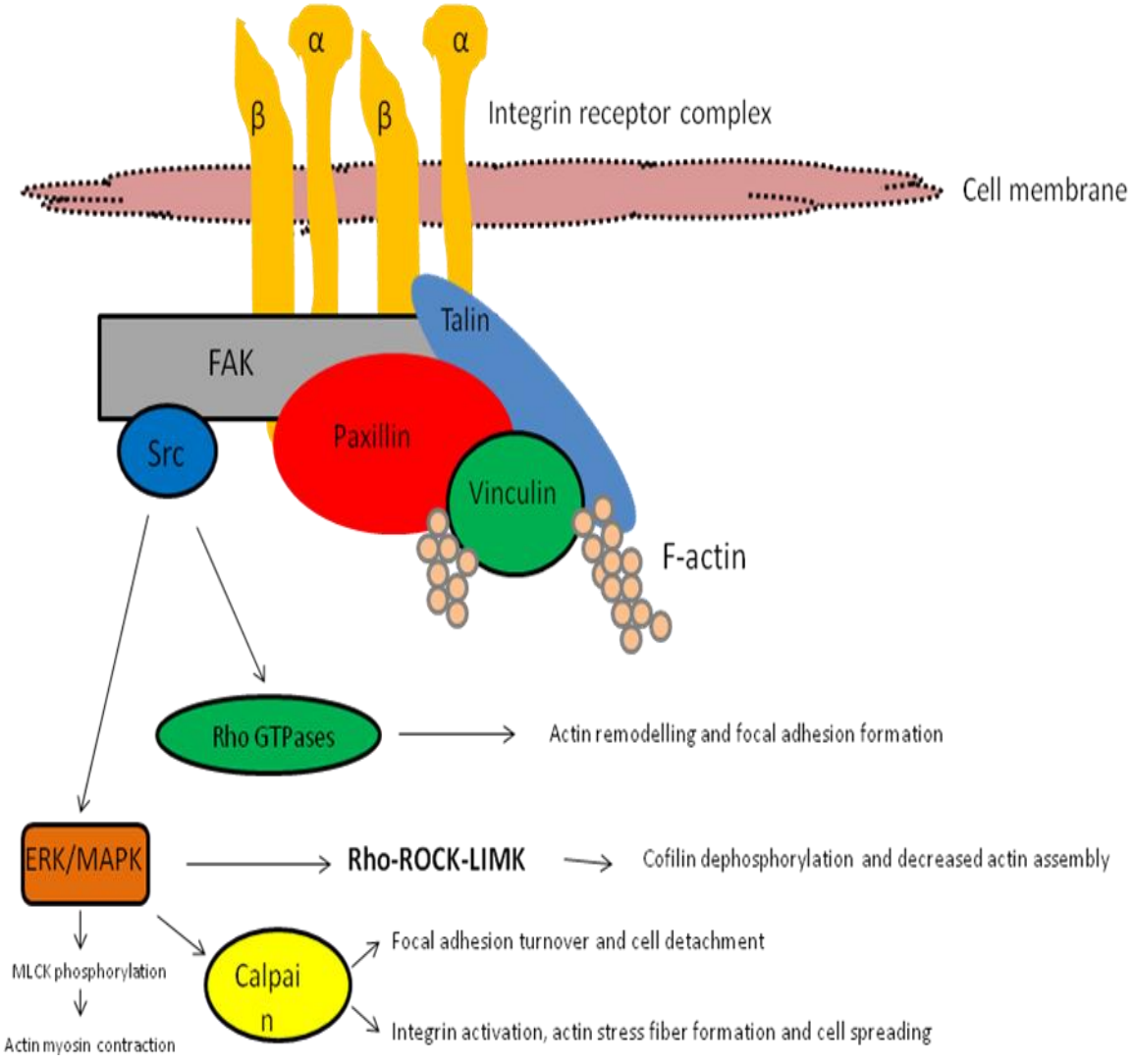

Figure 2.1: Schematic presentation of integrin-linked focal adhesion complex, which provide the main sites of cell adhesion to extracellular matrix and associated with the actin cytoskeleton to control cell movement.

2.4: Role of actin in cell motility:

To migrate, cells use dynamic rearrangements of the actin cytoskeleton for the formation of protrusive structures and for generation of intracellular forces that lead to net cell translocation. This is initiated by a transition from a non-polarized to a polarized state, dictated by the extracellular signals and their concentration gradient cues. These activated motile cells extend distinct protrusive regions in the direction of translocation with advancing front and retracting rear end (Moissoglu et al. 2006). Whereas several actin-rich structures have been described in motile cells, two cellular features are typically associated with cell migration (lamellipodia and filopodia) (Small, 1994). Another important aspect for directed movement is coordinated assembly and disassembly of these adhesion sites. When new focal adhesions are being established in the advancing end, they are also being disassembled at the rear end for retraction and transported to sites of active adhesion formation (Moissoglu et al. 2006).

During progressive movement, a motile cell forms protrusive structures which appear in the form of broad sheets (lamellipodium) and narrow finger like projections (filopodium). Lamellipodia and filopodia are composed of actin filaments. These are formed by polymerization of globular actin (G-actin), an ATP binding protein which exists as monomers bound to profiling and sequestering proteins such as thymosin-β4, into double stranded helical filaments (F-actin). These are structurally and kinetically polarized, possessing a faster growing (+)-end and a slower growing (−)-end. Once incorporated at the (+)-end, ATP-G-actin hydrolyses its bound ATP. After release of inorganic phosphate, ADP-actin molecules are left in the filament and finally dissociate

at the (−)-end (Figure: 2.2). ADP-actin monomers are subsequently reloaded with ATP and shuttle back to the barbed ends for a new round of polymerization. Addition of ATP-actin occurs preferentially at the positive (+)-ends and dissociation of ADP-containing molecules at the negative (−)-ends. Each end is in equilibrium with a monomer concentration called the critical monomer concentration. Under steady state conditions, when the monomer concentration lies between the critical concentrations of both ends, the number of actin molecules added at the fast growing ends balances the number of molecules dissociating from the pointed ends, resulting in a dynamic equilibrium called treadmilling (Wang et al. 1985). Migrating cells reach speeds of 1–20 μm/min depending on the cell type, implicating actin polymerization rates of 10–200 subunits/second. In contrast, the observed *in vitro* elongation rate is approximately 0.2–0.5 subunits/second (Zigmond et al. 1993). This discrepancy is due to the regulatory action of many actin binding proteins that accelerate several steps of the polymerization cycle, resulting in an efficient system that is optimised for progressive cell movement.

2.5: Control of actin polymerization:

In a resting cell, there is little or no need of an active turnover of actin filaments. Therefore, the fast growing ends are blocked (see below) and the large pool of actin monomers is in complex with polymerization-inhibiting or sequestering proteins. Upon cell activation by external stimuli (growth factors, chemoattractants etc) dramatic, often local, increases in actin polymerization are observed. This burst of actin polymerization

is initiated by uncapping (+)-ends, by severing existing filaments thereby creating free polymerizable ends, and by *de novo* polymerization (Pollard, 2003). Although neglected for a long time, *in vivo* nucleation is now considered as a major determinant in cell motility.

Three important nucleation mechanisms are now being suggested. Most of the time each of these relies on the proteins which form regulatory complexes. These proteins include WASP family proteins, Diaphanous related formins (DRFs) and Ena/VASP proteins. Current views indicate that the branched actin filament network in the lamellipodia are formed by WASP/Arp2/3, the contractile ring in dividing cells is organized by DRFs and F-actin bundles in filopodia and stress fibers by Ena/VASP proteins and DRFs, respectively (Nürnberg et al. 2011).

2.6: Role of ARP 2/3:

The Arp2/3-complex, in conjunction with WASP-family members, has emerged as the major factor responsible for *de novo* nucleation at the leading edge of a lamellipodium (Svitkina et al. 1999). The Arp2/3 complex is a multiprotein complex containing seven different subunits of which two are actin related (Arp2 and Arp3) (Svitkina et al. 1999). The Arp2/3-complex creates Y-shaped junctions on existing filaments resulting in the branched actin networks that are stabilized by cortactin (Machesky et al. 1994). The intrinsically inactive Arp2/3-complex is synergistically activated by pre-existing actin filaments (Mullins et al. 1998), by ATP (Weaver et al. 2002) and by proteins of the WASP/WAVE family.

2.7: Regulation of actin dynamics by WASP family proteins:

Rapid reorganisation of the actin cytoskeleton underlies morphological changes and motility of cells. WASP family proteins have received a great deal of attention as the signal-regulated molecular switches that initiate actin polymerization (Miki and Takenawa, 2003). The first member, WASP, was identified as the product of a gene of which dysfunction causes the human hereditary disease Wiskott-Aldrich syndrome. There are now five members in this protein family, namely WASP, N-WASP, WAVE/Scar-1, 2, and 3 (Parolini et al. 1997; Fukuoka et al. 1997; Hiroaki et al. 1998; Suetsugu et al. 1999).

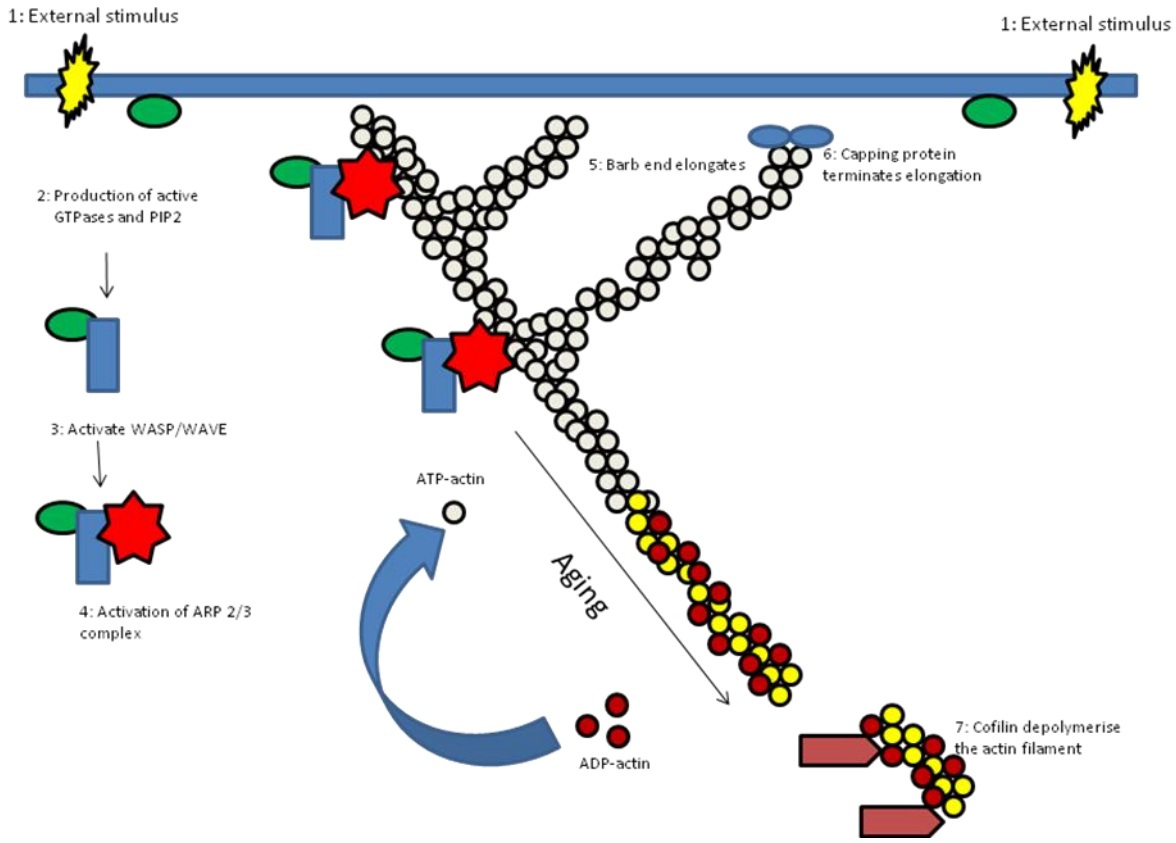

Figure 2.2: Dynamics of actin polymerisation and depolymerisation. (1) Extracellular signals activate receptors. (2) The associated signal transduction pathways produce active Rho-family GTPases and PIP2 which (3) activate WASP/WAVE proteins. (4) WASP/WAVE bring together Arp2/3 complex and an actin monomer on the side of a preexisting filament to form a branch. (5) Growth at the barbed end of the new branch pushes the membrane forward. (6) Capping protein terminates growth. Actin filaments age by hydrolysis of ATP bound to each actin subunit (white subunits turn yellow) followed by dissociation of the phosphate (subunits turn red). (7) Cofilin promotes phosphate dissociation, severs ADP-actin filaments and promotes dissociation of ADP-actin from filament ends. Profilin catalyzes the exchange of ADP for ATP (turning the subunits white), returning subunits to the pool of ATP-actin.

2.7.1: Wiskott-Aldrich syndrome:

The Wiskott-Aldrich syndrome (WAS) is a rare X-linked disorder with variable clinical phenotypes that correlate with the type of mutations in the *WAS protein* (*WASP*). This immunodeficiency disease presents with characteristic clinical phenotypes that include thrombocytopenia with small platelets, eczema, recurrent infections caused by immunodeficiency, and an increased incidence of autoimmune manifestations and malignancies (Sullivan et al. 1994). Clinical manifestations suggesting WAS are often present at birth and consist of petechiae, bruising, and bloody diarrhoea. Excessive hemorrhage after circumcision is an early diagnostic sign. Eczema is a frequent manifestation of classic WAS during infancy and childhood. The most consistent finding at diagnosis is thrombocytopenia and small platelets. Infections, including otitis media with drainage of mucoid purulent material, pneumonia most often caused by bacteria and rarely by *Pneumocystis carinii*, and skin infections, are frequent complaints during the first 6 months of life. Patients with variable presentation may have less problems with eczema and infections and often receive misdiagnoses of idiopathic thrombocytopenia (ITP), considerably increasing the actual age of diagnosis.

2.7.2: WASP and N-WASP:

In 1994, Derry et al., identified the gene that is mutated in WAS patients and named it Wiskott - Aldrich syndrome Protein (WASP) (Derry et al. 1994). Northern blotting analysis indicated that WASP is expressed exclusively in hematopoietic cells (Parolini et al. 1997). Two years later, a novel protein with ~50% amino acid identity to the WASP

gene product (WASP) was reported as a binding partner for the Grb2/Ash adapter protein. As compared to WASP, this protein was expressed ubiquitously, but its strongest expression was observed in nerve cells, and thus it was named Neural-WASP (N-WASP) (Fukuoka et al. 1997). These proteins share many structural and functional properties. Both proteins possess an EVH1 (or WH1) domain, a highly basic region, a GBD/CRIB motif, a proline-rich region, and a VCA region. The EVH1 domain binds the evolutionarily conserved WASP-interacting protein (WIP) family of proteins. The WIP family proteins are essential functional partners for WASP and N-WASP, probably responsible for regulation of their specific localization (Martinez-Quiles et al. 2001).

2.7.3: Structure of WASP-WAVE proteins:

In the mammalian world, WASP and WASP family verpolin homology (WAVE) proteins share a similar domain structure and each consist of approximately 500 amino acids. These proteins share two main regions of homology: a central segment rich in proline residues and a carboxy-terminal module comprising three characteristic domains called the VCA domain.The V domain is a monomeric actin binding site which binds to monomeric F-actin, the CA domain binds the Arp2/3 complex (Miki et al. 1998). The Arp2/3 complex is activated through binding with the VCA domain and this complex then catalyses actin polymerization (Machesky et al. 1999). Comparative analysis of the catalytic properties of the VCA module of WASP, N-WASP and WAVE revealed that the isolated domains display the unique kinetics of actin assembly. The VCA domain of N-WASP has a distinctly higher rate of nucleation than the VCA of both WASP and WAVE

domains which are distinctly shorter and have less activity (Machesky et al. 1999). The amino-terminal half of the molecule is defined by two functional groups on the basis of the presence of either WASP homology 1/Ena (Ena-vasodilator stimulated phosphoprotein) VASP homology 1 (WH1/EVH1) domain (found in WASP and N-WASP) or WAVE homology domain/suppressor of cAMP receptor (SCAR) homology domain (WHD/SHD), specific to WAVE isoforms (Takenawa et al. 2001). The N-terminal consists of more than 85% of the entire amino acid sequence (Takenawa and Suetsugu, 2007).

The molecular design of WASP family is organised in the form of a conserved C-terminal domain, responsible for output function of the molecule and divergent N-terminal region which is used for targeting by stimulants and also regulates the activity of the C-terminal or output domain (Takenawa and Suetsugu, 2007).

2.7.4: Role of WAVE-1:

WAVE-1 was identified as the third member of the WASP protein family with verprolin homology, functioning as a regulator of actin reorganization downstream of Rac and an essential step in the formation of membrane ruffles (Hiroaki et al. 1998). In the same time period, this protein was identified as SCAR, which is involved in tip formation and chemotaxis in Dictyostelium (Bear et al. 1998). In spite of its general function as a regulator of actin reorganization, its distribution and expression appeared to be limited to the brain (Nagase et al. 1998).

Mitochondrial fission and trafficking to dendritic protrusions have been implicated in dendritic spine development. There is indirect evidence that WAVE-1 is supposed to be responsible for depolarisation-induced mitochondrial movement into dendritic spines and filopodia and regulates spine morphogenesis (Sung et al. 2008). Depolarization-induced degradation of the p35 regulatory subunit of cyclin-dependent kinase 5 (Cdk5), with the resultant decreased inhibitory phosphorylation on WAVE-1, depends on NMDA receptor activation. Thus, WAVE-1 dephosphorylation and activation are probably associated with mitochondrial redistribution and spine morphogenesis (Sung et al. 2008).

The WAVE-1 expression was increased in children with acute lymphoblastic leukemia (ALL). Expression was more marked in children with more aggressive form of disease as compared to patients in complete remission. WAVE-1 might be implicated in the development of ALL and may serve as a marker for the evaluation of the severity of ALL in children (Wang et al. 2008).

The myelin sheath can be compared to the neuronal growth cone in that the unfurled sheath looks like a giant lamellum. WAVE-1 is critical for formation of oligodendrocyte lamellae and myelin sheaths. However some, but not all myelination seems to be impaired by knockout of WAVE-1 function and it appears that other regulators of actin nucleation help oligodendrocytes to produce myelin in parallel with WAVE-1 function. Oligodendrocyte maturation is also disturbed with WAVE-1 knockout and it has been proposed that proper localization and transport of signaling molecules relevant to the integrin signaling cascade were disrupted by loss of WAVE-1 function (Sloane, 2007).

WAVE-1 and WAVE-2 are overexpressed in mouse melanoma cell lines when these cell lines become metastatic (Kurisu et al. 2005). WAVE-1 is not essential for protrusion of the leading edge of lamellipodia but it is involved in the formation of dorsal ruffles, circular assemblies of actin filaments formed upwardly in the dorsal surface of cell. In WAVE-1-knockout cells, extension of the leading edge occurs faster than in wild-type cells (Kurisu et al. 2005). However, the leading edges in WAVE-1-knockout cells are unstable and have shorter half-lives than those of wild-type cells. Consistent with this finding, WAVE-1 is localised slightly behind the leading edge, and therefore, WAVE-1 might be important for the accumulation of actin filaments behind the leading edge to increase the mechanical force necessary for protrusion (Yamazaki et al. 2005).

2.7.5: Role of WAVE-2

WAVE-2 has been found to be located at front end of membrane protrusive structures, formed in the direction of cellular movement. Recruitment to these sites is facilitated by binding of WAVE-2 with compounds like PIP3 (Oikawa et al. 2004). It has been observed that WAVE-2 mediates the downstream effects of Rac, by activating ARP 2/3 complex mediated actin polymerization and formation of lamellipodium (Yan et al. 2003). WAVE-2 appears to be particularly important for directional mesenchymal cell migration in fibroblasts (Yamazaki et al. 2003). WAVE-2 plays an important role in migration of B16F10 melanoma cells in 3-D matrix. Knock down studies of WAVE-2 in B16F10 melanoma cells using siRNA (small interfering RNA) method showed, reduced cell migration and metastases in to the lungs via regulation of membrane protrusions

(Kurisu et al. 2005). Polarized cell movement is triggered by the development of a PIP^3 (phosphatidylinositol tri-phosphates) gradient at the leading edge of membrane. WAVE-2 binds to PIP^3 through its basic domain. The binding of PIP^3 to WAVE-2 seems essential for WAVE-2 mediated rearrangement of the actin cytoskeleton (Oikawa et al. 2004). WAVE-2 has been observed to be significantly over expressed and associated with poor prognosis in breast (Fernando et al. 2007), colorectal (Iwaya et al. 2007) and hepatocellular cancers (Yang et al. 2006).

2.7.6: Role of WAVE-3

WAVE-3 was originally found to be truncated and inactivated in a patient with ganglioneuroblastoma (Sossey-Alaoui et al. 2002). Inactivation of Scar/WAVE-3 was hypothesised to lead to an accumulation of neural crest cells that are defective in migration yet retain some potential for proliferation. The resulting enlarged ganglia would contain accumulated undifferentiated proliferating cells that could potentially be differentiated if given the right signals at a later time. This is a typical manifestation of ganglioneuroblastoma (Sossey-Alaoui et al. 2002). In recent studies, Scar/WAVE-3 was shown to accumulate at puncta, which appeared to be precursors to new filopodia and protrusions that latter became dendritic spines (Pilpel et al. 2005). These puncta were shown to be places of accumulation of F-actin and actually overexpression of Scar/WAVE-3 in hippocampal neurons, induced accumulation of F-actin in these regions (Pilpel et al. 2005).

From neuroblastoma work, Sossey-Alaoui and colleagues found that in general, Scar/WAVE-3 has a positive rather than a negative role in promoting the metastasis and invasion of cancer cells. Condeelis and colleagues found an upregulation of Scar/WAVE-3 in their microarray analysis of motile tumour cells (Condeelis et al. 2005). Scar/WAVE-3 expression appears to be increased in various cancer cell lines and in human breast cancer samples (Sossey-Alaoui et al. 2002, 2005, 2007). In one study, Scar/WAVE-3 was linked to expression of metalloproteases MMP-1, MMP-3 and MMP-9 which associated with cancer cell invasion (Sossey-Alaoui et al. 2005). Silencing of Scar/WAVE-3 using siRNA showed a reduced motility and invasiveness of cancer cells, using matrigel assays. These results were similar to what has been previously shown for WAVE-1 and WAVE-2. The loss of Scar/WAVE-3 led to an increase formation of actin stress fibres and focal adhesion complexes, indicating the possibility that the Scar/WAVE-3 or the balance of Scar/WAVE proteins in the cell can influence the mobility or contractility of the actin cytoskeleton (Sossey-Alaoui et al. 2005). *In vivo* studies showed reduction of Scar/WAVE-3 expression levels also led to a decrease in the number of lung metastases of breast cancer cells in SCID mice and also inhibited primary tumor establishment in the SCID mice (Sossey-Alaoui et al. 2007). Recent work from Fernando et al. has confirmed similar findings in prostate cancer cell lines, where WAVE-3 does not appear to change the growth rate but drastically reduces the motility and invasion of PC-3 and DU-145 prostate cancer cells (Fernando et al. 2009).

2.8: Role of matrix metalloproteinases (MMPs) in cancer invasion and metastasis:

Extracellular and intracellular proteases are integral parts of many developmental and embryological processes. Without these essential molecules cells cannot interact properly with the surrounding environment. Their role in development was first described in the process of involuting tadpole tail. It was observed that diffusible enzymes from the fragments of tail were able to degrade the native fibrillar collagen gels (Gross and Lapiere, 1962). Since the initial discovery multiple families of these proteins have been identified in uni and multi-cellular organisms, including humans. One particular closely related family of proteins, Matrix Metaloprotienases (MMPs), has been identified which depend heavily upon metal ions for their catalytic activity (Nelson et al. 2000). In addition to degradation of extracellular matrix, they also cleave the cell surface molecules and influence the cell behaviour in several ways. Through this role MMPs can influence processes like tissue development, wound repair, inflammatory diseases and neoplastic development (Nelson et al. 2000).

Matrix metalloproteinases are zinc containing endopeptidases which help to dissolute extracellular matrix proteins. At present, 25 vertebrate MMPs and 22 human homologues have been identified. All MMP family members share specific characteristics consisting of a pro-domain, a catalytic domain and a highly conserved active site domain. The active site domain contains HEXGHXXGXXH motif where the three histidine residues constitute three zinc ligands and the glutamic acid residue (Giannelli et al. 1997). With the exception of MMP-7 all MMPs exhibit a hemopexin-

homology domain which associates with substrate specificity. In addition MMP-2 and MMP-9 also contain a fibronectin type gelatin binding domain. MMPs are either secreted (MMPs 1–13 and 18–20) or anchored to the cell membrane through a transmembrane domain (MMPs 14–17). Functionally, MMPs are subdivided into collagenases, stromelysins and gelatinases, depending upon substrate preference.

Gelatinases have earned their name for their preferential degradation of denatured collagen. They include MMP-2 (Gelatinase A) and MMP-9 (Gelatinase B). Due to their ability to degrade collagen IV MMP-2 and MMP-9 are also known as 72kD collagenase IV and 92kD collagenase IV. Like other MMPs substrate specificity extends beyond collagen IV and also includes collagen I, V, and X for MMP-9 and laminin for MMP-2 (Birkedal-Hansen et al. 1993; Giannelli et al. 1997).

2.8.1: Regulation of MMP activity:

The physiological and pathological role of MMPs depends upon their presence in a specific environment, location and time interval. To achieve this, the activity of MMPs is usually regulated at four levels including transcription, post transcriptional modification, proteolytic activation of the zymogen form and inhibition of the active enzyme. It has been observed that MMPs are not expressed continuously but a variety of stimuli like growth factors, cytokines and cell to cell or cell to extracellular matrix (ECM) interactions can induce expression of MMPs (Vu, 2000).

2.8.2: Expression of MMPs

MMPs overlap with each other for their substrate specificities so biological function is largely controlled through their expression. Primary regulation is at the transcription level. MMP genes expression is influenced by numerous stimulatory and suppressive factors through multiple pathways (Vu, 2000). Expression of MMPs can be up or down-regulated by phorbol esters, integrin derived signals, ECM proteins, cell stress and changes in cell shape (Kheradmand et al. 1998). Type I collagen stimulates discoidin domain-containing receptor-like tyrosine kinases that induces MMP-1 expression and become inactive when it binds to MMP-1-cleaved collagen (Vogel et al. 1997). Expression of MMP-2 is controlled sparingly with modest up or down regulation under various circumstances (Birkedal-Hansen et al. 1993). MMP-1, MMP-2, MMP-3 and MT1-MMP expression can also be stimulated by the extracellular matrix metalloproteinase inducer (EMMPRIN). It is a cell surface glycoprotein from an immunoglobulin superfamily and also acts as surface receptor for MMP-1 (Guo et al. 2000).

In contrast to other gelatinases, MMP-9 expression is highly inducible by several cytokines and growth factors including interleukins, interferons, EGF, VEGF, PDGF and the extracellular matrix metalloproteinase inducer (EMMPRIN) (Hipps et al. 1991). This differential expression can be traced back to the promoter regions in the gene. The promoter region of MMP-2 lacks any binding sites for AP-1 and ETS transcription factors (Westermarck et al. 1999). Cytokines and growth factors activate expression of MMP-9 through mitogen activated protein kinase (MAPK) pathway which incorporates ERK 1/2, JNK/MAPK 1/2 and p38 proteins (Westermarck et al. 1999). The highly

inducible nature of MMP-9 by growth factors can be detected in invasive tumors in mice carrying a β-galactosidase gene under the control of MMP-9 promotor (Kupferman et al. 2000). The 5'-flanking regulatory regions of inducible MMPs contain an AP-1 *cis*-regulatory element in the proximal promoter, approximately 70 nucleotides upstream of the transcription initiation site (Fini et al. 1998). The promoter regions of AP-1 contains the PEA3 site, another important *cis*-element which binds members of the ETS family of transcription factors and cooperates with the AP-1 motif for optimal activation of the MMP-1, MMP-3 and MMP-9 promoters (Gum et al. 1996; Westermarck et al. 1997; Vu et al. 2000). Expression of ETS-1 has been observed in stromal fibroblasts near invading tumour cells and angiogenic vascular endothelial cells (Westermarck et al. 1997).

It is very important to emphasize that integrins and extracellular matrix mediated signals also control the expression of MMPs. It was initially observed that antibodies blocking the α5β1 integrin mediated adhesion, also reduced MMP expression in fibroblasts (Werb et al., 1989). Later studies showed that α2β1 integrin regulates MMP-1 expression (Riikonen et al. 1995; Dumin et al. 2001). Antibodies to α3β1 integrin-tetraspanin induced MMP-2 expression and $\alpha_M\beta_2$ integrin stimulated MMP-9 expression (Larjava et al. 1993; Wize et al. 1998). Integrins also appear to play important role in the delivery of MMPs to the cell surface as part of transport vesicles (Ginestra et al. 1997; Dolo et al. 1999; Taraboletti et al. 2002).

2.8.3: Activation of MMPs:

Most MMPs are produced in an inactive and latent form, known as zymogens and are activated once transported out from the cells. This inactive form is maintained by interaction between the sulphhydryl group of highly conserved cystine within the peptide and catalytic zinc ion. This interection essentially blocks the zinc dependent activation of the water molecules, required for attack on the peptide bonds (Van Wart and Birkedal-Hansen, 1990).

Treatment of latent MMPs by chaotropic agents, such as organomercurials, or partial proteolytic cleavage dissociates the covalent bond between zinc and the sulfhydryl group which leads to activation of the catalytic site (Nagase, 1997). Although many proteases can cleave the MMPs in vitro, the activation mechanism for the majority of MMPs *in vivo* remains unclear. Evidence from different experimental studies has demonstrated the close association of plasminogen activator and plasmin system with MMP activation (Mignatti et al. 1996). However studies from mice deficient in plasminogen have demonstrated adequate levels of MMPs, along with adequate invasive potential (Rosenthal et al. 1998). MMPs are capable of mutual and in some cases auto-activation (usually under *in vitro* condition). MMP-1 can activate latent MMP-2. MMP-13 can be activated by MT1-MMP, MMP-3 and MMP-10 (Knäuper et al. 1996).

2.8.4: Inhibition of MMPs

The proteolytic activity of MMPs is primarily controlled by tissue inhibitors of metalloproteinases (TIMPs), once released and activated in the tissues. These are small proteins of 21–28 kDa that specifically block MMP activity by binding to the highly

conserved zinc-binding site of active MMPs. There are currently four known TIMP family members. All four TIMPs possess 12 conserved cysteine residues, required for the formation of six disulfide bonds (Gomez et al. 1997). The amino-terminal domain is specifically required to inhibit activated MMP (Gomez et al. 1997). Data from several experiments based on synthetic peptides have demonstrated that many regions are involved in complex formation with interstitial collagenase (Bodden et al. 1994). Most importantly a specific sequence surrounding two of the disulfide bonds of TIMP-1 is highly effective in inhibiting collagenase activity (Bodden et al. 1994).

TIMP-1 and TIMP-2 inhibit the activity of most MMPs, and similar to TIMP-2 and pro-MMP-2, TIMP-1 can form a complex with pro-MMP-9 (Goldberg et al. 1992). The TIMP-1/proMMP-9 complex recruits MMP-3 resulting in formation of more stable tertiary complex composed of proMMP-9/TIMP- 1/MMP-3. The resulting complex inhibits active MMP-3 (Kolkenbrock et al. 1995). TIMP-3 inhibits the proteolytic activity of MMPs 1, 2, 3, 7, 9 and 13 (Knäuper et al. 1996). TIMP-4 inhibits the activity of MMP-2 and MMP-7. It also inhibits MMP-1, MMP-3 and MMP-9 to lesser extent (Liu et al. 1997).

2.8.5: Role of MMP in cell migration:

Cell migration is a complex process and a critical event in cancer progression and establishment of metastasis. In the initial phase of migration, the cell extends membrane processes such as lamellipodia and filopodia at the cell front. Lamellipodia are sheet like processes and filopodia are needle like projections (Lauffenburger et al. 1996). Invadopodia are a specialized form of needle like projections which are located

in basal part of cells and can be observed in two dimensional cell culture models (Chen et al. 1999). Invadopodia have been studied previously and are characterized by proteolytic degradation (Chen and Wang, 1999). Along the leading edge of invasive cell, new adhesion contacts by integrins and other molecules are also being established. This complex process requires integrins for adhesion/de-adhesion, as well as matrix metalloproteinases (MMPs) for localized proteolysis at the adhesion site.

Formation of adhesive contacts is regulated by the Rho family of GTPases and includes Cdc42, Rac and Rho. These adhesive sites further progress to make mature focal contacts which comprise a highly dynamic network of proteins (Zamir and Geiger, 2001). Formation of adhesive structures is accompanied by tyrosine phosphorylation of cystoskeleton associated proteins such as focal adhesion kinase (FAK), paxillin and tensin which are mediators of intracellular signaling (Weisberg et al. 1997). FAK is a 125-kDa tyrosine kinase which mediates multiple functions such as cell motility, survival and proliferation (Parsons et al. 2000). Increased expression of FAK in human tumours is associated with invasiveness (Owens et al. 1995) and inhibition of FAK through dominant negative mutant can reduce aggressiveness (Aguirre Ghiso et al. 1999).

FAK negative fibroblasts cannot exhibit migration; however viral Src-protien restores the migration through reactivation of Src pathway. Src is associated with integrins and uPAR and acts by linking FAK to integrins, such as $\alpha_V\beta_5$ in VEGF mediated stimulation. However it is quite interesting to note that although motility of FAK naive fibroblasts is recovered, invasion and expression of gelatinases is not restored. The authors suggested that FAK activity is required for synchronisation of motility and invasion (Hsia

et al. 2003). In a recent study, MT1-MMP and MT3-MMP activity was linked to proteolytic cleavage of FAK in vascular smooth muscle cells (Shofuda et al. 2004).

Generation of new adhesion is necessary at the advancing edge but also needs a mechanism to release them on the tail end. Release mechanism on the tail end involves multiple mechanisms including mechanical stretch from cytoskeleton, changes in integrin pathways (Lauffenburger et al. 1996) and proteases along with their inhibitors (Czekay et al. 2003). Only a few other proteins are involved in cell detachment at the tail end. These include tenascin-C, thrombospondin-1 and 2 and SPARC (secreted protein, acidic and rich in cysteine) (Murphy-Ullrich, 2001). Focusing on these concepts it is easy to understand that integrins and their ligand interactions are key regulators of cell migration. Relatively small changes in levels of integrins and their affinity to ligands can substantially change the speed of cell migration. In addition, inhibition of cell movement can be achieved not only by integrin blocking antibodies but also with antibodies that activate them and proteases which change matrix components (Schenk et al. 2003).

Kryczka et al demonstrated that MMP-2 is up-regulated in resected colorectal tumours and degrades β1 integrins with release of fragments containing the β1 I-domain. The β1 cleavage pattern is similar to that produced by digestion of α5β1 and α2β1 with MMP-2. This study suggested that MMP-2 amplifies the motility of colon cancer cells, not only by digesting the extracellular matrix components in the vicinity of cancer cells but also by inactivating their major β1 integrin receptors (Kryczka et al. 2012).

MMPs generate pro-migratory signals by cleavage of growth factors. MMP-9 can activate VEGF and TGF-β, promoting tumour growth and angiogenesis (Bergers et al.

2000; Yu et al. 2000). Gelatinases are also linked to cell spreading during cell migration. Activated Rho-A is necessary but not sufficient for cell invasion (Stam et al. 1998). MMP-9 co-localizes with activated Rho-A and constitutively active Rho-A increases the secretion of MMP-9 (Abécassis et al. 2003). Other evidence for MMPs involvement in cell spreading comes from studies involving inhibitors of MMPs. MMP-2 inhibition by over expression of TIMP-2 causes extensive cell spreading (Ray and Stetler-Stevenson, 1995). Inhibitors of MMPs augment cell adhesion by reducing cadherin cleavage and stabilize cell to cell contact by inhibiting ECM degradation (Ho et al. 2001).

2.8.6: MMPs in tumour progression:

It is important to emphasize that several MMPs were first cloned and have been repeatedly re-cloned as cancer-associated genes (Sternlicht and Werb, 1999). Increased expression of MMPs has been demonstrated in cancers of breast, colon, skin, lung, ovary and prostate. This phenomenon is often accompanied by increased aggressiveness of tumours and decreased survival among patients (Egeblad and Werb, 2002). Expression of MMPs may be variable at different stages of cancer, especially during different steps of metastasis. In melanoma, expression of MMP-9 is increased during the early stage of disease and the opposite is true in the later stages of the disease (van den Oord et al. 1997). Studies involving breast and colonic cancer have demonstrated that MMP-9 expression was associated with equivocal effect on survival and development of metastatic disease (Zeng et al. 1996; Takeha et al. 1997; Pacheco et al. 1998; Scorilas et al. 2001).

2.8.7: MMP in angiogenesis:

Every tumour needs the development of new blood vessels in order to meet the demands of oxygen and nutrients supply. MMPs, especially gelatinases, are involved in this critical step. This phenomenon has been well established *in vitro* (Schnaper et al. 1993; Seftor et al. 2001) and *in vivo* studies (Itoh et al. 1998; Vu et al. 1998). The exact underlying mechanism involved is still obscure and MMPs are thought to use multiple pathways. Bergers et al. demonstrated in a model of pancreatic islet carcinogenesis that MMP-2 and MMP-9 were up-regulated in angiogenic tumors (Bergers et al. 2000). In this study the up-regulation of MMPs resulted in release of VEGF which is a potent growth factor for angiogenesis. It was also observed that the phenomenon of angiogenesis was mainly dependent upon intact MMP-9 activity rather than MMP-2, in MMP knockout mice models (Bergers et al. 2000).

MMP-9 activity was required to expose a cryptic pro-migratory control site in collagen during retinal neo-vascularization (Hangai et al. 2002). A monoclonal antibody recognizes an epitope in denaturised collagen type IV (HUIV26). Exposure of this epitope is required for angiogenesis in vivo and is associated with $\alpha_V\beta_3$ binding to collagen type IV. Exposure of this epitope is crucial in angiogenesis and it involves $\alpha_V\beta_3$ binding to collagen type IV (Hangai et al. 2002). It is interesting to note that the appearance of HUIV26 epitope in melanoma tumour vasculature, takes place with the appearance of MMP-2 (Xu et al. 2001).

2.8.8: MMPs in cancer mediated inflammation:

Chronic inflammation associated with some tumours is thought to be associated with progression through release of MMPs by inflammatory cells (Coussens et al. 1999 and 2000). These cells include neutrophils, dendritic cells, macrophages, eosinophils and lymphocytes which can significantly alter the tumour micro-environment through provision of additional agents like cytokines, interferons and MMPs. Chemokines are important mediators of leucocyte recruitment in to tumors. They also modify endothelial and tumour cell chemotaxis and affect the migratory and invasive behaviour of tumour cells. These chemokines need to be proteolytically processed in order to get activated by different proteases, including MMPs. A prime example of this activity comes from platelet factor (PF)-4, a monokine induced by interferon IFN-γ, interferon inducible protein-10 (IP-10/CXCL-10) and stromal-cell derived factor-1 (SDF-1) representing angiogenic chemokines, which can be cleaved and activated by MMPs like gelatinases (Moore et al. 1998). MMP-9 has been implicated in the down regulation of the immune response to cancer by cleaving interleukin-2α receptor, activation of TGF-β and by shedding of ICAM-1 (Yu et al. 2000; Fiore et al. 2002; McQuibban et al. 2002). MMP-2 is able to influence the process of inflammation through proteolytically processing the chemoattractants for monocytes and suppression of inflammation *in vivo* (McQuibban et al. 2002). Due to the active role of inflammation in the dynamics of neoplastic process, different anti-inflammatory agents like cyclo-oxygenase inhibitors are added to anticancer treatment (Williams et al. 1999; Liu et al. 2002).

2.9: Aims of the study:

Cancer metastasis is a complex process and cellular motility plays an important and vital role. Growth factors provide important signals in the development of metastasis. Binding of growth factors leads to morphological changes in the actin cytoskeleton through a variety of pathways. There is some evidence in the literature that WAVEs play an important role in the regulation of actin cytoskeleton through regulation of the ARP 2/3 complex. The basic aim of this research project was to examine the role of WAVEs in prostate cancer, in response to growth factors and to dissect the underlying mechanism which can be potentially used as a common step to stop the process of metastasis.

The specific aims of the study were,

1: To study and determine the expression levels of different members of the WAVEs family of proteins in various epithelial cell lines.

2: To create prostate cancer cell lines through a process of cellular cloning, which are deficient in specific gene, for subsequent use in functional studies.

3: To determine the role of WAVE-3 in growth factor induced cellular changes including growth, cell matrix interaction, invasion and cellular motility.

4: To determine the role and interaction of different pathways which could potentially be responsible for morphological changes in prostate cancer cells.

Chapter 3
Materials and Methods

3.1: General materials:

3.1.1: Cell lines

Seven prostate cancer or prostatic epithelial cell lines were used in the study. PC-3 cells were acquired from the ECACC (European Collection of Animal Cell Culture, Salisbury, UK). PC3 cell line has high metastatic potential and was established in 1979 from bone metastasis of prostate cancer, in a 62-year-old Caucasian male (Kaighn et al. 1979). DU-145, LNCaP-FGC, CA-HPV10 and PZ-HPV-7 were supplied by the ATCC (American Type Culture Collection). DU-145 cell line was derived from brain metastases and has moderate metastatic potential (Stone et al. 1978). LNCaP cells are androgen-sensitive human prostate adenocarcinoma cells, derived from the left supraclavicular lymph node metastasis, from a 50-year-old Caucasian male (Horoszewicz et al. 1980). CA-HPV10 cells were derived from adenocarcinoma of prostate, followed by transfection with viral DNA from HPV (Weijerman et al. 1994). PZ-HPV-7 cell line was derived from peripheral zone epithelium of normal prostate and immortalized by transfection with viral DNA from HPV (Weijerman et al. 1994). PNT-1A and PNT-2C2 were generous gifts provided by Professor Norman Maitland (University of York, England, UK). PNT cell lines were derived from normal prostate epithelium, immortalized by transfection with a plasmid containing SV40 genome. All cells were routinely maintained in DMEM-F12 medium supplemented with 10% foetal calf serum and antibiotics.

3.1.2: Primers

Two different categories of primers were designed for this study. The first set was able to detect the mRNA level of a particular gene through conventional RT-PCR (Table: 3.1 & 3.2). The second set of primers was designed according to the secondary structure of a gene transcript, and was used to synthesize the hammerhead ribozymes for the gene silence study (Table: 3.3).

Molecule	Primer		PCR product	Annealing temperatures
WAVE-1	Forward	5″-CCTCCTCCACCACCTCTTC	526bp	55°C
	Reverse	5″-GCACACTCCTGGCATCAC		
WAVE-2	Forward	5'-CAAGCCATCCACCACCAG	595BP	55°C
	Reverse	5'-ACAGCAATGCGACGAGAC		
WAVE3	Forward	5″- TACTCTTGCCGCTATCATACG	532bp	58°C
	Reverse	5″- TGCCATCATATTCCACTCCTG		
β-Actin	Forward	5'-ATGATATCGCCGCGCTCG	580bp	55^{o}C
	Reverse	5'-CGCTCGGTGAGGATCTTCA		

Table: 3.1: Primers for RT-PCR used for detection of WAVEs.

Molecule	Primer		PCR product (bps)	Annealing temperatures
MMP-1	Forward	5″- GGATGCTCATTTTGATGAAG	110	55°C
	Reverse	5″- TAGAATGGGAGAGTCCAAGA		
MMP-2	Forward	5″- TGCAGCTCTCATATTTGTTG	472	55°C
	Reverse	5″- TTTGATGACGATGAGCTATG		
MMP-7	Forward	5″- GCTATGCGACTCACCGTGCTGTG	530	55°C
	Reverse	5″- AGCGTGTTTCCTGGCCCATCAAATG		
MMP-9	Forward	5″- AACTACGACCGGGACAAG	357	55°C
	Reverse	5″- ATTCACGTCGTCCTTATGC		
MMP-11	Forward	5″- GTGCCCTCTGAGATCGAC	88	55°C
	Reverse	5″- CAGGGTCAAACTTCCAGTAG		
GAPDH	Forward	5'- GGCTGCTTTTAACTCTGGTA	475bp	55^{o}C
	Reverse	5'- GACTGTGGTCATGAGTCCTT		

Table: 3.2: Primers for RT-PCR used for detection of MMPs.

	Name of primer	Sequence of primers
Ribozyme	T7F	5´-TAATACGACTCACTATAGGG
	RBBMR	5'-TTCGTCCTCACGGACTCATCAG
	RBTPF	5'-CTGATGAGTCCGTGAGGACGAA
WAVE-3 ribozyme-1	WAVE-3RIB1F	5˝-CTGCAGTTGTAAATATCAGCAACAGCTGATGAGTCCGTGAGGA
	WAVE-3RIB1R	5˝-ACTAGTTTCAAAGAACAGCATTCCTAATTTCGTCCTCACGGACT
WAVE-3 ribozyme-2	WAVE-3RIB2F	5'-CTGCAGCTTCCTCTGTGGTGACTGATGAGTCCGTGAGGA
	WAVE-3RIB2R	5'-ACTAGTAGCTGTGAAAGTGTTTTCGTCCTCACGGACT

Table: 3.3: Primers used to synthesize hammerhead ribozymes for the gene silencing study.

3.1.3: Antibodies

3.1.3.1: Primary antibodies

Full details about the primary antibodies used in this study are in Table 3.4.

Antitibody name	Host species	Predicted product size (kDa)	Antibody/dilution used	Supplier and catalogue number
Anti-WAVE- 3	Goat	55kDa	1:500	Santa Cruz Biotechnology Inc (sc- 10395)
Anti-rabbit (Whole molecule) IgG peroxidise	Goat	Dependent on primary	1:1000	Sigma (A-9169)
Anti-β-actin (C-II)	Goat	42 kDa	1:500	Santa Cruz Biotechnology Inc. (sc-1615)
Anti-paxillin	Mouse	68 kDa	1:500	BD Transduction Laboratories (610051)
Anti-phophorylated paxillin	Rabbit	68 kDa	1:250	Sigma (P-6368)
Anti-FAK	Mouse	125 kDa	1:500	BD Transduction Laboratories (610088)
Anti-Radexin	Goat	82 kDa	1:250	Santa Cruz Biotechnology Inc.SC-6408
Anti-Moesin	Mouse	77 kDa	1:250	Santa Cruz Biotechnology Inc.SC-13122
Anti-Ezrin	Goat	87 kDa	1:250	Santa Cruz Biotechnology Inc.SC-6409
Anti-GAPDH	Mouse	37 kDa	1:500	Santa Cruz Biotechnology Inc.SC-47724
Anti-MMP-2	Mouse	63 kDa	1:250	Santa Cruz Biotechnology Inc.SC-53630

Table: 3.4: Antibodies used for detection of different proteins in western blotting, immunoflourescence and immunocytochemistery experiments.

3.1.3.2: Secondary antibodies

Peroxidase (horseradish peroxidase, HRP) conjugated anti-goat IgG, anti-rabbit IgG and anti-mouse IgG antibodies were obtained from Sigma (Poole, Dorset, UK). TRITC conjugated secondary antibody to rabbit IgG was obtained from Sigma (Poole, Dorset, UK). FITC conjugated secondary antibodies to mouse and goat IgG were obtained from Santa-Cruz Biotechnology (Santa-Cruz, California, USA).

3.1.4: General reagents and solutions

3.1.4.1: Reagents and chemicals

Protein-A/G agarose beads used during immunoprecipitation were obtained from Santa-Cruz Biotechnology (Santa-Cruz, California, USA). The Super Sensitive^{TM} Wash Buffer (BioGenex, USA) was used in the immunofluorescent staining (IF). SDS-6H (Sigma-Aldrich, Inc., Poole, Dorset, England, UK), a protein molecular weight marker mixture was used to determine the protein size. The Supersignal^{TM} West Dura system (Pierce Biotechnology, Inc., Rockford, IL, USA), a highly sensitive chemiluminescence substrate was used to detect the horseradish peroxidase (HRP) in western blot. All other chemicals or reagents were purchased from Sigma, unless otherwise stated.

3.1.4.2: General solutions

The following solutions are generally used throughout the study.

Tris-boric acid-EDTA (TBE)

For a 5×TBE buffer, 540g Tris-Cl, 275g Boric acid and 46.5g EDTA was dissolved in 9.5 litres of distilled water, pH adjusted to about 8.3 using NaOH, and a final volume of 10 litres was made with distilled water.

Tris buffered saline (TBS)

A 10× stock solution was made by dissolving 24.228 Tris and 80.06g NaCl in 1 litre distilled H_2O and adjusting the pH to 7.4 with concentrated HC1. This solution contained 200mM Tris and 1.37M NaCl.

Balanced salt solution (BSS)

A 5 litre stock solution of 1 x BSS consists of 137mM NaCl, 2.6mM KCl, 1.7mM Na_2HPO_4 and 8.0mM KH_2PO_4 and was made by dissolving 40g NaCl, lg KCl, 5.72g Na_2HPO_4 and 1 g KH_2PO_4 in dH_2O and adjusting the pH to 7.4 with 1M NaOH.

0.05M EDTA in BSS

A 5 litre stock solution at 1x concentration contained 1g KCl, 5.72 Na_2HPO_4, 1g KH_2PO_4, 40g NaCl and 1.4g EDTA, and dissolved in 5 litres distilled H_2O and adjusted the pH to 7.4 before autoclaving.

Loading buffer (for DNA electrophoresis)

A stock solution was made by dissolving 25mg bromophenol blue and 4g sucrose in distilled water to a final volume of 10ml. Solution was stored at 4°C to avoid mould growing in the sucrose until use.

Ethidium bromide solution

A stock solution of ethidium bromide (10mg/ml) was made by dissolving 200mg ethidium bromide in 20ml distilled water, and protected from light by covering the tube in aluminium foil.

Transfer buffer (for Western blot)

Glycine in quantity of 72g and15.15g of Tris dissolved in distilled water along with 1 litre methanol, final volume of 5 litres was made with distilled water.

0.5% amino black staining solution

2.5g amino black, 50ml acetic acid, 125ml ethanol were added into 325ml distilled water to make a final volume of 500ml.

Amino black destaining solution

100ml acetic acid and 250ml ethanol were added into 650ml of distilled water for a 1 litre amino black destaining solution.

Running buffer (for SDS-PAGE)

A 10× stock solution was made by dissolving 303g Tris, 1.44kg glycine and 100g SDS in 10 litres distilled water.

3.2: Cell culture and storage

3.2.1: Preparation of growth medium and maintenance of cells

- The culture medium used in the study was Dulbecco's Modified Eagle's Medium (DMEM / Ham's F-12 with L-Glutamine; PAA, E15-813) (pH 7.3) containing; 2mM L-glutamine, 15mM HEPES and 4.5mM $NaHCO_3$.
- DMEM was then supplemented with 10% heat inactivated foetal calf serum (PAA Laboratories, Austria); 50 ml FCS in 500 ml DMEM/HAM F12.
- Antibiotics were added to the medium at a final concentration of 100 units/ml (60µg/ml) for benzylpenicillin (Britannia, Pharmaceuticals Ltd, UK) and 100 µg/ml for streptomycin (Streptomycin Sulfate salt, Sigma-Aldrich Co.). Benzylpenicillin (Britannia, Pharmaceutical Ltd, UK) powder 600mg ($1x10^6$units) in each bottle was dissolved in 5ml sterilized water, and kept at 4 ^oC in a fridge until ready for use. The concentration of streptomycin stock solution was 250mg/ml. 200µl of streptomycin was dispensed into each 500 ml of culture medium, to give a final concentration of 100µg/ml.

- The cell lines were cultured in monolayer either 25cm^2 or 80cm^2 culture flasks (Cell Star, Germany) at cell densities of 1x10^{5}cells/ml.
- Culture flasks were loosely capped and placed in an incubator at 37^{o}C with a 98% humidification (water tray in the incubator) and 5% CO_2.
- The flasks were then left until sub-confluent (2-3 days) for experimental work or fully confluent (7 days) for subculture.

3.2.2: Trypsinisation and counting of cells

- All handlings of cells were performed under sterile conditions using class II hoods and autoclaved instruments to keep sterile conditions.
- Following removal of culture medium, the flasks were rinsed once with 5ml of sterile HBSS (Hanks Balanced Salt Solution) (137mM NaCl; 8mM Na_2HPO_4; 3mM KCl; 1.5mM KH_2PO_4) buffer to remove all possible traces of serum, which would inhibit the enzymatic action of trypsin.
- 1-2ml of trypsin EDTA, which has trypsin 0.01% (w/v) and EDTA 0.05% (w/v) in BSS buffer, was added to the flasks, which were incubated for 5 minutes at 37^{o}C to allow cell detachment.
- Once the cells had detached from the surface of the flask, the effect of trypsin was neutralised by the addition of 5ml of DMEM and placed in a universal container.

- The cells were centrifuged at 1,500 rpm for 5 minutes.
- The excess medium was aspirated and the pellet re-suspended in 5mls of DMEM.
- The cells were then either re-cultured in flasks or counted for immediate experimental work or stored by freezing in liquid nitrogen (see below).
- Cell counts were performed using an improved Neubauer haemocytometer counting chamber with an inverted microscope (Reichert, Austria) at 10×10 magnification.

3.2.3: Storage of cell lines in liquid nitrogen

- The cell lines were stored in liquid nitrogen by resuspending at a cell density of $1x10^6$ cells/ml in DMEM, containing 10% (v/v) dimethylsulphoxide (DMSO; Fisons, UK).
- 1 ml aliquots of cell suspension were transferred into cryopreserve tubes;
- Transferred to -80^{o}C for 24 hours before storage in liquid nitrogen (-196^{o}C) until required.

3.2.4: Resuscitation of cells

- After removal from liquid nitrogen, the cells were allowed to thaw rapidly to 37^{o}C in 1-2 minutes;

- The cell suspension was transferred to a universal container, with 2ml of pre-warmed DMEM. The cells were then incubated at 37^{o}C for 10 minutes.
- The cells were then centrifuged at 1600 g for 5 minutes and the excess medium removed.
- The cell pellet was re-suspended in DMEM and washed twice to remove any possible trace of DMSO.
- After the final wash, the cell pellet was re-suspended in 5ml of DMEM and the cell suspension transferred to a 25cm^2 tissue culture flasks. The cells were incubated at 37°C, 98% humidification and 5% CO_2.

3.3: Methods for detecting mRNA

3.3.1: Total RNA isolation

Ribonucleic acid (RNA) is present within the nucleus, cytoplasm and mitochondria of all living eukaryotic cells. The total cytoplasmic RNA is representative of three main sub types which are classified as; ribosomal (rRNA), transfer (tRNA) and messenger (mRNA) RNA. Although mRNA accounts for only 1-2% of total cellular RNA, it is of particular importance as it carries the genetic information for protein formation. The presence of specific mRNA sequences indicates which protein is being produced by a cell at any given time.

RNA is susceptible to degradation by RNases and therefore, special care must be taken to minimize this during its isolation. All methods involving RNA isolation rely on the use of strong denaturants to inhibit the action of endogenous RNases for preserving intact RNA during the isolation. Guanidine, thiocyanate and chloride used for the RNA isolation are amongst the most effective protein denaturants and inhibitors of ribonucleases. The guanidine thiocyanate method described by Chomczynski and Sacchi in 1987 (Chomczynski and Sacchi, 1987), has evolved as a rapid procedure which combines acid guanidium thiocyanate, phenol and chloroform in a single step RNA extraction. Using this method, the extraction of RNA is set under acidic conditions, so that the DNA is selectively partitioned into the organic phase whilst the RNA remains in the aqueous phase. The quality and concentration of the RNA isolated can then be detected using a spectrophotometer at a wavelength of A260nm/A280nm.

3.3.1.1: Homogenisation

After aspiration of culture medium, cells in the mono-layer were lysed directly in the culture flask by adding the RNA reagent (1ml/3.5cm petri dish, or 1ml/5-10 x 10^6 cells). The resultant cell lysate was transferred immediately to eppendorf or polypropylene tubes. Washing the cells before addition of the RNA reagent was avoided as this might increase the possibility of mRNA degradation.

3.3.1.2: RNA extraction

Following homogenisation,

- The homogenate was stored for 5 minutes at 4°C to permit the complete dissociation of nucleoprotein complexes.
- 0.2ml of chloroform per 1ml of RNA reagent was added, shaken vigorously for 15 seconds and placed on ice at 4°C for 5 minutes.
- The homogenate was centrifuged at 12,000g (4°C) for 15 minutes.

Centrifugation resulted in separation of homogenate in two phases: the lower phase, organic phase and the upper aqueous phase. DNA and proteins are present in the organic phase and in the interface while RNA is present in the aqueous phase. The volume of the aqueous phase thought to be about 40–50% of the total volume of the homogenate plus chloroform.

3.3.1.3: RNA precipitation

- The aqueous phase was carefully transferred to a fresh tube while taking care not to disturb the interface.
- An equal volume of isopropanol was added and samples were stored for 10 minutes at 4°C.
- The samples were centrifuged at 12,000g (4°C) for 10 minutes.
- RNA precipitation formed a white pellet at the bottom of the tube after the centrifugation.

3.3.1.4: RNA wash

- The RNA pellet washed twice with 75% ethanol (prepared using DEPC treated distilled water) by vortexing and subsequent centrifugation for 5 minutes at 7,500g (4°C).
- At the end of the procedure, the pellet was dried briefly at 50°C for 5–10 minutes in a hybridiser drying oven.
- Care was observed not to let the RNA pellet dry completely, as it can greatly decrease its solubility. The RNA pellet was dissolved in 50–100µl of DEPC treated water by vortexing for 1 minute.

3.3.1.5: Qualification and quantification of RNA

The concentration and purity of RNA was determined by measuring its absorbance at wavelength A260nm/A280nm (WPA UV 1101, Biotech Photometer). The ratio of A260nm/A280nm can give an estimate of the purity of the RNA. Pure RNA solutions have an optical density ratio of 2.0. Optical density values less than 1.5 indicates ethanol or protein contamination. The RNA samples were either stored at -80^{o}C until used later or used for reverse transcription (RT).

3.3.2: Reverse transcription (RT)

RT-PCR is a simple, versatile and sensitive technique, which has greatly enhanced the study of genes and how they are controlled. It provides an alternative and more sensitive approach for the analysis of mRNA, compared with other procedures such as;

Southern blots for DNA analysis and Northern blots for RNA analysis. This technique has the advantage over more traditional methods because it requires a smaller amount of RNA, and yet is more sensitive and rapid. In this study, complimentary DNA (cDNA) was synthesized by using the DuraScript^{TM} RT-PCR KIT (Sigma-Aldrich, Inc.). According to the manufacturer's instructions, a 20-µL-reaction mixture was added in a polypropylene tube (Eppendorf):

0.25µg of total RNA template (volume depends on concentration)

PCR H_2O (volume=8µL – volume of the RNA template)

1µL of deoxynucleotide mix (500 µM of each dNTP)

1µL of anchored oligo (dT)

The samples were heated at 70°C for 10 minutes to denature RNA secondary structure which allowed for more efficient reverse transcription, and were then placed on ice. The following components were added to the samples:

6 µL PCR H_2O

2µL 10×buffer for DuraScript RT

1µL RNase inhibitor

1 µL DuraScript reverse transcriptase

The resultant total volume in each eppendorf tube was 20 µL. The samples were incubated at 50^{o}C for 50 minutes. The cDNA samples were then diluted to 1:4 by adding 60 µL of PCR H_2O. The samples were stored at -20^{o}C until required.

3.3.3: Polymerase chain reaction (PCR)

The polymerase chain reaction is a very powerful technique for enzymatically amplifying a nucleic acid target sequence. It was devised by Karey Mullis in 1983, for which he was awarded the Nobel prise in 1994. A particular gene was amplified by using a REDTaq^{TM} ReadyMix PCR reaction mix (Sigma-Aldrich, Inc.). A 12-µl-reaction mixture was prepared in a thin walled PCR tube:

1µL of cDNA template

1µL of forward primer (at a working concentration of 1 µM)

1µL of reverse primer (at a working concentration of 1 µM)

6µL of 2×REDTaq^{TM} ReadyMix

3µL of PCR H_2O

Cycling conditions for the 12-µL-reaction mixture were 94˚C for 5min, followed by 30-36 cycles of 94˚C for 30s, 55˚C for 30s, and 72˚C for 40s. This was followed by a final extension of 10 min at 72˚C. PCR products were visualized on a 0.8% or 2% agarose gel through staining with ethidium bromide after electrophoresis.

3.3.4: Agarose gel DNA electrophoresis

Agarose gel electrophoresis is the easiest and commonest way of separating and analyzing DNA. The purpose of the gel might be to look at the expression of DNA, to quantify it or to isolate a particular band. The DNA is visualised in the gel by addition of ethidium bromide. This binds strongly to DNA by intercalating between the bases and is

fluorescent by means of absorbing invisible UV light and transmits the energy as visible orange light.

A 0.8% gel was used for of large DNA fragments (1–10kb), while a 2% gel showed good resolution for small fragments (<1kb). In the present study, 20mls of agarose gel solution at the appropriate concentration was poured into an universal container (Sterilin, UK) and cooled to about 55˚C before casting the gel in the mould. A well forming comb was then inserted into the gel mould and the gel was allowed to set at room temperature for about 30-40 minutes.

Once the gel had set, TBE buffer was carefully poured into the electrophoresis tank until it reached a level of about 5mm from the surface of the gel. The PCR products were loaded into the wells (6µL per well) by placing the gel loading tip through the buffer and locating it just above the bottom of the well. The sample was slowly and delicately delivered into the well. This procedure was continued until all the samples had been loaded into the gel. A 1Kb DNA ladder (Cat No. 15615-016, Invitrogen Inc., USA) was prepared according to the manufacturer's instructions, and delivered into the well (5µl per well) in the same manner as for the PCR products.

A power pack (Gibco BRL, Life Technologies Inc.) was connected to the electrophoresis apparatus and the gel was run at a constant voltage of 100 Volts. Electrophoresis was continued for 30-50 minutes or until the samples had migrated about two-thirds of the way down the agarose gel (depending on the size of the PCR products). The PCR products were stained using ethidium bromide (10mg/ml) for 5 minutes with continuous agitation to ensure even staining of the agarose gel. This was followed by destaining in

distilled water for about 1 hour, to reduce the background staining. PCR products were then visualised on the agarose gel using an UV Transilluminator (UVP, Inc, Cambridge, England, UK). Gel images were printed using a Mitsubishi thermoprinter (Mitsubishi UK, London) and saved as a TIFF image file using a default image saving facility.

3.3.5: Quantitative real time PCR (Q-RT-PCR)

Real time quantitative PCR is a sensitive technique to determine quantitatively prevalent levels of messenger RNA of the gene of interest. Q-RT-PCR is capable of detecting very small quantities of cDNA within a sample and carries minimal chances of error if standards are followed. In our laboratory we used real-time quantitative PCR, based on the Amplifluor™ technology, modified as previously reported (Jiang et al. 2005). The cDNA used in this technique was generated by this same technique as described before. This cDNA was used to make up a master reaction mixture containing the following amounts of each component per reaction

Forward Z primer – 0.3 µL (1 pmol/µL)

Reverse primer - 0.3 µL (10 pmol/µL)

Q-PCR master mix (Hot-start Q-master mix ABgene, Surrey, UK) - 5 µL

Probe Ampiflour (FAM-tagged probe) - 0.3 µL (10 pmol/µL)

PCR H2O – 2.1 µL

cDNA - 2 µL

Pairs of PCR primers were designed using the Beacon Designer™ software (version 2, Palo Alto, CA, USA), but added to one of the primers was an additional sequence, known as the Z sequence (5'actgaacctgaccgtaca'3) which was complementary to the universal Z probe (Intergen Inc., Oxford, UK). In each reaction one of the primer pair contained a Z sequence at 1/10 concentration of the other primer and probe. The Ampiflour system was used to detect and quantify transcript copying number. The ampiflour probe consists of a region specific to their Z sequence together with a hairpin structure labelled with a fluorescent tag (FAM). While in the hairpin structure this fluorescent tag is effectively quenched and produces no signal. However the specificity of the 3' region of the ampiflour probe to the Z sequence causes the incorporation of this uniprimer. Subsequent DNA polymerisation, following the incorporation, results in the destruction of the hairpin structure and effective signalling of the fluorescent tag within the structure. The degree of fluorescence within each sample is compared to a range of standards of known transcript copying number, allowing the calculation of transcript copying number within each sample. Detection of β-actin copy number within each sample was subsequently used to allow further standardisation and normalisation of the samples.

Sample cDNA was amplified and quantified over a large number of shorter cycles using i-cycler IQ thermal cycler and detection software (BioRad laboratories, Hammelhempstead, UK) and experimental conditions as outlined below.

Step 1: Initial denaturing period - 94ºC for 5 minutes

Step 2: Denaturing step - 94ºC for 10 seconds

Step: 3: Annealing step - 55ºC for 15 seconds

Step 4: extensions step - 72ºC for 20 seconds

Step 2 to 4 was repeated over 60 cycles.

The camera used for detection of fluorescence in the system was set to detect fluorescent signal during the annealing stage. The experimental procedure was repeated twice and data are representative of expressional trends of different messenger RNAs. In this established method, approximately 20 cycles were required for the generation of Z-tagged products. Quality standards were maintained using specific Q-PCR primers verified using a positive control known to express molecule of interest and a negative control. PCR water replaced DNA in the negative control and it also helped to rule out contamination of the reaction.

3.4: Methods for detecting protein:

Two different methods were employed in present study to assess the expression of a certain gene at the protein level. These included western blot and immunofluorescent staining.

3.4.1: SDS-polyacrylamide gel electrophoresis (SDS-PAGE) and western blot

3.4.1.1: Preparation of cell lysates

- Cells were removed from the base of the culture flask using a disposable cell scraper. Cells were transferred using a pipette in to a clean universal container.
- Samples were centrifuged at 2,000 rpm for 5 minutes.
- The supernatant discarded and cell pellet resuspended in 200-300 µL of lysis buffer (20 µL per 500,000 cells) and the resultant lysates transfered into 1.5ml eppendorf tubes.
- Samples were incubated at 4˚C for 40 minutes with continuous rotation in order to extract protein from the cell lysate.
- Samples were centrifuged at 13,000 rpm for 15 minutes in order to remove cellular debris. The supernatant was transfered to a new tube and the pellets were discarded. The protein samples were quantified and utilised for SDS-PAGE, or were stored at -20˚C until used.

3.4.1.2: Determination of protein concentration of cell lysates

This method was based on a protocol supplied by BIO-RAD, from whom the protein assay kit was purchased.

- Preparation of working reagent. 20 µL of reagent S was added to each ml of reagent A which was required for the run.
- Bovine serum albumin stock with known concentration (Sigma; 100mg/ml) was diluted serially and prepared in the same cell lysis buffer to give a working concentration range between 0.50-0.79 mg/ml. A standard curve was prepared

each time the assay was performed. For best results, the standard was always prepared in the same buffer as the sample.

- 5 µL of standards and samples were added into a 96-well plate.
- 25 µL of reagent A (see note from step 1) and 200 µL of reagent B were added into each well.
- After 15 minutes, absorbance was read at 590 nm. The absorbance is usually stable for about 1 hour.
- A standard protein curve for the bovine serum albumin was constructed and the unknown protein concentrations of the cell lysate samples were determined.
- Protein concentrations were adjusted to a working range of 1-2 mg/ml by diluting in cell lysis buffer.
- Crude cell lysates were prepared for SDS-PAGE by diluting a portion of the quantified lysate sample with a 2x sample buffer (containing 2x mercaptoethanol).
- Crude cell lysate samples were denatured by boiling at 100˚C for 5 minutes. Cooled at room temperature for 5 minutes and centrifuged to collect droplets.
- The samples were subsequently loaded on a gel, or stored at -20˚C until required.

3.4.1.3: Preparation of immunoprecipitates

Immunoprecipitation is an invaluable technique used to analyse intracellular phosphorylation events occurring following extracellular stimulation. The process of immunoprecipitation involved cell lysis, followed by the addition of a specific antibody directed against the phosphorylated protein present within the cell lysate sample. The resultant antigen-antibody complexes were then collected by the addition of staphylococcal protein A, protein G or their mixture, which was covalently attached to agarose beads. These immune complexes were precipitated by centrifugation, separated by SDS-PAGE and analysed by immunoprobing. A brief description of the immunoprecipitation method used in this study is outlined in the following paragraph.

- Specific quantities of PY20/PY90 antibody were added to the cell lysate. The concentration or dilution of the antibody followed the corresponding instruction of the antibody used.
- Samples were incubated at 4˚C for 1 hour with constant agitation on a rotating wheel.
- 50µL of conjugated A/G protein agarose beads (Santa Cruz Biotechnology, supplied by Insight Biotechnologies Inc, Surrey, England, UK) were added into each sample, and then the samples rotated on the rotating wheel for 1 hour to allow the antibody-antigen complex to get attached to the beads.
- Samples were centrifuged at 7000 - 8000 rpm for 5 minutes, to remove unbound protein or excess antibodies from the supernatant fraction.
- Protein pellets were washed twice using 200-300µL of lysis buffer.

- The pellets were resuspend in 40-60µL of 2x sample buffer, and denatured by boiling at 100˚C for 5 minutes.
- The samples were stored at -20˚C until required for use.

3.4.1.4: Gel preparation

- Four glass plates (2 large rectangular and 2 small rectangular plates) were dried, cleaned and assembled in pairs of gel cassettes on a casting stand. Alignment was checked by a card to verify glass plates and spacers were aligned properly. Glass plates were held in place securely by tightening the thumb screws.
- The space between the glass plates was filled with some alcohol to test the seal for leaks.
- Polyacrylamide resolving gel was prepared after adding the specified amount of TEMED and 10% APS, with gentle stir to mix.
- Using another plastic pipette, immediately the resolving gel was applied carefully by running the solution down from one side between the glass plates until it reached a level about 1 cm below the top of the smaller plate.
- Using a new pipette, the top of the resolving gel was covered with 0.1% solution of SDS until a layer of about 2mm formed on top of the gel solution. This ensured the gel would set with a smooth surface.

- Gels were left to polymerize at room temperature for about 30 minutes. When the gel had set a sharp refractive change at the overlay/gel interface could be observed on polymerization. Furthermore, the unused resolving gel in the universal container was also used to confirm the setting of gel.
- SDS solution was removed and the gel surface rinsed with deionized or distilled water.
- The stacking gel was prepared as per instructions specified by manufacturer remembering not to add the TEMED and APS until ready to use.
- The stacking gel solution was added immediately to the gel cassette (on top of the resolving gel) in the same manner as the resolving gel, until its upper surface was flush with the smaller glass plate.
- A well forming Teflon comb was inserted carefully, (taking care not to trap bubbles between the glass plates) into the layer of stacking gel, until it reached within 1mm from the top of the spacers.
- The stacking gel was allowed to polymerize for 30minutes at room temperature.
- Once the stacking gel had set, the Teflon comb was removed without tearing the edges of the polyacrylamide wells. The wells were rinsed with distilled water and gel cassettes were placed in a gel electrophoresis rig with the small glass plate facing the silicone gasket.

- The gel rig was placed into the electrophoresis chamber and central reservoir, formed by the gel plates was filled with running buffer so that the top of the wells was completely covered.
- Subsequently the chamber was filled with sufficient 1x running buffer to immerse the thumb screws.

3.4.1.5: Loading the samples

- Equal volumes (10µL) of crude cell lysates or precipitated proteins (containing sample buffer) were inserted into the wells. This was accomplished using a 50µL syringe (Hamilton) with a flat-tipped needle, and carefully locating the tip of the needle just above the bottom of the wells and then slowly delivering the protein into the well.
- Control wells were loaded with 10µL of pre-stained molecular weight standard. Documentation regarding the sequence of the protein samples was completed. The lid of the tank over the apparatus was replaced and leads were connected.

3.4.1.6: Running the gel

- High voltage lead wires were connected according to manufacturer instructions. The gel was allowed to run on constant current 40mA at 125V (20mA per gel) until the ladder had reached within 1 cm of gel bottom. The usual running time was about 40-60 minutes.

3.4.1.7: Preparation of membrane

- A nitrocellulose membrane (Hybond C, Ammersham, Cardiff) was cut to the dimensions of the gel (7.5×7.5cm) and immersed in 1× transfer buffer for about 10-20 minutes to ensure proper binding of the protein to the membrane. Similarly, four sheets of filter paper of the same dimensions (7.5×7.5cm) were cut and soaked in 1× transfer buffer for 10-20 minutes.
- Upon completion of the electrophoresis, the gel was separated from the glass plates by disassembling the apparatus and it was transferred in to a container with transfer buffer.

3.4.1.8: Electroblotting

- The pre-soaked nitrocellulose membrane was placed on the two sheets of soaked filter papers previously placed on electrode. The gel was transferred on top of the nitrocellulose membrane taking care not to trap air bubbles between the gel and membrane and maintaining the orientation of loaded samples.
- Two more sheets of wet filter paper were placed on top of the gel creating a sandwich of paper-nitrocellulose-gel-paper (Figure 3.1).
- Any air bubbles were removed by rolling a glass rod across the surface to ensure good contact between the gel and nitrocellulose membrane.

- The surface of this sandwich was carefully smoothed out, using a transfer pipette as a rolling pin to remove the formation of air bubbles which may interfere with protein transfer.
- Finally the cover, containing the cathode plate of the blotter was positioned on top of the transfer “sandwich” and high voltage leads connected to the power supply. A constant current at 5 Volts, 500 mA and 8 Watts for 30-40 minutes, was applied.
- After transfer was complete, the cathode plate of blotter was removed after turning off the power supply. Complete transfer was assured before removal of membrane from sandwich.

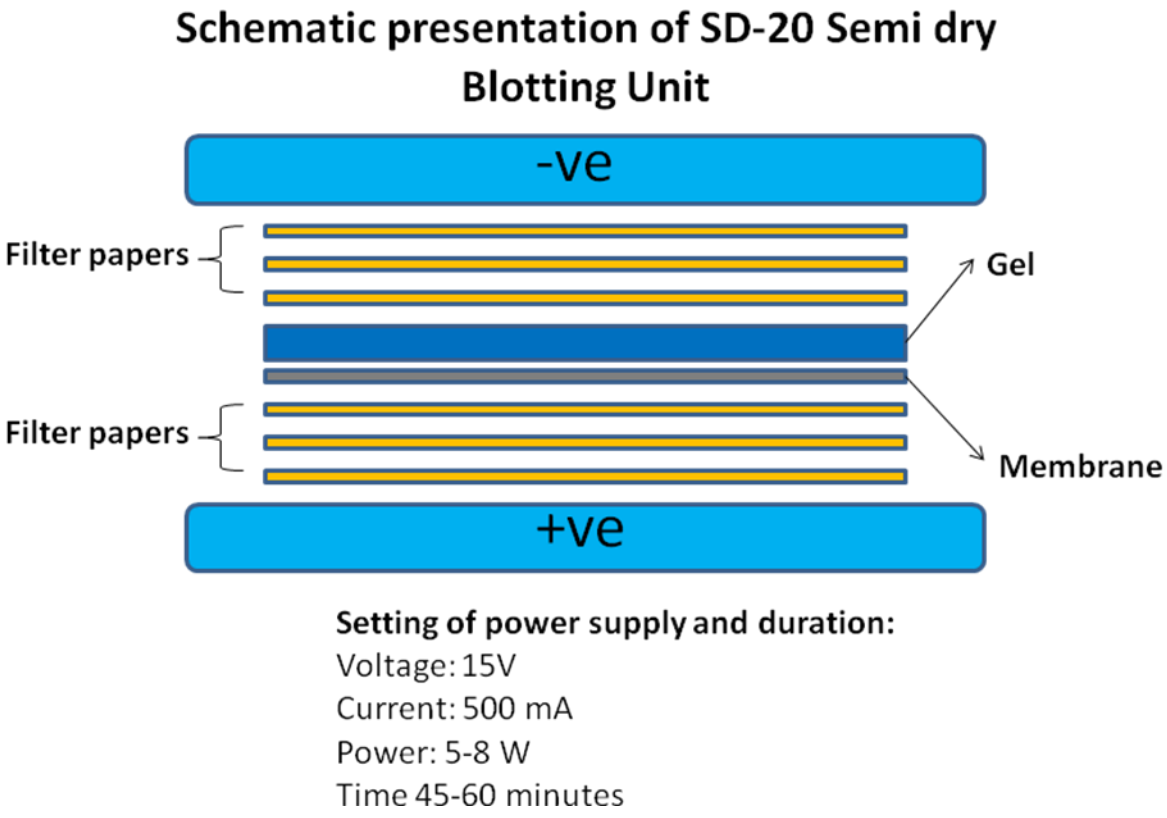

Figure 3.1 Diagram of assembling the semi dry blotting unit.

3.4.1.9: Specific protein detection – Immunoprobing procedure

Specific solutions for membrane blocking and washing were prepared, including

Solution A

10% milk powder (5g)

0.1% Tween 20 (50ul)

Dissolved above in 50ml TBS

Solution B

3% milk powder (3g)

0.1% Tween 20 (100ul)

Dissolved above in 100ml TBS

Solution C

0.2% Tween 20 (60ul) in 30ml TBS

- The blotted membrane was incubated in this blocking solution (solution A) with agitation for 40-60 minutes at room temperature, in order to block non-specific protein binding of the antibody on membrane.

- Followed by incubation of the membrane with 10ml of solution B for 15 mins.
- Diluted primary antibody (1:200 diluted in the solution B) was added and the membrane was left on a roller for one hour at room temperature.
- Membranes were washed for 30 minutes with agitation, changing the wash medium every 10 minutes with 10ml of solution B.
- Then the membranes were treated with 5 ml of diluted Horse Reddish Peroxidase (HRP) conjugated secondary antibody (typically 1:1,000 in solution B) with agitation for one hour at room temperature.
- The membrane was washed again with 10ml of solution B twice, each for 15 mins.
- Finally membranes were washed twice using 10ml per wash of the solution C, and than washed twice for 15 minutes each in TBS to remove residual detergent and transferred to weighing boats containing TBS solution using forceps until ready for chemiluminescent detection.

3.4.1.10: Chemiluminescent detection of protein

- The Supersignal^{TM} West Dura system (Pierce Biotechnology, Inc., Rockford, IL, USA), which has a highly sensitive chemiluminescence substrate, was used to detect the horseradish peroxidase (HRP) in western blot. The two substrate components were mixed at a 1:1 ratio with a final volume of 0.125ml/cm^2 (for a mini gel – 4ml of each reagent).

- Excess TBS buffer was removed from the membrane by draining the membrane over a piece of folded tissue paper and briefly touching the edge of the membrane.
- The membrane with protein side down was immersed in a clean tray containing the chemiluminescence working solution and agitated for 5 minutes.
- The membrane was wrapped in the saran wrap and placed in a plastic tray with the right-side facing up. The chemiluminescence signal was captured and visualised by using a UVITech imager (UVITech, Inc., Cambridge, England, UK). The protein bands were then quantified by using UVIband software (UVITEC, Cambridge, UK).

3.4.1.11: Amido black staining protocol

- After protein band visualization the membrane was immersed in Amido black stain for approximately 15-30 seconds.
- The membrane was destained in a solution containing 10% acetic acid /10% isopropanol until bands were clearly observed.
- The Amido black stain provided a permanent record of the membrane which can then be compared to corresponding images from the chemiluminescence assay, to aid in the orientation of the membrane.

3.5: Zymography:

Numerous methods have been developed to measure the expression and activity levels of proteolytic enzymes in different tissues and biological fluids (Cheng et al. 2008). Zymography is a technique now routinely used for the detection of MMPs in complex biological samples (Snoek-van Beurden et al. 2005). It was first pioneered by Granelli-Piperno and Reich (1978) and subsequently described by Heussen and Dowdle (1980) as a method for detecting plasminogen activators in gelatin substrate slab gels.

Zymographic analysis involves the electrophoretic separation of proteins under denaturing but non-reducing conditions through an SDS-polyacrylamide gel containing a co-polymerised protease substrate such as gelatin. Upon electrophoresis, resolved proteins are renatured in non-ionic detergent which removes the SDS, and susbsequently incubated in a buffer system which supplies the chloride and zinc ions, the enzymes require to be active. As previously known, zymogen forms of MMPs are activated through this process of gentle denaturation and renaturation; and they can therefore be detected in zymograms along with the active forms based on their different molecular weights (Kleiner et al. 1994). Following Coomassie Blue staining, MMPs are visualised as clear zones in gelatin containing gel, which represent proteolytic activity resulting in degradation of the gelatin substrate. Zymography has been described as an extremely sensitive technique. Leber and Balkwill (1997) reported the detection of less than 10 pg of MMP-2 on gelatine zymograms which can be compared favourably with techniques like Enzyme-Linked immunosorbent Assays (ELISA) (Kleiner and Stetler-Stevenson, 1994). Moreover, zymography has been used extensively in the qualitative evaluation of proteases

present in tumours and cell culture media (Kleiner and Stetler-Stevenson, 1994). In this study, gelatin zymography was employed which is routinely used for the detection of the gelatinases MMP-2 and MMP-9.

3.5.1: Conditioned medium collection:

As described before cells were seeded into $60mm^3$ culture dishes at a density of $5xl0^5$ cells/dish and allowed to form a monolayer. Medium was removed and cells were rinsed with PBS. For zymographic analysis of MMP expression, cells were cultured overnight in the lowest possible culture medium volume (1ml per dish) to increase the MMP concentration in the collected medium. Cells were cultured in serum free medium to eliminate contamination with exogenous constitutively expressed MMPs contained in the FCS of routine culture medium. The serum-free medium was removed, centrifuged at low speed to remove cellular debris and the supernatant was collected. It was stored at -4ºC until used.

3.5.2: Substrate gel electrophoresis:

Gelatinase zymography was performed in 10% SDS polyacrylamide Gel. The gels were prepared as described before with addition of gelatin and final concentration of gelatin 0.1% was achieved (Table: 3.5). Prior to loading, culture medium samples were combined with an appropriate amount of non-reducing sample loading buffer (Ix; see buffer appendix), vortexed, pulsed and incubated for 30 minutes at RT to allow coating

of the proteins with SDS. Samples were not boiled before electrophoresis. Following incubation, samples were applied to the gel as described in western blotting alongside the protein molecular weight marker. A standard volume of 40 µl was loaded for each sample. Gels were electrophoresed at 70V for 4 hours at 4°C to prevent spontaneous enzyme activation.

3.5.3: Staining and destaining

Following electrophoresis, gels were washed in the detergent Triton X-100 (2.5% in H_2O) three times for a total of 1 hour to allow renaturation of the MMP proteins contained in the gel matrix before overnight incubation in activation buffer (see buffer appendix) at 37°C to allow digestion of the gelatine substrate by the enzymes. Upon overnight incubation, gels were briefly rinsed in distilled water. A stain stock solution (0.2%) was prepared by dissolving one Phast Blue® tablet (GE Healthcare, UK) in 80ml of distilled water, adding 120ml of methanol, and stirring until all dye was dissolved, according to manufacturer's recommendations. The solution was then filtered through Whatman filter paper to remove undissolved stain particles. A stain working solution was prepared by adding a certain volume of stain stock solution to an equal amount of glacial acetic acid (0.2% in water). Gels were incubated in stain working solution (200ml per gel) on a rotor-shaker for 6 hours and then washed in destain solution (see buffer appendix) until clear bands against a dark blue background appeared. Gels were subsequently scanned on digital scanner and digital images were saved for subsequent analysis.

Table 3.5: Resolving gel for zymography.

	8% (w/v) gel (10 ml)	Final concentration in gel
Acrylamide/bis-acrylamide 30% solution (ratio 29:1)	2.7 ml	8 % (w/v)
H_20	3.6 ml	-
1% gelatin stock solution	1ml	0.1%
Tris(1.5M,pH8.8)	2.5 ml	375mM
SDS (10% solution in H_20)	100 µl	0.1% (w/v)
APS (10% solution in H_20)	100 µl	0.1% (w/v)
TEMED	40µl	0.4% (v/v)

3.6: Immunofluorescent staining (IFC)

This fluorescent staining method was previously reported (Jiang et al. 1999; Parr et al. 2001; Martin et al. 2003) and currently used.

- 20,000 cells in 200µl aliquots per well were seeded into a 16-well chamber slide (Nalge NUNC International, LAB-TEK®), and then incubated at 37ºC with 5% CO^2 overnight.
- After incubation and treatment with HGF (40 ng/ml), medium was aspirated and cells fixed with ice-cold ethanol at -20ºC for 20 minutes.
- Cells were rehydrated in BSS buffer for 20 minutes at RT.
- Cells were permeabilised with 0.1% Triton×100 for 5 minutes.
- Blocking was performed for 20 minutes using blocking buffer (2 drops of horse serum in 5ml wash buffer).
- Samples were washed twice with wash buffer after blocking.
- Samples were probed with primary antibody for 1 hour (1:100 made up in wash buffer with horse serum for blocking).
- Samples were washed twice with wash buffer.
- Samples were incubated with specific secondary antibody for 1 hour in the dark according to the primary antibody used which labelled with FITC or TRITC (1:100 made up in wash buffer with horse serum for blocking).
- Samples were washed twice with wash buffer.

- Slides were mounted with a fluorescence mounting medium, Flour-Save, CalBiochem, Nottingham, England).
- Cells were viewed under a fluorescent microscope (Olympus) and photos were taken. Analysis was carried out using Cell Analyser software (Olympus).

3.7: Immunocytochemistry (ICC):

Specific solutions for blocking and washing were prepared, including,

- ABC Complex:

  8 drops Reagent A to 20 ml of wash buffer;

  5 drops Reagent B to the same mixing bottle and mixed immediately

  (ABC Reagent allowed to stand for about 30 minutes before use)

- DAB Chronogen:

  Agents added in order and shaken each time in 5 ml distilled water

  2 drops buffer

  4 drops DAB

  2 drops hydrogen peroxide

  Wash Buffer

- 20xWash Buffer, Super SensitiveTM Wash Buffer (Bio Genex, USA)

- PC-3 cells (PC-3^{WT}, PC-3^{pEF} and PC-$3^{WAVE\text{-}3KD}$) were seeded in chamber slides (Nunc, Denmark), at a density of 20,000 cells/well.
- Cell culture medium was removed by aspiration and washed twice with TBS buffer to remove culture medium proteins. Buffered formalin (4%) was added and incubated at RT for 10 minutes.
- The fixative was aspirated and cells were washed twice with TBS buffer. Permeabilization buffer mixture (0.1% Triton in TBS buffer) was added and incubated for 10 min.
- Cells were washed twice with washing buffer following aspiration of permeabilization buffer.
- Non specific protein block was performed with diluted horse serum for 20 minutes (1 drop to 5 ml washing buffer).
- Chambers were washed again in washing-buffer for 4 times.
- Cells were incubated with diluted primary antibody (anti-MMP diluted 1:100 in blocking buffer) at 37˚C, for 1 hour.
- Cells were washed again in washing buffer for 4 times to remove any unbound primary antibodies.

- Secondary antibodies were added (anti-mouse, rabbit or goat depending upon the origin of primary antibodies, with a dilution of 1:250 in blocking buffer) and incubated for 30 minutes at room temperature.
- Cells were washed again in washing buffer for 4 times to remove any unbound antibodies.
- ABC complex was added and incubated for 30 minutes at RT.
- DAB chromogen was added for 5 minutes in the dark after washing again four times (covered by a tray).
- Excess chromogen was removed by washing with water for 2 minutes.
- Cells were counterstained with Mayer's Haematoxylin for 1 minute. Finally they were washed in water for 5 minutes to remove excess of Haematoxylin.

3.8: Knockdown of gene transcripts using ribozyme transgenes

Ribozyme stands for ribonucleic acid enzyme and represent RNA molecule capable of catalyzing a chemical reaction. Kruger et al. (1982) were the first ones to use this term, followed by pioneering work from Cech and Altman (Cech, T.1990; Altman, S. 1995). Ribozymes are found ubiquitously in nature and many of them catalyze hydrolysis of their own phosphodiester bonds are responsible for hydrolysis of bonds in other RNA molecules. The hammerhead ribozyme got its name due to the peculiar appearance of its molecular shape. It was first discovered as a self cleaving domain in the RNA genome of many plant viroids and virusoids. With the advancement in understanding regarding their role in cells, it was demonstrated that the hammerhead motif could be incorporated in to short synthetic oligonucleotides and transformed in to a true catalyst which was capable of cleaving many varieties of RNA.

All hammerhead motifs share a typical secondary structure consisting of three helical stems (I, II and III) that enclose a junction characterized by several invariant nucleotides (i.e., the ‘catalytic core’). In most trans-acting hammerhead ribozymes, helix II is formed intramolecularly by the catalyst, whereas helices I and III are formed by hybridization of the ribozyme with complementary sequences on the substrate. The best triplets in terms of cleavage rates were found to be AUC, GUC and UUC.

We synthesised ribozymes with a Touchdown PCR procedure, and cloned ribozymes in a suitable vector which was followed by transformation and transfection using an electroporator. After 3-4 weeks selection with a specific antibiotic, a stable cell line with

a transgene was verified by using RT-PCR and Western-blot. This method has been extensively used and reported previously in our laboratory (Jiang et al. 2001, 2003 and 2005).

3.8.1: Production of ribozyme transgenes:

Messenger RNA for WAVE proteins was targeted by specifically developed transgenes targeting WAVE mRNA. The secondary structure of mRNA was predicted using Zuker's RNA Mfold software (Zuker 2003). It can predict the stem and loop structure of mRNA with quiet reliable accuracy, under optimal condition. From this predicted structure a suitable GUC codon was selected. In this programme usually the codons which are located in the loop segment of secondary structure, are targeted. It allows easy access of the ribozyme to the codon. Once designed the transgenes were ordered from Invitrogen (Invitrogen Corporation, California) as sense/antisense strands (Table: 3.3) and combined in to transgene using touchdown PCR, under conditions as follows:

Step 1: Initial denaturing period: 94˚C for 5 minutes

Step 2: Denaturing: 94˚C for 20 seconds

Step 3: Annealing: 72˚ C for 15 seconds for 1st cycle

60˚ C for 15 seconds for 2nd cycle

58˚ C for 15 seconds for 3rd cycle

54˚ C for 15 seconds for 4th cycle

Step 4: Extension: 72˚ C for 50 seconds

Step 3: Final extension period: 72˚ C for 8 minutes

Step 2-4 were repeated for 32 cycles. Once combined, the transgenes were run electrophoretically on 2% agarose gel to confirm their presence and accurate size before they were inserted in to empty pEF[6] plasmids.

3.8.2: Topo TA cloning

The TOPO TA Expression system provides a highly efficient, 5 minute, one step cloning strategy ("TOPO Cloning") for the direct insertion of *Taq* polymerase amplified PCR products into a plasmid vector for high-level expression in mammalian cells. No ligase, post-PCR procedure, or PCR primers containing specific sequences are required. Once cloned, analysed, and transfected into a mammalian host cell line, the PCR product can be constitutively expressed. Cloning of ribozyme transgenes was carried out according to manufacturer's recommendations and using the kit provided.

Spontaneous ligation between vector and appropriate insert occurs when they are combined in specific concentration and conditions. Cloning reaction was set up by adding 4 µl of PCR product, 1 µl of salt solution and 1 µl of TOPO® vector in the PCR tubes. The solution was gently mixed and incubated at room temperature for 30 minutes and stored in ice until ready to proceed with one shot chemical transformation. Following ligation, the cloning reaction was transformed immediately into *E. coli*, to prevent any compromise for the transformation efficiency.

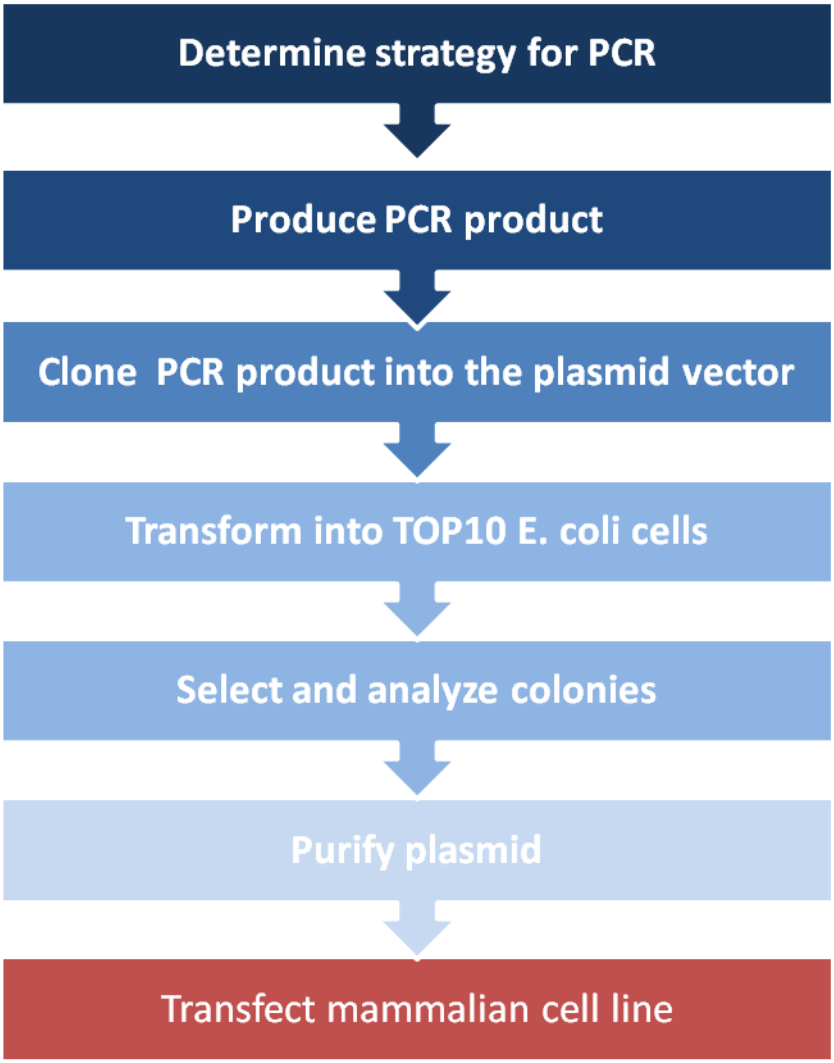

Figure 3.2: Schematic presentation of cloning reaction

3.8.3: Transferring plasmid into E.coli

The cloning reaction was transferred into the chemically competent *E. Coli* cells (OneShot^{tm} TOP10 E.Coli, Invitrogen Inc.) through following process: a 100 µl aliquot of the chemically competent bacteria (stored at -70°C) was thawed by immersion in to an ice-bath for 5 minutes. Following this, the cloning reaction was added and gently mixed using a pipette; this suspension was then placed on ice for 30 minutes. Cells were heat-shocked, in a water bath, at exactly 42°C for 30 seconds, then immediately placed back on ice for 2 minutes. Following which, 250µl of SOC medium was added. These cells were incubated for 60 minutes at 37°C with continuous shaking at approximately 225 rpm. The resultant transformation mix was plated out (at two different volumes) onto pre-warmed selective LB-agar plates containing ampicillin (50 µg/ml). LB medium was prepared by dissolving l0 g tryptone, 5 g yeast extract, and l0 g NaCl in 950 ml deionised water. The pH was adjusted to 7.0 with NaOH, and final volume made up to 1 liter. The solution was autoclaved and Ampicillin was added. This medium was then stored at room temperature. To create LB plates, 15g of agar was added to the one liter of LB medium before autoclaving. Following cooling, it was added to plates and allowed to set. Once prepared these plates were stored in an inverted position, at 4°C.

3.8.4: Selection and analysis of colonies

Following overnight incubation, the plates revealed a large number of bacterial colonies containing the plasmid vector. The plasmid vector encodes a gene to enable resistance to Ampicillin and when transformed into the *E. coli*, it confers this resistance to these

cells. Thus, selection occured in the presence of Ampicillin, as cells without the plasmid vector will not survive. The next step was to establish a population of bacteria containing plasmid with correct orientation of inserted transgene, in order to get correct and effective ribozyme transgene. Analysis of the individual colonies was performed to determine which of the colonies grown on the plate contained the vector plus insert in the correct arrangement, prior to amplification.

At least 10 colonies were screened with PCR, to amplify the target sequence of insert DNA at the correct position within the plasmid vector. Samples were obtained by touching individual colonies with a pipette tip then transfering those cells into the PCR reaction cocktail ready for specific amplification of the desired sequence. This was achieved through the use of the forward primer for the plasmid and the reverse primer specific for the inserted PCR products. This ensured that amplified products, at the expected size, are that of the plasmid and insert in the correct orientation. Once confirmed from the results of PCR, these colonies were then ready for amplification.

3.8.5: Amplification and purification of plasmid DNA

Following identification of positive colonies with the appropriate vector and insert positioning, a single positive colony was transferred, aseptically, to inoculate 2ml of LB medium, containing Ampicillin at a final concentration of 100µg/ml, and incubated until the culture grew to mid-log phase at 37°C in a rotary shaker. At which stage, the resultant culture was then added into 100 ml LB medium (plus ampicillin), and

incubated overnight at 37°C under rotation. The resulting amplification of recombinant plasmids within *E.coli,* was extracted using a plasmid DNA purification kit (Filter Maxi System, QIAGEN, West Sussex, UK), as described below.

This method using QIAGEN Maxi filter cartridges has the capacity to recover plasmid DNA from the 100 ml of bacterial cells. To harvest the culture, cells were centrifuged in a refrigerated centrifuge (at 4 ^{o}C) at 6000g for 15 minutes. Medium was removed so that only bacterial cells could be collected as a pellet. This pellet was then resuspended in 10 ml of resuspension buffer, containing RNase inhibitors (available in the pack). To lyse the cells, 10 ml of cell lysis buffer was added and the solution mixed gently to avoid shearing of genomic DNA. Following 5-minute incubation at room temperature, 10 ml of neutralization buffer was added and mixed, and then transferred to the QIAGEN filter cartridge. After 10 minutes at room temperature, the cell lysate was filtered into the barrel of the QIAGEN tip, which was then allowed to enter the resin by gravity flow. The plasmid DNA binds to the anion-exchange resin.

To remove all contaminants from the plasmid preparation, the resin was washed throughly with wash buffer. RNA, proteins, dyes, and low molecular weight impurities were removed by this medium-salt wash. The DNA was eluted from the resin through the addition of a high salt elution buffer, and was collected in a 50 ml universal tube. Plasmid DNA was then concentrated and desalted by isopropanol (10.5ml) precipitation, followed by a series of centrifugation and washing steps. The pellet was then dried and resuspended in a suitable volume of water. The yield of DNA was determined through

quantification, following which, a small amount of plasmid DNA was run on agarose gel (0.8%) to check both plasmid purity and size.

3.9: Transfection via electroporation of mammalian cells

Once the plasmid DNA had been isolated, purified and quantified, it was ready to be introduced into cultured mammalian cells. The method employed during this study, utilized electroporation of cultured cells to allow plasmid DNA to be incorporated into the cells. The electroporation technique used the Easy Jet Plus system (Flowgen, Staffordshire, UK), which passed a voltage of up to 310 volts across the cells to produce small perforations in the cell wall integrity, thus allowing passage of plasmid DNA across cell membranes to be integrated into the cells.

For a transfection, 3 pg of plasmid DNA was added to resuspended cells and mixed. The mixture was left to stand at room temperature for 2-5 minutes. The mixture was then transferred into an electroporation cuvette (Euro Gentech, Southampton, UK) ready for electroporation. The cuvette was loaded into the electroporator and a pulse of electricity (310 volts) was passed through the cuvette. The mixture was then immediately (within 10 seconds) transferred into 10 ml of pre-warmed culture medium. These cells were then cultured under the usual incubation conditions, as described before in methodology (Chapter 3; 3.2).

3.10: Establishing a stable expression mammalian cell line

To create a stable cell line that does not expresses the WAVE-3 gene; the culture was designed to yield only a population of cells expressing the plasmid-insert. The above electroporated cells were allowed to grow to semi-confluence, prior to exposure to selection conditions. Selection of plasmid positive cells relies on the presence of an additional drug (Blasticidin) resistance gene in the plasmid. Plasmids used in this study have dual resistance genes, i.e. one for prokaryotic selection (as already mentioned earlier) and one for mammalian selection. For the latter, modified antibiotics that are capable of entering mammalian cells are used, such as blasticidin (for pEF^{6}/V5-His-TOPO). Thus the respective antibiotic was added to cultured cells at an appropriate concentration (5pg/ml for blasticidin) to kill cells lacking appropriate plasmid. This antibiotic selection period was continued for a week, at which point the cells remaining should all contain the plasmid and the inserted DNA fragment. Cells were routinely tested for the presence of the plasmid and insert, using RT-PCR. This was achieved through study of expression for different WAVEs mRNA and expression of the protein itself. The transfectants cell populations were then employed in a series of *in vitro* studies, to examine for the influence of WAVE-3 gene knock down.

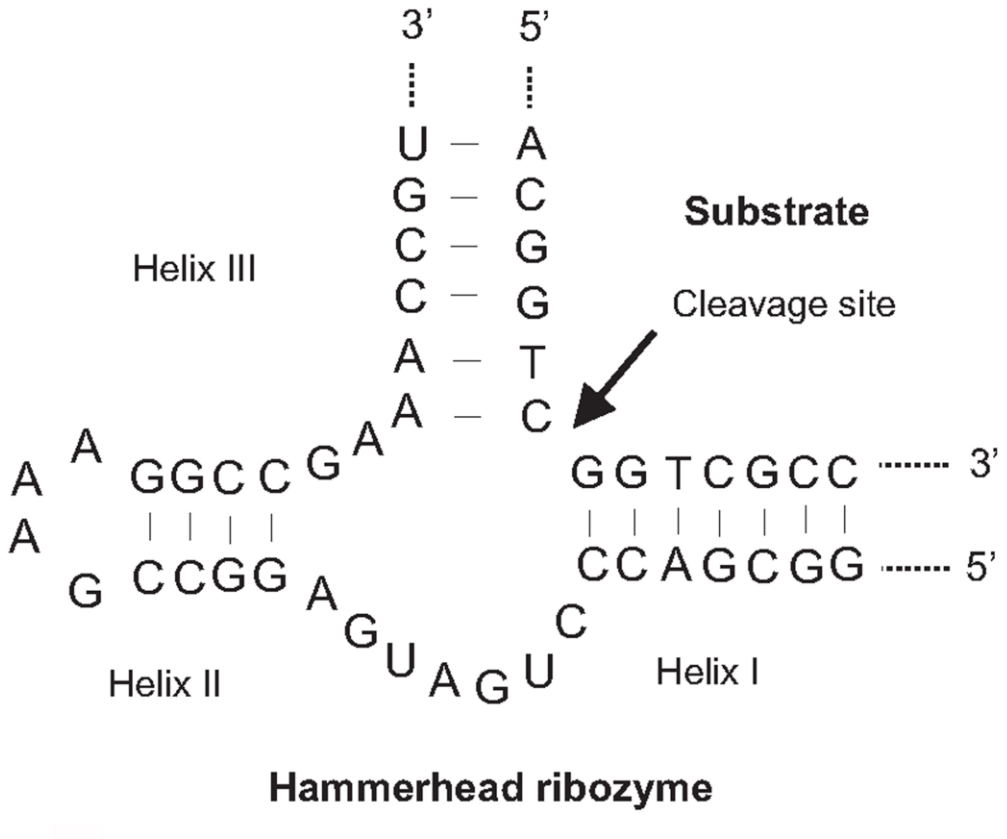

Figure 3.3 Secondary structure of the hammerhead ribozyme with bound substrate.

3.11: *In vitro* functional assays:

3.11.1*: In vitro* cell growth assay

We used the method previously reported in literature (Jiang et al. 2005). Briefly, an equal number of the respective cells were plated into a 96-well plate (2,500cells/well). Cells were fixed in 10% formaldehyde on the day of plating; days 1, 3, and 5 after plating; and then stained with 0.5% (w/v) crystal violet. Following washing, stained crystal was extracted with 10% (v/v) acetic acid and absorbance determined at a wavelength of 540nm by using a spectrophotometer (BIO-TEK, ELx800, Wolf Laboratories, York, England).

3.11.2: *In vitro* migration assay (wounding assay)

The migration of cells across a wounded surface of a near-confluent cell monolayer was examined, which has been described in a previous study (Jiang et al. 1999). Cells at a density of 50,000/well were seeded into a chamber slide and allowed to reach near confluence. The layer of cells was then scraped with a fine gauge needle to create a wound of approximately 200 mm. A treatment was then added with appropriate control. The movement of cells to close the wound was recorded using a time lapse video recorder and analysed using the motion analysis feature in a software package Optimas 6.0.

3.12.3: *In vitro* motility assay using Cytodex-2® beads

We followed the protocol described by Rosen and Jiang (Rosen et al. 1990; Jiang et al. 1995). 1×10^6 cells were incubated with 100µl of beads in 10 ml DMEM overnight. The beads were washed to remove dead cells in 5ml DMEM twice, and then resuspended in 800µl DMEM. 100µl of beads/cells were transferred into each well of a 24-well plate, and repeated in triplicate. After incubation for 4 hours, the medium was aspirated and cells were fixed with 4% formalin for 5 minutes. They were then stained with 0.5% crystal violet for 5 minutes. The cells were washed and allowed to dry before counting. Counting was performed randomly in 3 random fields per well. This was adopted to make sure that more than 9 counts were performed for each sample when experiment was set up in triplicate fashon.

3.12.4: *In vitro* invasion assay

This technique was previously reported and modified in our laboratory (Jiang et al. 1995). The technique works upon the principle that a culture plate is equipped with an insert which has one end sealed with a polycarbonate membrane with a pore size of 8µm in diameter, sufficiently large enough to allow cells to migrate through it. The surface of this membrane is then coated with an extracellular matrix protein solution, Matrigel (rich in basement membrane), to form a thin layer of gel matrix. Since this technique determines the capacity of tumour cells to penetrate through the gel matrix and porous membrane, it represents an indication of invasive capacity. The following method briefly outlines the procedure used during this study.

Cell culture inserts (Becton-Dickinson) for *in vitro* invasion, were placed into a 24 well plate (Nunclon) using forceps. To prevent irreversible gelling of Matrigel the following procedure was carried out at 4°C. A stock solution of Matrigel was prepared at a concentration of 0.5mg/ml in pre-cooled sterile water and 100µL aliquots of Matrigel (50µg per insert) were added to these pre-chilled cell culture inserts. Once the inserts had a thin even coating of Matrigel, they were incubated at 45°C in a drying oven, to dry out the Matrigel. Prior to use, the Matrigel layers were rehydrated by incubating at room temperature for 1 hour using 300µL of sterile water, and then aspirating the water from each insert.

Cell suspensions were added to each insert and treated. After a culture time of upto 72 hours at 37°C, the Matrigel layer together with the non-invasive cells were removed from the inside of the insert using a cotton swab. This step was performed as the Matrigel is stained in addition to the cells, thus making it difficult to resolve between invading cells and background. The cells which had invaded into the Matrigel and migrated through the porous membrane were fixed in 4% formaldehyde, for 10 minutes at room temperature. The cells were washed twice using distilled water and stained with 0.5% crystal violet for 10 minutes at room temperature. Excess stain was removed by washing the cells twice in distilled water. The cells were allowed to air dry and the numbers of invading cells were counted using a light microscope, prior to being photographed.

3.12.5: *In vitro* cell-matrix adhesion assay

100µL serum free medium that contained 5µg Matrigel (BD Matrigel™ Matrix, Matrigel™ Basement Membrane Matrix, Cat No. 354234) was added in each well of 96-well plate (NUNC™, TC Microwell 96F, Cat No. 167008), and then the Matrigel was dried at 55°C for about one hour in oven. Matrigel was rehydrated in 100µL sterile water per well at room temperature for 40 minutes, and then the medium was aspirated. 40,000-50,000 cells per well were seeded since the plates with Matrigel were ready. The cells were incubated with or without treatment of hepatocyte growth factor (HGF) at 37°C with 5% CO_2 for 40 minutes. After the incubation or treatment with hepatocyte growth factor (HGF), the medium was discarded. The non adherent cells were washed off 3-4 times using BSS buffer. The cells were then fixed with 100µl per well of 4% formaldehyde for a minimum of 5 minutes. The formaldehyde was discarded and the cells washed with BSS buffer. 100µl of crystal violet solution (0.5% crystal violet in distilled water) was added into each well for up to 5 minutes, washed with BSS buffer, and then left to dry at RT. The number of adherent cells were counted under a microscope, from random fields in a triplicate fashion and compared to the number of adherent cells that remained on the Matrigel after HGF/SF treatment.

3.13: Statistical analysis

Data from independent runs of experiments were recorded on Microsoft Excel software and latter imported in to statistical software SPSS 12.0.1 for further analysis. One way ANOVA (analysis of variance) was mainly used to compare the means for any statistical significance. In this method analysis of variance is used to test the hypothesis that several means are equal. This technique is an extension of the two-sample t-test. It is important to understand that the one way ANOVA test can only determine that at least two groups are different in the particular experiment. However it is easy to determine which groups are different by performing the post-hoc test. There are multiple tests available for post-hoc test. Levene's homogeneiety of variance test is used first to determine the variance in the samples. If equal variance is assumed, Bonferroni, Sidak and Dunnett test can be performed for multiple comparisons. If equal variance is not assumed than Tamhane's-T2, Dunnett's T3 and Dunnett's-C can be performed.

Chapter 4
WAVE-3 in prostate cancer cell lines: Expression and knock down.

4.1: Introduction:

WAVE-3 was identified in 1999 as part of the Wiskott-Aldrich Syndrome Protein family (WASP) (Suetsugu et al. 1999). This diverse family of proteins plays a critical role in actin polymerisation, organisation of the cytoskeleton and cellular motility. The expression profiles of WAVE genes have demonstrated overlapping expression of all three WAVE transcripts in many embryonic and adult tissues. These proteins have been frequently found to be co-localised indicating their involvement in similar processes. WAVE-3 was originally found to be truncated and inactivated in a patient with ganglioneuroblastoma. It was hypothesized that loss of this molecule resulted in accumulation of neural crest cells due to their abnormal migration but at the same time retaining their growth potential (Sossey-Alaoui et al. 2002).

Expression of WAVE-3 has been well documented in breast cancer cell lines (Sossey-Alaoui et al. 2005; Fernando et al. 2007). Its expression appears to be up regulated in motile cancer cells. Genetic silencing of WAVE-3 using different techniques has demonstrated a reduced motility and invasiveness of prostate cancer cell lines. The loss of WAVE-3 results in increased formation of stress fibers and focal adhesion complexes which may indicate its importance in maintaining the balance of cellular motility (Sossey-Alaoui et al. 2005).

HGF is a well-documented cytokine found in patients with aggressive and metastatic prostate cancer. It induces growth, cellular motility and interaction of malignant cells with its environment resulting in increasing invasive and metastatic potential of prostate

cancer. HGF promotes these effects through multiple mechanisms. However the role of HGF in WAVE-3 dynamics has not been studied before.

The aim of the current study was to document the expression of WAVE-3 in different cell lines. In the second part of this study we also analyzed the effect of HGF on expression of WAVE-3 in PC-3 cell line, following variable concentration and timed exposure of HGF. Thirdly, we wanted to generate and confirm a prostate cancer cell line, deficient in WAVE-3 through the process of cellular cloning and use of hammerhead ribozymes.

4.2: Materials and methods:

4.2.1: Expression of WAVE-3 in prostate cancer cell lines.

Complimentary DNA samples were selected from a stock of ready prepared kit in the department, derived from different cell lines. These cell lines included PC-3, DU-145, CAHPVN, LNCaP, PZHPV-7, PNT1A, PNT2C2, HECV and MRCJ. Real time PCR (RT-PCR) was used to document the expression of WAVE-3 using predefined forward and reverse primers, as previously described in the methods section. GAPDH expression was also analysed to document the quality of complimentary DNA samples. It also helped to normalize the DNA samples from different cell lines.

The final products from PCR were separated using agarose gel electrophoresis. The gel was stained with ethium bromide (10mg/ml) for five minutes, followed by a wash in BSS buffer to remove any background staining. The gel was placed on ultraviolet

transilliminator (WPA UV 1101; Biotech Photometer, Cambridge UK). The obtained images were saved as pictures for subsequent analysis and records.

Following documentation of good expression for WAVE-3 in PC-3 cell line, the effects of HGF at different concentrations as well as exposure over a variable time period were studied. Cells were exposed to concentration ranging from 1ng/ml to 100ng/ml over a time period of one hour. Similarly cells were exposed to a 40ng/ml concentration of HGF ranging from five minutes to 24 hours. Complimentary DNA was prepared as described before in the methods chapter (3.3.1 & 3.3.2).

4.2.2: Knock down of WAVE-3 expression:

4.2.2.1: Construction of ribozyme transgenes targeting at WAVE-3.

A hammerhead ribozyme was designed based on the secondary structure of the WAVE-3 mRNA. The secondary structure of WAVE-3 was generated using Zuker's RNA mFold programme (Zuker, 2003). The sequence in the mFold programme was the entire coding region of human WAVE-3. According to both the cleavage site of target gene and the sequence of hammerhead ribozyme, the primers were designed (refer to Table: 3.3). These oligo primers had the following characteristics: restriction sites (Spe1 (TGATCA) on the 5' end of the reverse primer and Pst1 (CTGCAG) on the 5' end of the forward primer) were included for cloning purposes; the primers permit template free amplification during PCR; Hammerhead ribozyme and antisense were pre-arranged in order that correctly oriented ribozymes were amplified.

The ribozymes were synthesized by using touchdown PCR (Figure 4.3 A). The ribozymes thus generated carried an A- overhang at the 3' end of the product. The ribozyme was subsequently TA cloned into a mammalian expression pEF^6/V5-His-TOPO plasmid vector (Invitrogen Ltd., Paisley, UK), using a protocol as already described in chapter:3 (3.8). Following ligation, the vector was then transformed into E. Coli, using the heat shock method. After one-hour incubation in SOC medium which allows the bacteria with transgenes to generate resistance to the antibiotic, the bacteria were plated and incubated overnight at 37˚C. The colonies were then analysed using direction specific PCR, which verified both presence and direction of the ribozymes in the clone (Figure 4.3 B). Each colony was tested using two separate PCR reactions: one using T7F primer coupled with RBBMR primer and the other using T7F with RBTPF primer (sequences of primers in Table: 3.3). Colonies with T7F/RBBMR reaction positive (and with the correct /sided product) and T7F/RBTPF negative were regarded as the colonies with correctly oriented ribozyme insert were grown. These colonies were then carefully picked and grown up in a large volume of LB medium (with ampicillin). The respective plasmid was finally extracted, and verified using DNA electrophoresis (Figure: 4.3-C).

4.2.2.2: Transfection of PC-3 cells and establishment of the stable transfectants.

Ribozyme transgenes and empty plasmid vectors were transfected into separate groups of PC-3 cells using an electroporator (Easjet Plus, EquiBio Ltd, Kent, UK), with a voltage at 270V. The cells were immediately transferred to 25 cm^3 tissue culture flasks

containing 5ml of pre-warmed culture medium. Selection of transfectants began when the cells reached 50%-70% confluence. The selection of positive cells was with a medium that contained the antibiotic blasticidin (Sigma-Aldrich, Inc., Poole, Dorset, England, UK) at 5µg/ml. After identification of colonies that survived the selection, they were then expanded into a larger population, and used for verification for the presence of the ribozyme and effects of the ribozymes on the expression of the respective target gene transcript using RT-PCR. Suitable strains were cultured in maintenance medium (blasticidin 0.5µg/ml) and grown to sufficient numbers for experimental studies. The selection took up to 2 weeks.

4.2.2.3: RT-PCR for WAVE-3 and β-actin.

RNA was isolated from the cells, and cDNA was synthesised by reverse transcription using 0.25µg RNA in a 20-µl-reaction mixture as described in the methods section (Chapter: 3; 3.3.1 & 3.3.2). PCR was undertaken using a REDTaq^{TM} Ready Mix PCR reaction mix (Sigma-Aldrich, Inc.). Cycling conditions for the 12-µl-reaction mixture were 94ºC for 5min, followed by 30-40 cycles of 94ºC for 30 s, 55 ºC for 30 s, and 72 ºC for 40 s. This was followed by a final extension of 10 min at 72 ºC. The products were visualized on a 2% agarose gel and stained with ethidium bromide after electrophoresis. The PCR primers used are listed in chapter: 3 (Table: 3.1).

4.2.2.5: Western blot analysis of WAVE-3 and GAPDH.

Cells were lysed and after extraction, protein concentrations were measured using the DC Protein Assay kit (BIO-RAD, USA). Samples were diluted using the lysis buffer in order that same concentration was obtained. These protein samples were then mixed with a 2×sample buffer which contained SDS, glycerol and a loading dye. After electrophoresis, proteins were blotted onto nitrocellulose sheets, followed by blocking before probing with specific primary antibody (anti-WAVE-3 1:100 and anti-GAPDH 1:250 dilution), and corresponding peroxidase-conjugated secondary antibodies (1:1000). Protein bands were visualized with a SupersignalTM West Dura system (Pierce Biotechnology, USA).

4.3: Results:

4.3.1: Expression of WAVE-3 in different cell lines:

A range of epithelial cell lines were screened for 3 different members of the WAVE family. These included prostate cell lines (PC-3, DU-145, CA-HPV-10, LNCaP, PZ-HPV-7, PNT1A, PNT2-C2), HUVEC (human umbilical vein endothelial cells) and MRC-5 (human lung cells). The WAVE-3 was abundantly expressed by prostate cancer cell lines including PC-3, DU-145, CA-HPV-10, LNCaP, and PNT1A. However PZ-HPV-7 and PNT2-C2 did not show any significant expression of WAVE-3. HUVEC and MRC-5 showed good expression but it appeared to be weaker than prostate cell lines (Fig: 4.1). PC-3 (WT) cells were exposed to variable concentrations over fixed time period of 17.5 hours. Expression of WAVE-3 was noted in middle range concentration (25 ng/ml) as

well as high concentration (75 and 100 ng/ml) of HGF (Figure 4.2). On the other hand maximum expression of WAVE-3 was noted following one hour treatment with concentration of 40 ng/ml (Figure: 4.2). This treatment time and concentration of HGF in the medium, was used during subsequent *in vitro* experiments.

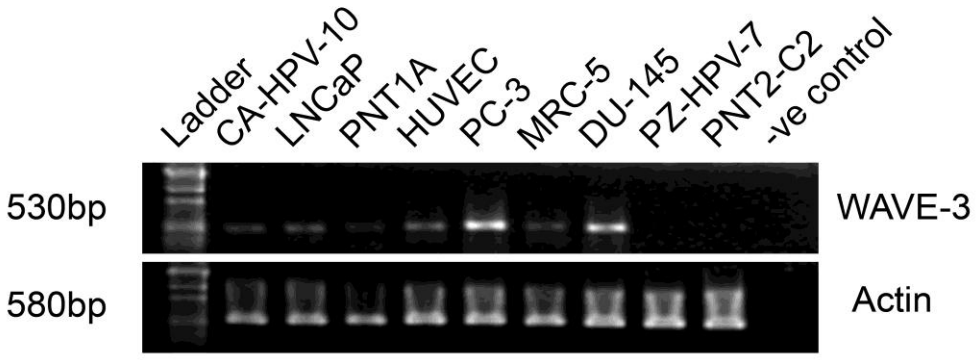

Fig 4.1: PCR showing expression of WAVE-3 in different cell lines.

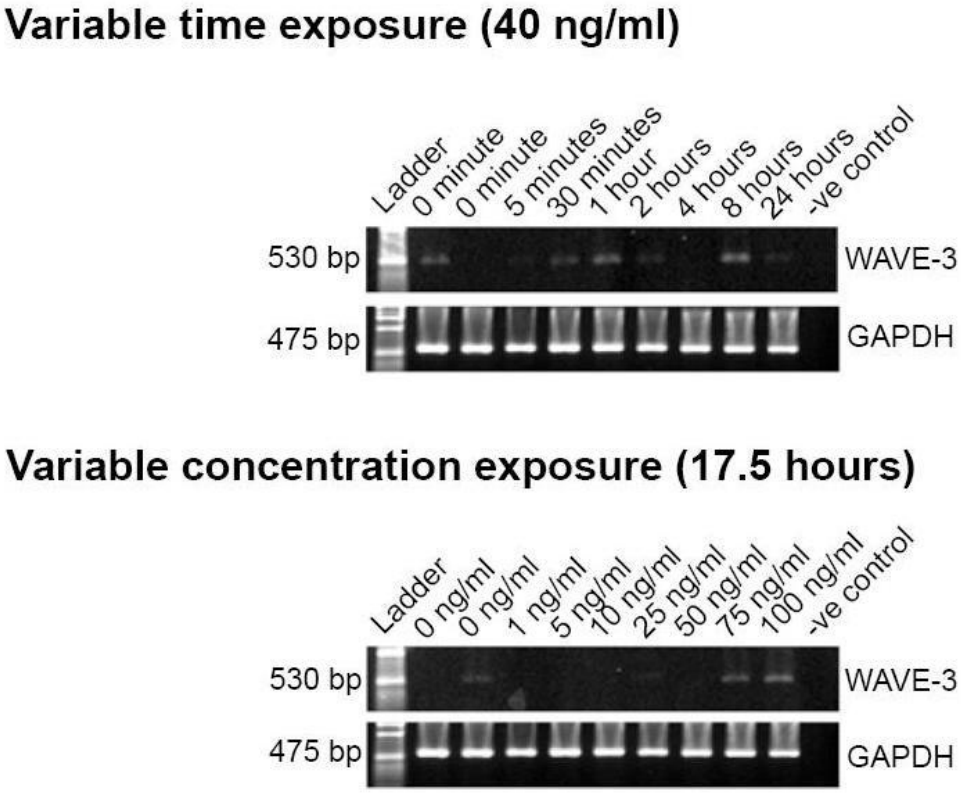

Figure 4.2: Expression of WAVE-3 in PC-3 cell line, in response to HGF. PCR showing the expression of WAVE-3 RNA in PC-3 (WT) cell line following exposure to HGF over variable time (0-24 hours at fixed concentration of 40 ng/ml) and variable concentration (0-100 ng/ml) over 17.5 hours)

4.3.2: Knock down of WAVE-3:

4.3.2.1: Generation of pEF plasmid containing WAVE-3 ribozyme transgene:

Suitable sites were selected for generation of two hammerhead ribozymes based upon the predicted secondary structure of human WAVE-3 RNA transcript, created through mRNA folding programme. Touchdown PCR was used to synthesize anti-WAVE-3 ribozyme transgene. These ribozymes were inserted in to empty pEF plasmids and transferred in to E.Coli. These bacteria were allowed to grow in the Ampicillin selection which ensured the growth of pEF plasmid containing bacteria only. Isolated random colonies were selected and checked for correct orientation of ribozyme transgene insertion to deliver correct and active viable product. Correct orientation was indicated by the presence of a band approximately 140 bp in the T7F Vs RbBMR reaction whereas band of 140bp bp in the T7F Vs RbToP was taken as incorrect orientation. Following selection, the colonies were amplified by overnight incubation. The plasmid was extracted (as described previously in chapter: 3; 3.8.2) and confirmed by gel electrophoresis on a 0.8% agarose gel with a band corresponding to approximately 5890bp (Fig: 4.3).

4.3.2.2: Expression of WAVE-3 protein in PC-3$^{\Delta WAVE\text{-}3}$ transfected cells:

Expression of WAVE-3 was significantly reduced in successfully transfected cells. This phenomenon was exclusively observed on RT-PCR and western blotting (Fig: 4.4).

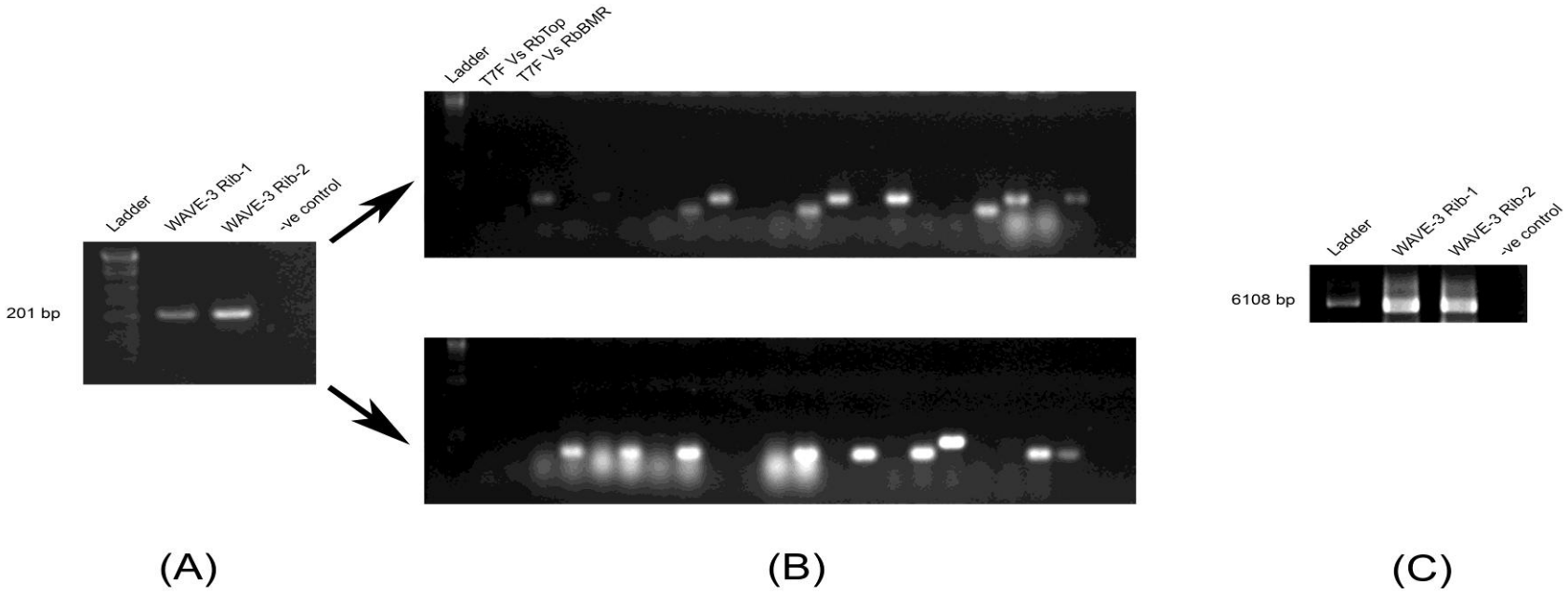

Figure 4.3: Cloning of WAVE-3 Ribozyme-1 & 2 (WAVE-3 Rib-1 and WAVE-3 Rib-2)

(A): PCR showing the successful generation of the WAVE-3 ribozyme transgenes as indicated by the correct predicted product size.

(B): PCR screening of E.Coli colonies to select those with correct orientation of the ribozyme transgene in the pEF6 plasmid. Correct orientation is indicated by a band of approximately 140bp in the T7F Vs RbBMR reaction, whereas a band of 140bp in the 7TF Vs RbToP is considered incorrect orientation.

(C): PCR confirming purified pEF6 plasmid containing the ribozyme (6kb) following extraction from E.Coli.

4.3.3: Expression of WAVE-3 transcripts in Q-PCR:

To confirm the knock down of WAVE-3 in the transfected cell, Q-PCR was used to determine the levels of mRNA expression, in addition to RT-PCR and western blotting. Table 4.1 and graph 4.1 shows that cells transfected with the WAVE-3 ribozyme-2 (W3R2) transgene (PC-3 $^{\Delta WAVE\text{-}3}$ Rib2) exhibited a reduced level of WAVE-3 expression at the mRNA level. Data regarding the expression of different WAVEs was normalized against the expression of house keeping gene (β-actin). In contrast, cells transfected with the WAVE-3 ribozyme-1 transgene (PC-3 $^{\Delta WAVE\text{-}3}$Rib1) failed to knock down WAVE-3 expression as demonstrated by the presence of transcripts. Similarly, both wild type (PC-3^{WT}) and pEF6 transfected (PC-3^{pEF6}) cells exhibited transcripts for WAVE-3 expression. The β-actin transcript was present in all samples screened and was used as a quality control. There was no significant change observed in expression of WAVE-1 and WAVE-2 following WAVE-3 knock down on Q-PCR, among different cell lines (Table4.1 & Graph 4.1).

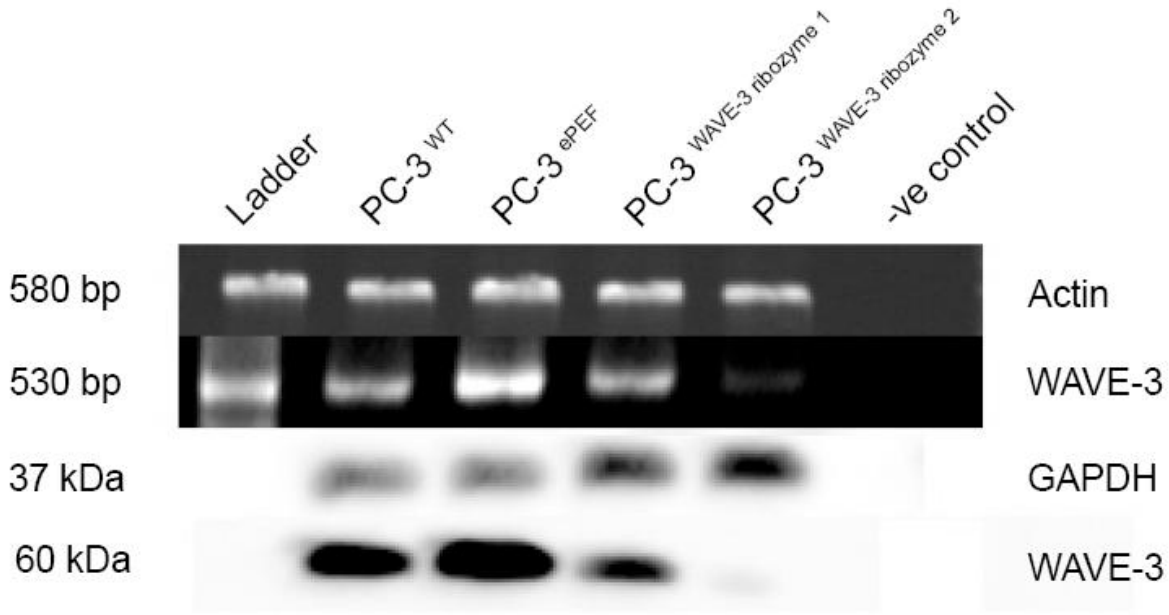

Figure 4.4: RT-PCR and Western blotting for mRNA and protein levels of WAVE-3 in PC-3 cells following knockdown by ribozyme transgenes.The expression of WAVE-3 was almost completly knocked down on RT-PCR (A) and western blotting (B) in WAVE-3 (Ribozyme-2) as compred to WAVE-3 (Ribozyme-1).

Molecule	Number of transcript copies of mRNA in cell lines			
	PC-3 WT	PC-3 pEF	PC-3 ^{W3Rib1}	PC-3 ^{W3Rib2}
β-Actin	$1.35x10^7$	$1.29x10^7$	$1.44\ x10^7$	$1.01\ x10^7$
WAVE-1	9188.19	6478.76	6546.61	11389.23
WAVE-2	952.39	919.08	792.58	544.81
WAVE-3	1414.39	3045.94	865.09	7.53

Table 4.1: Number of transcript copies on real time Q-PCR in four different cell lines (normalized against the expression of β-actin).

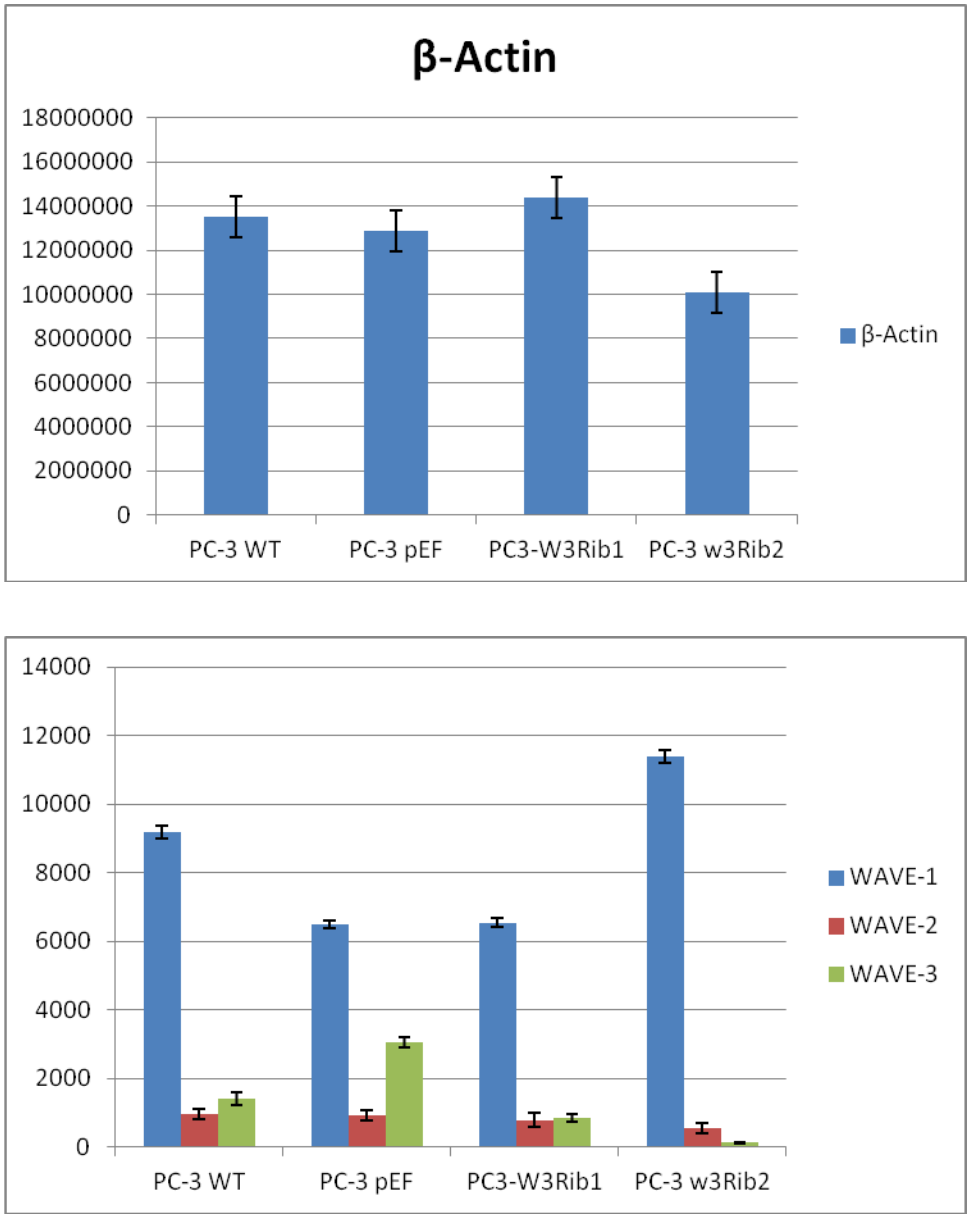

Graph 4.1: Real time Q-PCR showing number of transcript copies for WAVE-1, WAVE-2 & WAVE-3 along with β-actin in different cell lines.

4.4: Discussion:

The first aim of this part of the study was to document the expression of WAVE-3 in different prostate tissue cell lines. The seven prostate cell lines used in this study may represent different clinical characteristics of prostate cancer according to their origin. PC-3, DU-145, LNCaP and CA-HPV-10 represent prostate carcinomas which were derived from either primary tumor or secondary tumor, whereas PZ-HPV-7, PNT-1A and PNT2-C2 are immortalised prostate epithelial cell lines. Among the four prostate cancer cell lines, PC-3, DU-145 and LNCaP were derived from various metastatic sites and are more aggressive than CA-HPV-10, which was isolated from a primary tumor. LNCaP is an androgen sensitive cell line, whereas PC-3 and DU-145 represent androgen insensitive cell lines. These cell lines have been used in different models for the *in vitro* and *in vivo* investigation of prostate cancer. Strong expression of WAVE-3 in PC-3, DU-145, CA-HPV-10 and LNCaP, observed in this study probably indicates its active role in prostate cancer dynamics.

The second aim of this part of study was to generate a clone of prostate cancer cells deficient in WAVE-3 for subsequent studies, with particular emphasis on its effect in dynamics of prostate cancer metastasis. The cellular cloning involved in our experiment comprised silencing the specific gene expression which is usually expressed under normal circumstances. Specific gene expression can be modified at transcriptional and posttranscriptional levels. Transcriptional genetic silencing involves histone modifications through creation of an environment of heterochromatin around the gene, resulting in the gene being inaccessible to cellular machinery like RNA polymerase and

other transcriptional factors (Perry et al. 2010). Post-transcriptional modification involves mRNA of a specific gene being destroyed through introduction of specific agents targeted specifically against the gene of interest. A common mechanism is the introduction of small interfering RNAs (siRNA) which prevent the translation of specific gene mRNA. This concept has been used successfully in therapeutic implications of diseases like cancer and has shown promising results. Major targets of this therapy include silencing of genes involved in process of angiogenesis, metastasis, apoptosis and resistance to chemotherapy (Ramachandran et al. 2012). These RNAs can be delivered directly to intracellular environment or production can be induced through the delivery of plasmid DNA.

We successfully utilized the hammerhead ribozymes to knock down the expression of WAVE-3 after transcription *in vitro*. This particular technique used in this study is highly effective and had dramatically reduced the levels of the representative molecule at protein and messenger RNA level. The hammerhead is able to reduce target gene expression through its capability for multiple turnovers and acts in trans or cis forms for irreversible cleavage of target RNA. The hammerhead ribozyme can potentially target against any substrate mRNA provided it contains a specific combination of nucleotides, which allow formation of the correct secondary structure to permit cleavage. Although this method is long and time consuming, it provides reliable and stable knock down of a specific gene and can be applied in variety of cell lines.

One study has indicated the possible role of micro RNAs in this process. Sossey-Alaoui et al (2007) demonstrated an inverse correlation between WAVE-3 and miR200 microRNA expression levels in invasive *versus* non-invasive breast cancer cells

(Sossey-Alaoui et al. 2007). The expression of miR200 microRNA is lost during epithelial to mesenchymal transition (EMT) and therefore cancer metastasis. This mciro RNA directly targets the 3′-UTR of the WAVE-3 mRNA and inhibits its expression. This study also stressed that the miR200-mediated inhibition of WAVE-3 expression is specific for WAVE-3 because it does not affect the expression levels of the other members of the WAVE family.

These focused genetic tools not only allow construction of experimental models to determine the role of specific molecules in cellular function but also have potential role in therapeutic applications (Bertrand et al. 1994; Tang et al. 1998).

Chapter 5
Hepatocyte growth factor (HGF) induced migration and invasion of prostate cancer cells in vitro is dependent on WAVE-3

5.1: Introduction:

The invasive and metastatic potential of any cancer is dependent upon expression of different cellular characteristics at various steps of the metastatic cascade. Cellular motility and cytoskeleton changes are integral parts of this process and depend upon actin polymerization. The WASP (Wiskott-Aldrich syndrome protein) and WAVE (WASP Verpolin homologous) family are structurally related and responsible for regulation of actin polymerization through their interaction with Actin related proteins 2&3 (ARP2/3). The WASP gene family includes WASP muted in and responsible for Wiskott-Aldrich syndrome and widely distributed N-WASP. The WAVE gene family is comprised of WAVE-1, 2 and 3. The WASP and WAVE families of protiens act as downstream regulators of small GTPase responsible for signal transduction generated by different regulatory factors. Rac (GTPase) controls the formation of lamellipodia through regulation of WAVE family. WAVE-1 appears to be crucial for dorsal ruffles, while WAVE-2 is necessary for formation of lamellipodia. WAVE-3 has been found to be an aetiological factor in the development of low grade neuroblastoma (Sossey-Alaoui et al. 2002). Prior studies have shown that elimination of WAVE-3 from breast and prostate cancer cell lines reduces their invasive potential through reduction in motility and reduced expression of enzymes responsible for extra cellular matrix degradation (Sossey-Alaoui et al. 2005 and 2007; Fernando et al. 2009).

Hepatocyte growth factor/scatter factor (HGF/SF) is known to play a crucial role in the metastatic process through its effects on proliferation, dissociation, migration and invasion (Tajima et al. 1991; Sugawara et al. 1997; Gmyrek et al. 2001). Normally

hepatocyte growth factor/scatter factor (HGF/SF) is expressed by supportive mesenchymal cells (Kasai et al. 1996), while Met is expressed by epithelial cells (Rong et al. 1993). HGF/SF derived from prostate stroma, promotes proliferation, differentiation, motility, and invasion of malignant epithelial cells indicating possible involvement in the progression of prostate cancer (Gmyrek et al. 2001). The serum levels of HGF and PSA are found to be significantly increased in prostate cancer patients as compared to a control group (Hashem and Essam, 2005). Higher plasma levels of SF/HGF in men with hormone-refractory prostate cancer are associated with a decreased patient survival (Humphrey et al. 2006).

Previous studies have clearly demonstrated the loss of an aggressive phenotype in different cell lines following elimination of WAVE-3, including prostate cancer cell lines (Sossey-Alaoui et al. 2005; Fernando et al. 2009). WAVE-1 and WAVE-2 have been previously addressed as important mediators of PDGF induced cell migration (Suetsugu et al. 2003; Yan et al. 2003; Oikawa et al. 2004). This study tried to examine the effects of HGF on prostate cancer cells, following WAVE-3 knockdown in order to establish the role of WAVE-3 in mediation of HGF induced aggressive changes in prostate cancer, known previously.

5.2: Material and methods:

The PC-3 cell line was obtained from ECACC, Sailsbury, UK. Cells were maintained in Dulbecco's modified eagle medium (DMEM)-F12 medium supplemented with 10% fetal

calf serum and antibiotics. Anti-WAVE3 antibodies were obtained from Santa Cruz Biotechnology, Santa Cruz, CA. Other kits and reagents were obtained from Sigma-Aldrich, Poole, UK. The recombinant human HGF/SF was from HGF/SF cDNA transfected Chinese hamster ovary cell and was a kind gift from Dr. T. Nakamura, Osaka, Japan.

Zuker RNA mFold program was used to construct anti WAVE-3 ribozyme transgene, based on the secondary structure of the gene generated. Following synthesis, ribozymes were cloned in to pEF6/V5-His TOPO TA Expression kit (Invitrogen, Paisley, UK) according to the protocol provided. Plasmid vectors containing anti WAVE-3 transgenes and empty plasmids were transfected in to PC-3 cells using Easyjet Plus electroporator (EquiBio, Kent, United Kingdom). Cells were put in the selection medium containing Blasticidin (5ng/ml) for 5 days followed by maintenance medium (0.5 ng/ml). Transfection was confirmed by the absence of WAVE-3 transcripts and WAVE-3 protein in selected cells.

5.2.1: RNA isolation and PCR:

RNA was isolated from selected cells using total RNA isolation reagent (ABgene, Surrey, UK). Following quantification, this RNA was used to construct complimentary DNA using DuraScript reverse transcriptase-polymerase chain reaction (RT-PCR) kit (Invitrogen, Paisley, UK). This DNA was used for routine PCR and Q-PCR to confirm the knock down of WAVE-3.

5.2.2: Sodium dodecyl sulfate-polyacrylamide gel electrophoresis (SDS-PAGE) and western blot:

Equal amounts of proteins were separated from cell lysates using the DC Protein Assay kit (Bio-Rad Laboratories, Hemel Hempstead, UK). These proteins were separated using sodium dodecyl sulfate-polyacrylamide gel electrophoresis (SDS-PAGE) and blotted on to nitrocellulose membrane. Membrane was treated with milk to block non-specific proteins prior to probing with anti-WAVE-3 primary antibodies, followed by peroxidise conjugated secondary antibodies. Protein bands were visualized and analysed using Supersignal West Dura system and documented using a gel documentation system (UVITech, Cambridge, United Kingdom).

5.2.3: Cell growth assay:

Cell growth was assessed using previously described method (Jiang et al. 2005). In this method, 3000 cells were added from each cell line in 96 well plates and growth was assessed after 72 and 120 hours, in the presence or absence of HGF (40ng/ml) containing medium. Crystal violet was used to stain the cells, which was extracted and subsequently used to quantify through absorbance of light (wave length 540 nm) using an ELx800 spectrophotometer. Amounts of absorbance represented the number of cell and change was calculated by percentage increase as compared to baseline reading. At least five independent repeats were done and each repeat was done in quadruplicate.

5.2.4: Cell matrix adhesion assay:

Following cell counting, a total of 30,000 cells were added to a 96 well plates, which were previously coated with Matrigel (5µg/well). Cells were incubated for 40 minutes with or without HGF/SF (40ng/ml). Non-adherent cells were washed with BSS buffer. Adherent cells were stained with crystal violet (200µL/well) for 20 minutes. Excess of stain was removed by gentle washing with BSS buffer. Cells were counted in each well using uniform magnification on an inverted microscope. At least five independent repeats were performed and each repeat was done in quadruplicate.

5.2.5: Invasion assay:

Transwell inserts with pore size of 8 µm were used for the invasion assay as previously described (Jiang et al. 1995). Inserts were precoated with Matrigel (50µg/well, BD Biosciences, Oxford UK) which mimics the basement membrane to study the invasive potential of cells. A total of 20,000 cells were added to each insert along with medium. The experiment was run in duplicate for each cell line with or without HGF/SF (40 ng/ml). After 72 hours of incubation, the number of cells that had invaded through the basement membrane were counted following staining with crystal violet solution as described above in adhesion assay. At least five independent repeats were done in duplicate.

5.2.6: Cell motility assay using cytodex-2 beads:

Cell motility was assessed by dissociation from cytodex-2 micro carrier beads following treatment with HGF/SF (40 ng/ml) or not and was adapted from previous published

methods (Jiang et al. 2003). Cells at a density of 1×10^5 cells/ml were cultured in 10 ml of DMEM medium containing 250 µg/ml of beads for 24 hours at 37°C. The cell/bead complex was seeded into a 24 well plate in triplicate, and cultured with (40 ng/ml) or without HGF for 4 hours at 37°C. Cells that had migrated from the beads and adhered to the bottom of each well were fixed in 4% formalin for 5min and stained in 0.5% crystal violet. The stained cells were counted with a light microscope at fixed magnification and three fields per well were scored. Duplicated experiment for each cell line was repeated at least 5 times.

5.2.7: *In vitro* cell migration (wounding) assay:

A wounding assay assesses the migratory properties of cells. In health, cells respond to wounding of a monolayer by converging and closing the initial wound. Using a method adapted from Jiang *et al.* (Jiang et al. 1999), this process can be recorded and analysed. 500,000 cells of each line were seeded into a single well of a 24 well plate. Subsequent serial dilutions reduced the number of cells seeded by a factor of 2, until 6 wells were seeded. The plate was left for 24-48 hours until an appropriate monolayer had formed in one well. The wounding was performed using a 21G needle to scrape three parallel lines across the well. The medium was changed immediately after to pre-warmed HEPES medium, and the cells given 15 minutes to recover. They were then transferred to a heated plate (Lecia GmbH, UK) and tracked using a camera attached to a Lecia DM IRB microscope (Lecia GmbH, UK). Images were captured at 0, 15, 30, 45, 60, 75 and 90 minutes time points. Images were retrospectively reviewed using Image J software and distances between the opposing wound edges were measured. The

arbitrary figure was converted to μm by multiplying by 0.8 as previously calibrated using a calibration grid. This method has been previously used exclusively in the host laboratory (Parr et al. 2001).

5.3: Results:

5.3.1: Effect of WAVE-3 knock down on cellular growth:

WAVE-3 knock down did not demonstrate any effect on growth of PC-3 cells at 72 and at 120 hours. Assessment of growth response was terminated at 120 hours which was in line with the time frame for assessment of invasion assay as well. There was a marked growth spurt with addition of HGF (40ng/ml) but the growth response between the different cell lines was not statistically significant at 3 days (Table 5.1 & graph 5.1) and 5 days interval (Table 5.2 & graph 5.2).

Cell type	Percentage increase after 3 days +/-SD	Significance p value <0.05	
PC-3 WT	45.28 +/- 4.81	**A**	**B**
PC-3 ePEF	51.29 +/- 10.46	WT Vs ePEF P=0.19	PC-3 WT without HGF Vs PC-3 WT with HGF P=0.024
PC-3 $W3^{KD}$	43.9 +/- 7.33	WT Vs $W3^{KD}$ P=0.68 ePEF Vs $W3^{KD}$ P=0.18	PC-3 ePEF without HGF Vs PC-3 ePEF with HGF P=0.004
PC-3 WT with HGF	99.09 +/- 20.01	WT Vs ePEF P=0.89	
PC-3 ePEF with HGF	97.3822 +/- 19.78		
PC-3 $W3^{KD}$ with HGF	109.11 +/- 7.03	WT Vs $W3^{KD}$ P=0.23 ePEF Vs $W3^{KD}$ P=0.16	PC-3 $W3^{KD}$ without HGF Vs PC-3 $W3^{KD}$ with HGF P=0.0096

Table 5.1: Growth assay representing percentage increase after 3 days among three trangenic cell lines. Difference in percentage growth did not reach a statistical significance among the different cell lines with or without HGF (A). However there was significant increase in the cell growth among all cell lines with addition of HGF (B). The mean difference was significant at the 0.05 level.

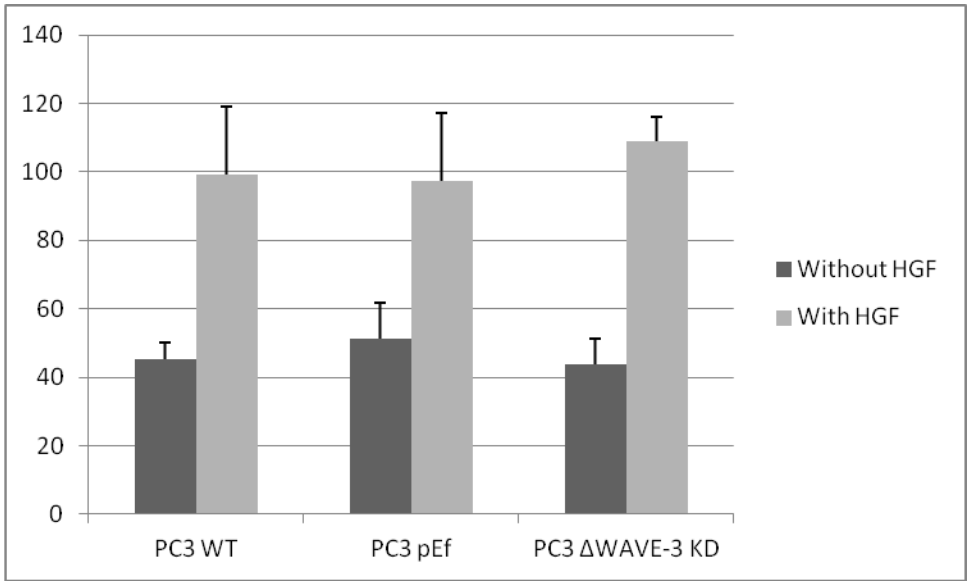

Graph 5.1: Percentage increase in cellular growth (+/- SD) after 3 days, among different cell lines with and without HGF. There was marked cellular growth following addition of HGF, but the difference in percentage growth did not reach statistical differeence (p value <0.05) among different cell lines (with and without HGF).

Cell type	Percentage increase after 5 days +/-SD	Significance p value <0.05	
PC-3 WT	239.66 +/-24.16	**A**	**B**
PC-3 ePEF	238 +/- 32.48	WT Vs ePEF P=0.91	PC-3 WT without HGF Vs PC-3 WT with HGF P=0.016
PC-3 $W3^{KD}$	238.22 +/- 48.59	WT Vs $W3^{KD}$ P=0.94 ePEF Vs $W3^{KD}$ P=0.99	PC-3 ePEF without HGF Vs PC-3 ePEF with HGF P=0.0017
PC-3 WT with HGF	324.57 +/- 33.1	WT Vs ePEF P=0.48	
PC-3 ePEF with HGF	336.38 +/- 21.9		
PC-3 $W3^{KD}$ with HGF	322.18 +/- 48.02	WT Vs $W3^{KD}$ P=0.91 ePEF Vs $W3^{KD}$ P=0.49	PC-3 $W3^{KD}$ without HGF Vs PC-3 $W3^{KD}$ with HGF P=0.029

Table 5.2: Growth assay representing percentage increase after 5 days among three trangenic cell lines. Difference in percentage growth did not reach a statistical significance among the different cell lines with or without HGF (A). However there was significant increase in the cell growth among all cell lines with addition of HGF (B). The mean difference was significant at the 0.05 level.

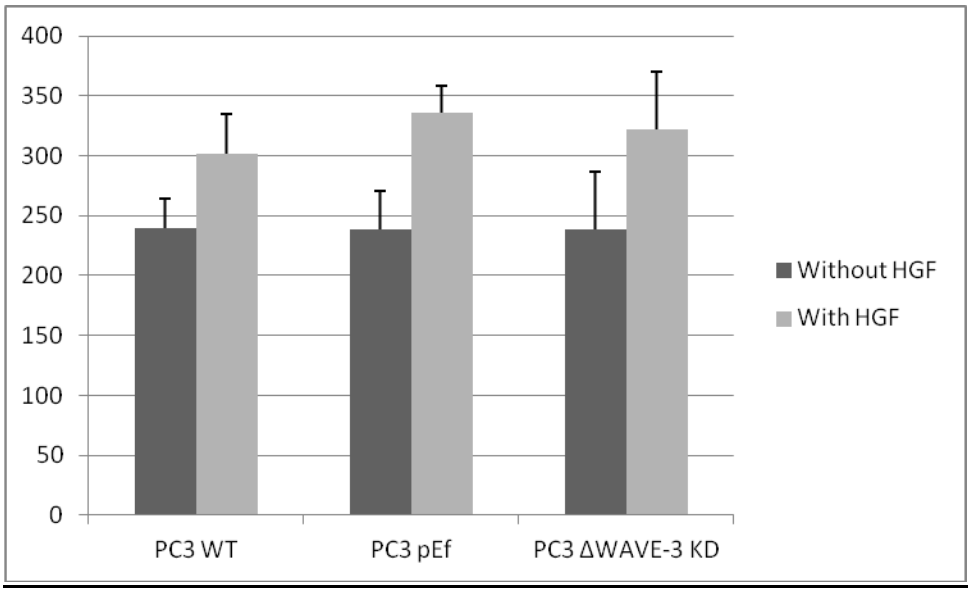

Graph 5.2: Percentage increase in cellular growth (+/- SD) after 5 days, among different cell lines with and without HGF. There was marked cellular growth following addition of HGF, but the difference in percentage growth did not reach statistical differeence (p value <0.05) among different cell lines (with and without HGF).

5.3.2: Effect of WAVE-3 knock down on cellular motility:

Elimination of WAVE-3 resulted in a reduction of motile cells on cytodex-2 beads assay. The mean number of motile cells (+/-SD) in PC-3^{WT} and PC-3^{pEF} were 10.9 +/-1.35 and 11.0+/-2.0 as compared to 5.93+/- 0.99 in $PC3^{WAVE\text{-}3\ KD}$ cell line. With the addition of HGF (40 ng/ml), the number of motile cells increased significantly in PC3-WT (23.56 +/- 2.46) and PC-3^{pEF} (21.46 +/- 1.8) as compared to $PC3^{WAVE\text{-}3\ KD}$ cell line (7.0 +/- 0.84) (Table: 5.4). As described before, there was no significant change in the adhesion assay which indicates an independent effect on cellular motility in the presence or absence of HGF. Bonferroni multiple comparisons between the PC-3 transgenic cell lines for the number of motile cells, showed a statistically significant difference in cell motility in $PC3^{WAVE\text{-}3\ KD}$ cell line with or without addition of HGF (Table 5.4).

Table 5.3: Descriptive statistics for cell motility assay

Cell line	N	Mean	Std. deviation	Std. error	95% Confidence interval for mean		Minimum	Maximum
					Lower bound	Upper bound		
PC-3^{WT} without HGF	5	10.9333	1.35067	.60404	9.2563	12.6104	9.25	13.00
PC-3^{PEF} without HGF	5	11.0000	2.06912	.92534	8.4309	13.5691	9.50	14.50
PC-3$^{WAVE\text{-}3\ KD}$ without HGF	5	5.9333	.99548	.44519	4.6973	7.1694	4.50	7.00
PC-3^{WT} with HGF	5	23.5667	2.46620	1.10292	20.5045	26.6289	20.25	26.38
PC-3^{PEF} with HGF	5	21.4667	1.83579	.82099	19.1872	23.7461	19.25	23.75
PC-3$^{WAVE\text{-}3\ KD}$ with HGF	5	7.0000	.84779	.37914	5.9473	8.0527	5.75	8.00

Table 5.3: Number of motile cells in three cell lines without and with hepatocyte growth factor (HGF) (40 ng/ml)

Table 5.4: Bonferroni multiple comparisons in between the PC-3 transgenic cell lines for number of motile cells

Cell type		Mean difference	Sig.	95% Confidence interval	
				Lower boundary	Upper boundary
PC-3^{WT} without HGF	PC-3 ^{PEF} without HGF	-.06667	1.000	-3.5627	3.4293
	PC-3 $^{WAVE-3\ KD}$ without HGF	5.00000*	.001*	1.5040	8.4960
	PC-3 ^{WT} with HGF	-12.63333*	.0001*	-16.1293	-9.1373
	PC-3 ^{PEF} with HGF	-10.53333*	.0001*	-14.0293	-7.0373
	PC-3 $^{WAVE-3\ KD}$ with HGF	3.93333*	.018*	.4373	7.4293
PC-3^{PEF} without HGF	PC-3 ^{WT} without HGF	.06667	1.000	-3.4293	3.5627
	PC-3 $^{WAVE-3\ KD}$ without HGF	5.06667*	.001*	1.5707	8.5627
	PC-3 ^{WT} with HGF	-12.56667*	.0001*	-16.0627	-9.0707
	PC-3 ^{PEF} with HGF	-10.46667*	.0001*	-13.9627	-6.9707
	PC-3 $^{WAVE-3\ KD}$ with HGF	4.00000*	.016*	.5040	7.4960
PC-3$^{WAVE-3\ KD}$ without HGF	PC-3 ^{WT} without HGF	-5.00000*	.001*	-8.4960	-1.5040
	PC-3 ^{PEF} without HGF	-5.06667*	.001*	-8.5627	-1.5707
	PC-3 ^{WT} with HGF	-17.63333*	.0001*	-21.1293	-14.1373
	PC-3 ^{PEF} with HGF	-15.53333*	.0001*	-19.0293	-12.0373
	PC-3 $^{WAVE-3\ KD}$ with HGF	-1.06667	1.000	-4.5627	2.4293

Table showing the statistical comparison of the effect of WAVE-3 silencing (PC-3$^{WAVE-3KD}$) to the wild type (PC-3^{WT}) and control (PC-3^{PEF}) using Bonferroni multiple comparisons in between the groups. * The mean difference is significant at the .05 level.

5.3.3: Effect of WAVE-3 knock down on cellular invasion through matrigel basement membrane:

WAVE-3 knockdown in PC-3 prostate cancer cells significantly decreased the invasion of cells through the matrigel artificial basement membrane. In this technique of *in vitro* invasion assay, cells have to move through the pores of 8 µm size, following degradation of basement membrane. The final results are from counts of cells that successfully reach the other side of the inserts used (Fig: 5.1). This assay also takes in to account the fact that there is no effect of WAVE-3 elimination on the cell growth, in same time interval. It was observed that there was a significant decrease in the invasiveness of PC-$3^{WAVE\text{-}3\ KD}$ cells as compared to PC-3^{WT} and PC-3^{pEF} cell lines. The mean (+/-SD) number of cells invaded in PC-$3^{WAVE\text{-}3\ KD}$ was 22.10+/-5.13 as compared to PC-3^{WT} 53.23+/-2.5 and PC-3^{pEF} 48.64+/-7.33 respectively (p value <0.05). At the same time there was no statistically significant difference between PC-3^{WT} and PC-3^{pEF} (p value 1.0) (Table: 5.6).

With the addition of HGF 40µg/ml to the medium in inserts and bottom wells (for all three cell lines), resulted in stimulation of the invasive potential of the different cell lines to variable degrees (Table: 5.6 & 5.7). HGF significantly increased the number of invasive cells in PC-3^{WT} (110.65+/-6.82) and PC-3^{pEF} (99.42+/-4.3) cell lines (p value <0.05, when compared to the number of cells that invaded without the presence of HGF). However this trend of change was not observed in the PC-$3^{WAVE\text{-}3\ KD}$ (23.17+/-2.48) cell line. In addition it was also observed that invaded cells in PC-3^{WT} and PC-3^{pEF} types were significantly higher than PC-$3^{WAVE\text{-}3\ KD}$, even after the addition of HGF induced stimulation (Table: 5.5 & 5.6).

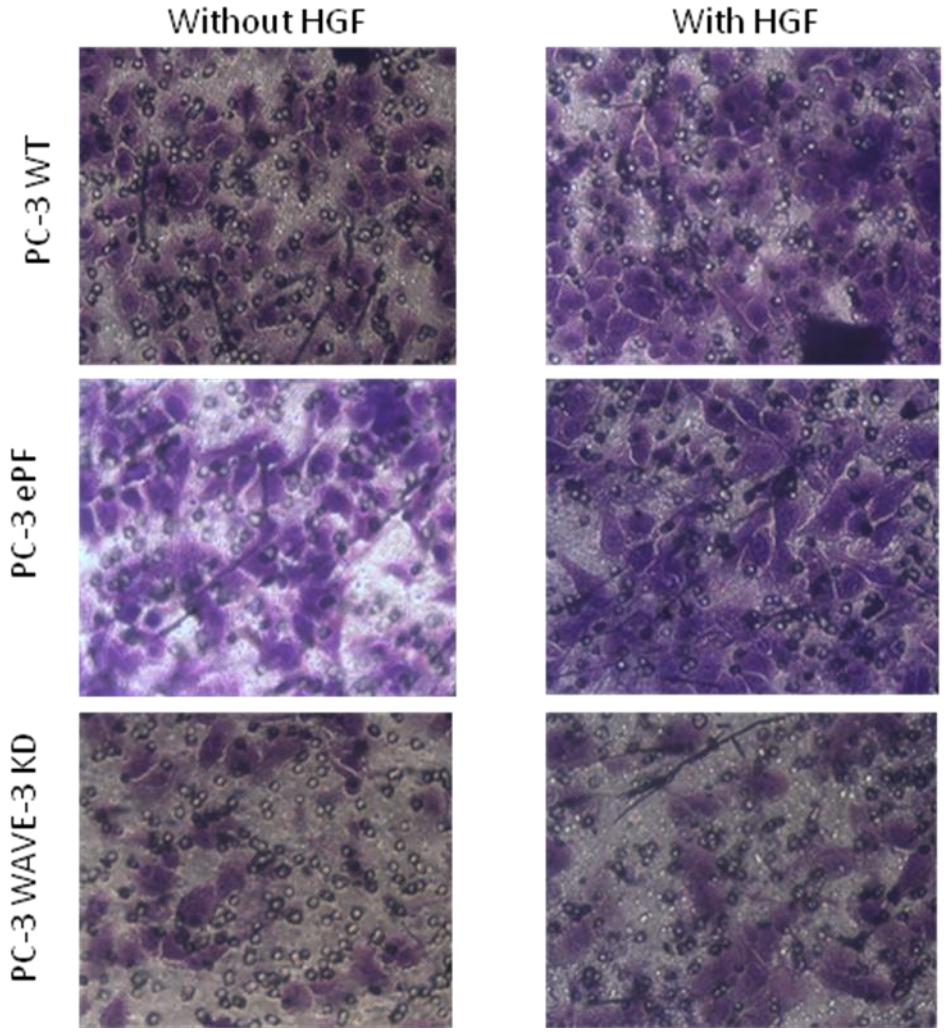

Fig 5.1: Figure illustrating the cells invaded through matrigel basement membrane and reached on the bottom of inserts, in different transgenic cell lines on invasion assay (magnification 20X). There is markedly reduced number of cells visible in PC-3$^{WAVE\text{-}3\ KD}$ cell line. This effect persisted even following addition of HGF to the medium.

Table 5.5: Descriptive statistics for cell invasion assay.

Cell line		Mean	Std. deviation	Std. error	95% confidence interval for mean		Minimum	Maximum
					Lower bound	Upper bound		
PC-3^{WT} without HGF	5	53.2344	2.50795	1.12159	50.1203	56.3484	49.50	56.50
PC-3^{PEF} without HGF	5	48.6406	7.33042	3.27827	39.5387	57.7425	36.44	55.00
PC-3$^{WAVE\text{-}3\ KD}$ without HGF	5	22.1094	5.13687	2.29728	15.7311	28.4876	14.19	28.50
PC-3^{WT} with HGF	5	110.6594	6.82422	3.05188	102.1860	119.1328	101.00	120.14
PC-3^{PEF} with HGF	5	99.4219	4.27734	1.91289	94.1109	104.7329	94.63	105.06
PC-3$^{WAVE\text{-}3\ KD}$ with HGF	5	23.1797	2.48220	1.11007	20.0976	26.2617	20.09	26.75

Table showing number of invaded cells in three cell lines without and with Hepatocyte growth factor (HGF) (40 ng/ml).

Table 5.6: Bonferroni multiple comparisons in between the PC-3 transgenic cell lines for number of invaded cells through the matrigel basement membrane

Cell type		Mean difference	Sig.	95% confidence Interval	
				Lower bound	Upper bound
PC-3^{WT} without HGF	PC-3^{ePEF} without HGF	4.59375	1.000	-5.9626	15.1501
	PC-3 $^{WAVE-3\ KD}$ without HGF	31.12500*	.0001*	20.5687	41.6813
	PC-3 ^{WT} with HGF	-57.42500*	.0001*	-67.9813	-46.8687
	PC-3 ^{PEF} with HGF	-46.18750*	.0001*	-56.7438	-35.6312
	PC-3 $^{WAVE-3\ KD}$ with HGF	30.05469*	.0001*	19.4984	40.6110
PC-3^{PEF} without HGF	PC-3 ^{WT} without HGF	-4.59375	1.000	-15.1501	5.9626
	PC-3 $^{WAVE-3\ KD}$ without HGF	26.53125*	.0001*	15.9749	37.0876
	PC-3 ^{WT} with HGF	-62.01875*	.0001*	-72.5751	-51.4624
	PC-3 ^{PEF} with HGF	-50.78125*	.0001*	-61.3376	-40.2249
	PC-3 $^{WAVE-3\ KD}$ with HGF	25.46094*	.0001*	14.9046	36.0173
PC-3$^{WAVE-3\ KD}$ without HGF	PC-3 ^{WT} without HGF	-31.12500*	.0001*	-41.6813	-20.5687
	PC-3^{PEF} without HGF	-26.53125*	.0001*	-37.0876	-15.9749
	PC-3^{WT} with HGF	-88.55000*	.0001*	-99.1063	-77.9937
	PC-3^{PEF} with HGF	-77.31250*	.0001*	-87.8688	-66.7562
	PC-3 $^{WAVE-3\ KD}$ with HGF	-1.07031	1.000	-11.6266	9.4860

Table showing the statistical comparison of the effect of WAVE-3 silencing (PC-3$^{WAVE-3KD}$) to the wild type (PC-3^{WT}) and control (PC-3^{PEF}) using Bonferroni multiple comparisons in between the groups. * The mean difference is significant at the .05 level.

5.3.4: Effect of WAVE-3 knock down on cellular matrix adhesion:

Elimination of WAVE-3 did not significantly affect the cell adhesion to the matrix, as observed in our *in vitro* cellular adhesion assay (Table: 5.8 & 5.9). The mean number of adherent cells in PC-3^{WT} and PC-3^{pEF} was 46.45 +/-7.5 and 47.02 +/- 14.6 respectively, as compared to PC-$3^{WAVE\text{-}3\ KD}$ 57.4 +/- 11.23. The small difference between the cell lines did not reach statistical significance. With the addition of HGF (40 µg/ml), the mean number of adherent cells in PC-3^{WT}, PC-3^{pEF} and PC-$3^{WAVE\text{-}3\ KD}$ were 61.2 +/-10.2, 61.68 +/- 18.7 and 63.13 +/- 14.7 respectively. As evident from cell number (Table: 5.9), there was an increase in adhesive potential of cells but there was no statistical difference between the various cell lines (p value <0.05).

Table 5.7: Descriptive statistics for cell adhesion assay

Cell type	N	Mean	Std. deviation	Std. error	95% confidence interval for mean		Minimum	Maximum
					Lower bound	Upper bound		
$PC\text{-}3^{WT}$ without HGF	5	46.4531	7.51732	3.36185	37.1191	55.7871	39.33	59.00
$PC\text{-}3^{PEF}$ without HGF	5	47.0214	14.69330	6.57104	28.7772	65.2655	29.63	70.33
$PC\text{-}3^{WAVE\text{-}3\ KD}$ without HGF	5	57.4094	11.23154	5.02290	43.4636	71.3552	43.63	71.08
$PC\text{-}3^{WT}$ with HGF	5	61.2094	10.27046	4.59309	48.4569	73.9618	44.55	71.82
$PC\text{-}3^{PEF}$ with HGF	5	61.6813	18.78015	8.39874	38.3626	84.9999	37.16	89.37
$PC\text{-}3^{WAVE\text{-}3\ KD}$ with HGF	5	63.1344	14.72992	6.58742	44.8448	81.4240	44.72	84.66

Table showing the number of adherant cells in three cell lines without and with hepatocyte growth factor (HGF) (40 ng/ml)

Table 5.8: Bonferroni multiple comparisons in between the PC-3 transgenic cell lines for number of adherent cells to the matrigel basement membrane

Cell line	Cell line	Mean difference	Sig.	95% confidence interval	
				Lower bound	Upper bound
$PC\text{-}3^{WT}$ without HGF	$PC\text{-}3^{ePEF}$ without HGF	-.56823	1.000	-28.1357	26.9993
	$PC\text{-}3^{WAVE\text{-}3\ KD}$ without HGF	-10.95625	1.000	-38.5237	16.6112
	$PC\text{-}3^{WT}$ with HGF	-14.75625	1.000	-42.3237	12.8112
	$PC\text{-}3^{PEF}$ with HGF	-15.22812	1.000	-42.7956	12.3394
	$PC\text{-}3^{WAVE\text{-}3\ KD}$ with HGF	-16.68125	.904	-44.2487	10.8862
$PC\text{-}3^{PEF}$ without HGF	$PC\text{-}3^{WT}$ without HGF	.56823	1.000	-26.9993	28.1357
	$PC\text{-}3^{WAVE\text{-}3\ KD}$ without HGF	-10.38802	1.000	-37.9555	17.1795
	$PC\text{-}3^{WT}$ with HGF	-14.18802	1.000	-41.7555	13.3795
	$PC\text{-}3^{PEF}$ with HGF	-14.65990	1.000	-42.2274	12.9076
	$PC\text{-}3^{WAVE\text{-}3\ KD}$ with HGF	-16.11302	1.000	-43.6805	11.4545
$PC\text{-}3^{WAVE\text{-}3\ KD}$ without HGF	$PC\text{-}3^{WT}$ without HGF	10.95625	1.000	-16.6112	38.5237
	$PC\text{-}3^{PEF}$ without HGF	10.38802	1.000	-17.1795	37.9555
	$PC\text{-}3^{WT}$ with HGF	-3.80000	1.000	-31.3675	23.7675
	$PC\text{-}3^{PEF}$ with HGF	-4.27188	1.000	-31.8394	23.2956
	$PC\text{-}3^{WAVE\text{-}3\ KD}$ with HGF	-5.72500	1.000	-33.2925	21.8425

Table showing the statistical comparison of the effect of WAVE-3 silencing ($PC\text{-}3^{WAVE\text{-}3KD}$) to the wild type ($PC\text{-}3^{WT}$) and control ($PC\text{-}3^{PEF}$) using Bonferroni multiple comparisons in between the groups.

5.3.5: Effect of WAVE-3 knock down on cellular motility (wounding assay):

In this time lapsed motility assay we analyzed the rate of cell movement in order to close the wound margins (Figure: 5.2 & 5.3). This method was adapted from a prior study and can be recorded as continuous process as well (Parr et al. 2001). The mean distance moved by the cells, over 90 minutes, was determined for each cell line. Cell motility was first assessed without any treatment, then monitored upon the addition of HGF/SF (40 ng/ml). Cells were shown to migrate a far greater distance following the addition of HGF. Although again, this HGF/SF induced motility was significantly reduced in PC-$3^{WAVE\text{-}3\ KD}$ cell line as compared to PC-3^{WT} and PC-3^{pEF} (Graph: 5.3 & 5.4).

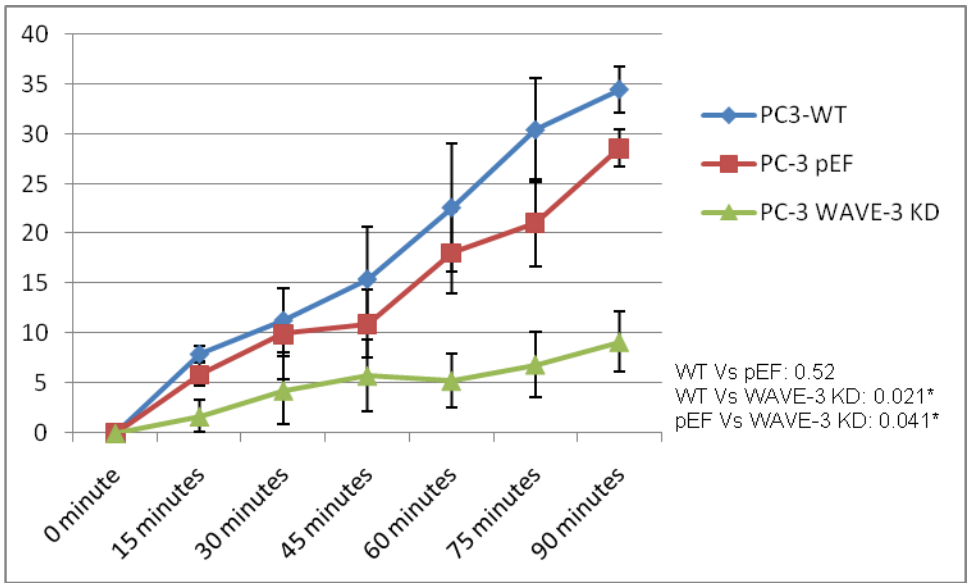

Graph 5.3: Wounding assay of different cell lines without HGF, demonstrating the effect of WAVE-3 knock down on cell migration. There was statistically significant reduction in the distance covered by PC-3$^{WAVE\text{-}3\ KD}$ cell line as compared to PC-3^{WT} and PC-3^{pEF} cell lines (* p value <0.05).

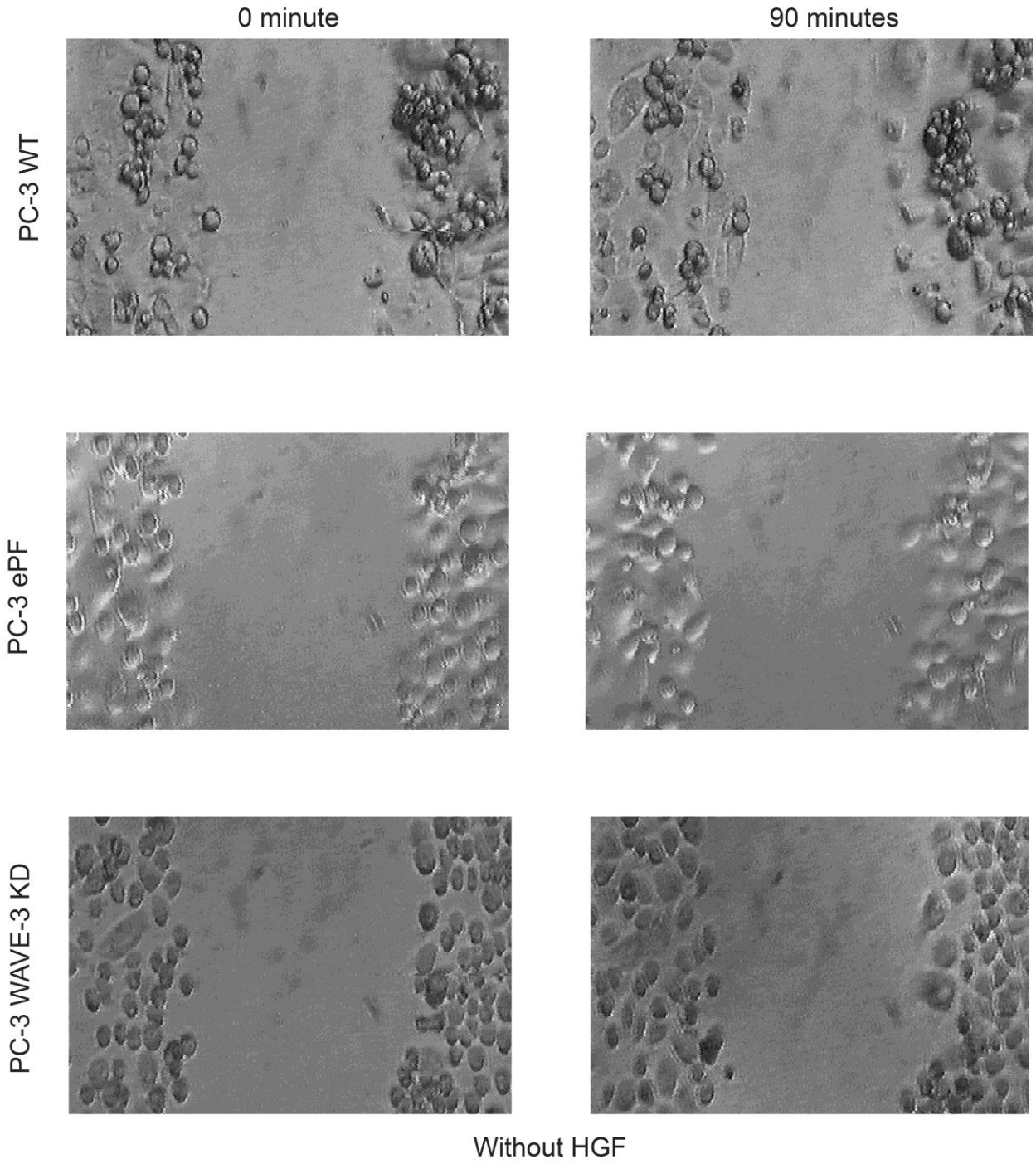

Fig 5.2: Wounding/cell migration assay in three transgenic cell lines without HGF, showing the extent of wound closure and cell movement over 90 minutes time period

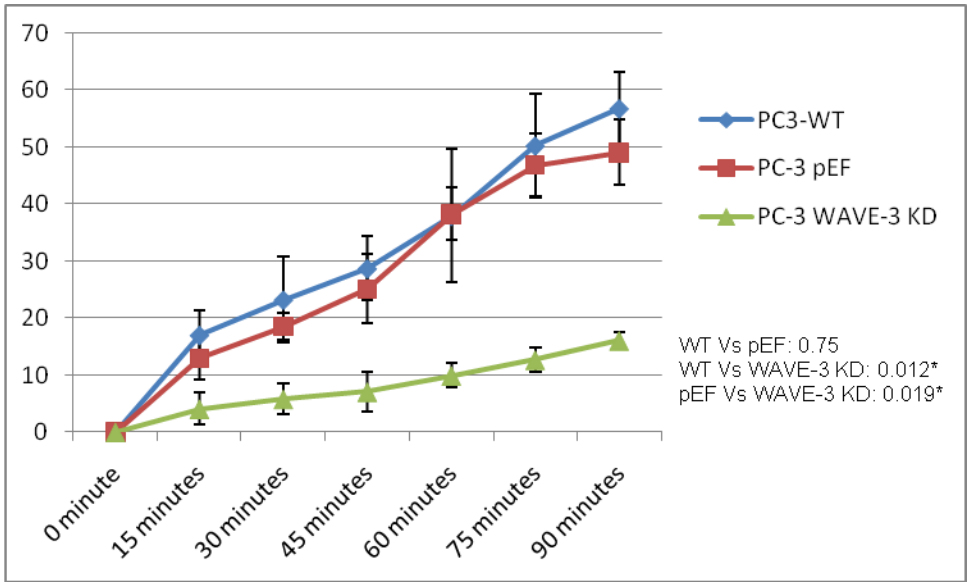

Graph 5.4: Wounding assay of different cell lines with HGF, demonstrating the effect of HGF treatment on cell migration. PC-3 ^{WT} and PC-3^{pEF} cell lines showing increased cell migration with reduced effect on PC-3$^{WAVE\text{-}3KD}$ cell line. There was statistically significant reduction in the distance covered by PC-3$^{WAVE\text{-}3\ KD}$ cell line as compared to PC-3^{WT} and PC-3^{pEF} cell lines (* p value <0.05).

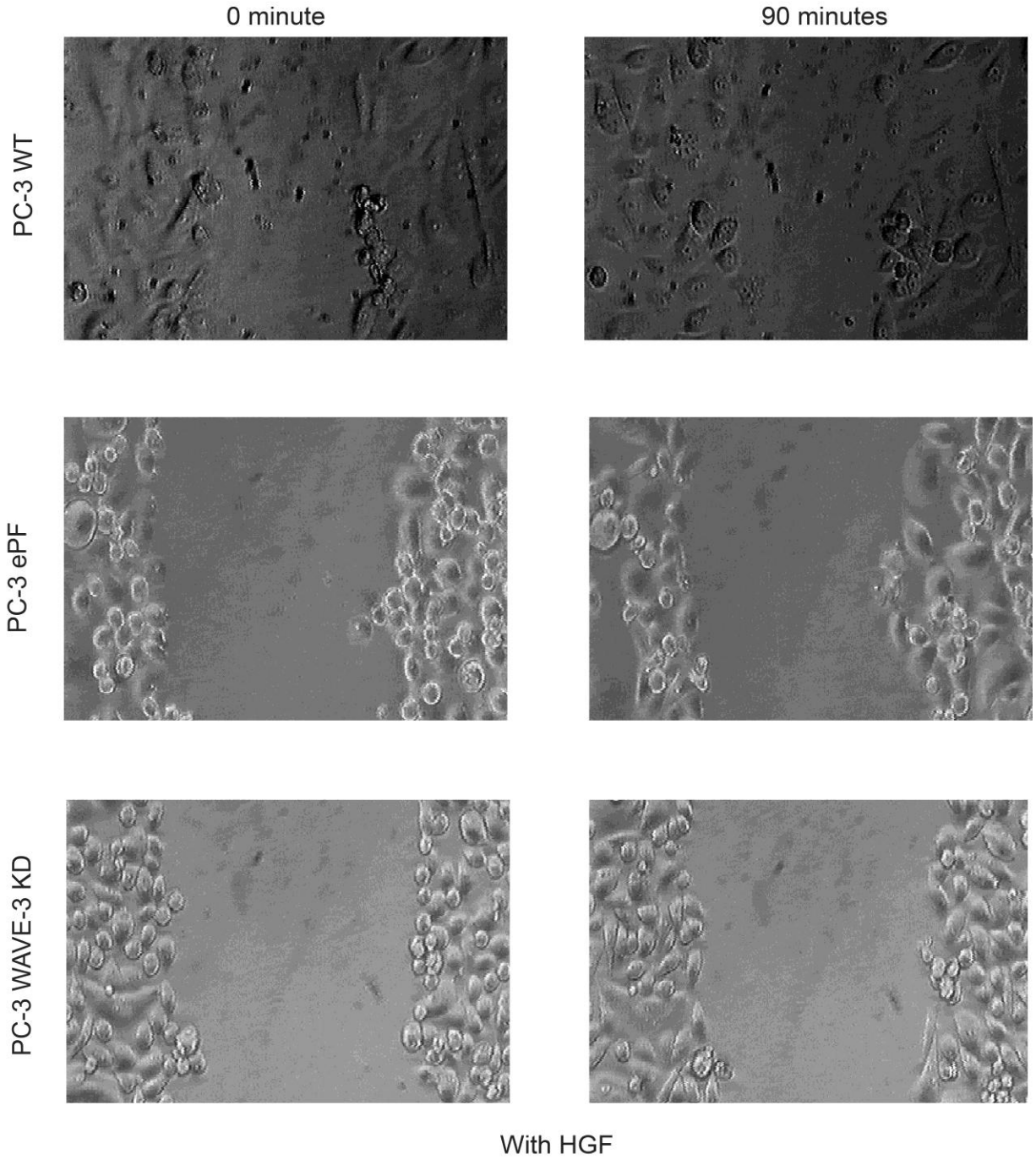

Fig 5.3: Wounding/cell migration assay in three transgenic cell lines with HGF, showing the extent of wound closure and cell movement over 90 minutes time period

5.4: Discussion:

Many actin-binding regulatory proteins have been identified and classified according to their effects on actin filaments. These proteins do not function independently but are involved in maintenance of perfect harmony to regulate the pivotal role of actin in cellular movement. Cell migration through the extracellular matrix (ECM) begins with the formation of cell protrusions that contain filamentous actin (F-actin). This process involves cell stimulation through multiple pathways involved in cellular polarization towards a specific direction. The processes of these cell protrusions heavily depend upon polymerization of F-actin. If this process of polymerization can be inhibited, it can result in inhibition of cellular movement resulting in potential prevention of invasion and metastasis. This crucial step of actin polymerization is controlled by actin related protein 2/3 (ARP 2/3). WASP family proteins play an important role by triggering the activation of the complex in response to mitogenic stimuli via the Rho family of peptides (RhoA, Rac, and Cdc42) (Etienne-Manneville et al. 2002). WASP is derived from the clinical condition called the “Wiskott-Aldrich syndrome”, which manifests due to malfunction of the actin cytoskeleton in the immune system, resulting in a clinical triad of immunodeficiency, thrombocytopenia, and eczema, due to inadequate cellular movement. WAVE-1, 2 and 3 are members of the WASP family along with N-WASP and WASP. The role of WAVE-3 in cellular movement has been documented in knock down studies involving breast cancer cells MDA-MB-231 (Sossey-Alaoui et al. 2007) and prostate cancer cell lines (Fernando et al. 2010).

The role of hepatocyte growth factor/scatter factor (HGF/SF) is well established in metastatic process through its effects on proliferation, dissociation, migration and invasion. Higher HGF levels have been demonstrated in hormone refractory prostate cancer and associated with poor prognosis. Strong expression of WAVE-3 has been documented in prostate cancer specimens and invasive cancer cell lines from earlier studies in our department (Fernando et al. 2010). In this study we focused on the role of WAVE-3 in the mediation of these changes with emphasis on prostate cancer cell lines. Our present study provides evidence that WAVE-3 has an important role in HGF induced cellular motility and possible metastasis without a significant effect on cellular growth. Following genetic silencing of WAVE-3, analysis of functional studies revealed a statistically significant reduction in HGF induced cellular motility as compared to control cell lines. HGF promotes cell invasion through the matrigel basement membrane in vitro which appears markedly reduced following WAVE-3 knock down. In our cellular motility experiments, HGF was able to induce non-directional (cytodex beads assay) as well as directional movement (wound closure assay) in the parent cell line (PC-3) and the control cell line with empty plasmid (PC-3^{PEF}). HGF was not able to induce these effects following elimination of WAVE-3. This phenomenon can possibly be attributed to reduced lamellipodia formation on the leading edge of cellular movement, as suggested from prior studies (Sossey-Alaoui et al. 2007; Fernando et al. 2010).

Following skeletal muscle injury, muscle satellite cells proliferate and migrate toward the site of muscle injury to start the process of regeneration. This migration is mainly stimulated through the secretion of HGF from injured and intact muscle fibers. Kawamura et al, utilized mouse derived skeletal muscle cells and demonstrated that

HGF promotes directional movement in these cells. Knock-out experiments involving WAVE-2 and N-WASP resulted in prevention of lamellipodia formation and cellular movement, in response to HGF. Moreover, exogenous expression of wild-type N-WASP or WAVE2 promoted lamellipodia formation and migration (Kawamura et al. 2004).

Similarly Sossey-Alaoui et al, demonstrated that WAVE-3 was in the leading edge of cell during cell migration in MDA-MB-231 cells. Platelet derived growth factor treatment induced chemotactic migration towards PDGF in three dimensional migration chambers. Knock down of WAVE-3 in these cells through small interfering siRNAs resulted in reduced migrational potential of these cells. With the addition of PDGF treatment, these cells failed to show any significant increase in migration and lamellipodia formation.

Our findings from this study indicate the important role of WAVE-3 in growth factor induced cell migration in prostate cancer cells. The role of WAVE-1 and WAVE-2 in cell migration has been documented previously in different cell lines. However it is very important to consider that these important members were well expressed in our cell lines, which makes the role of WAVE-3 even more important in this setting.

Chapter 6
Role of paxillin in reduced cellular motility following WAVE-3 knock down.

6.1: Introduction:

A metastatic cancer cell has to undergo a remarkable transition in cell shape during the process of metastasis. Dynamic modifications in the actin cytoskeleton mediate these changes in shape and cellular movement. Cancer cells interact with the surrounding micro environment through formation of small cell projections known as lamellipodia and filopodia. Formation of these small cell projections is controlled by small GTPases Rac and Cdc42 respectively (Suetsugu et al. 2003). The small projections transiently interact with the extracellular matrix and focal adhesion complex sites. Ezrin/Radixin/Moesin (ERM) proteins were shown to be required for the formation of focal adhesion complexes and stress fibers downstream of Rho GTPases activation (Mackay et al. 1997). Ezrin is involved in the dissociation of cell-cell contacts triggered by HGF stimulation through its interaction with the Fes kinase and in the formation of membrane extensions (Naba et al. 2008). Ezrin promotes cell motility in response to HGF treatment as measured by the ability of epithelial cells to close a wound (Crepaldi et al. 1997). Following HGF stimulation of epithelial cells, ezrin is rapidly recruited to the lateral membrane and to the leading edge of migrating cells where it is supposed to play a role in the control of actin polymerization (Crepaldi et al. 1997). Altogether these data show that ERM proteins convey signals elicited by membrane receptors to the actin cytoskeleton to regulate cell migration. However, it remains unclear how ERM proteins control the reorganization of the actin cytoskeleton during cell migration. A likely hypothesis is that through their phosphorylation ERM proteins will recruit regulators of actin polymerization. These interactions play a key role in linking the external

environment with intracellular machinery. The functional status of these proteins may be an important factor in tumor progression. In a comparative study, involving protein profiles of pancreatic cancers without and with lymph node metastasis indicated an increased expression of moesin and radixin in the lymph node metastasis-positive group and a change in ezrin phosphorylation, but not expression.

Integrins are important constituents of focal adhesions and act as intermediate molecules between substrates in the microenvironment and actin cytoskeleton. Extracellular surface projections of these molecules serve as receptor for different growth factors while intracytoplasmic tail ends recruit a variety of cytoplasmic proteins which mediate different cellular activities. Paxillin is a key member of integrins, which acts as a nexus to control the activity of small GTPases. Primarily paxillin is thought to be involved in coordination of cellular movements but with the passage of time its role in other activities is also emerging. Although we will be focusing our attention on the role of paxillin in the regulation of the actin cytoskeleton through which paxillin exerts its effect on pathological processes such as tumor cell invasion (Azuma et al. 2005). Paxillin is a well preserved gene in cancer and no mutations have been documented in a wide variety of tumors. Kim et al. analyzed somatic paxillin mutations in 45 lung, 45 gastric, 45 colorectal, 45 breast, 45 liver and 45 prostate cancers by polymerase chain reaction and single-strand conformation polymorphism assay. Paxillin mutation was absent in lung cancers and other common solid cancers, suggesting that paxillin mutation may not play a principal role in cancer development (Kim et al. 2011). However it has been suggested that an increase in paxillin phosphorylation is correlated with the metastatic ability of the cell (Rodina et al. 1999). Phosphorylation of the FAK

and paxillin proteins is involved in multiple signal transduction pathways during metastatic cascade, such as interaction with extracellular matrix. Phosphorylation of paxillin and FAK appears to be dependent upon the Src family of protein kinases (v-Src) (Richardson et al. 1997). Multiple sites of phosphorylation exist on the paxillin molecule which is targeted by different kinases in response to binding of growth factors like HGF (Jiang et al. 1996). Multiple cytokines have been identified which play important roles in local progression and promotes metastatic potentials. Hepatocyte growth factor is one of these cytokines which has been identified as a promoter of aggressive disease and metastasis in prostate cancer (Gupta et al. 2008).

Results from our prior study have demonstrated that WAVE-3 knock down results in reduced cellular motility in prostate cancer cells. Interestingly these cells were not able to elaborate any significant changes in their motility even after addition of HGF. In this part of our study we tried to investigate the role of different important intermediary proteins which are responsible for mediating the changes in the cell cytoskeleton, in response to HGF stimulation.

6.2: Materials and methods:

6.2.1: Cell lines:

The human prostate cancer cell line PC-3 was used throughout this study. This was originally obtained from the European Collection for Animal Cell Culture (ECACC, Porton Down, Salisbury, UK). Cells were routinely cultured with Dulbecco's modified

Eagle medium (DMEM) supplemented with 10% foetal calf serum, penicillin and streptomycin (Gibco BRC, Paisley, Scotland). The PC-3 cell line with WAVE-3 knock down and control cell line with empty plasmid were generated and maintained in the maintenance medium as described before in chapter:3 (3.2). This cloning technique has been tested and extensively used previously (Jiang et al. 2001 and 2005). Expression of WAVE-3 knock down was confirmed both on RNA and protein levels.

6.2.2: SDS-polyacrylamide gel electrophoresis (SDS-PAGE) and western blot:

Western blotting was used to evaluate the expression of different cytoskeletal proteins in cell lysate from prostate cancer cell lines. All three cell lines including PC-3 ^{WT}, PC-3 ^{pEF} and PC-3$^{WAVE\text{-}3KD}$ were cultured to confluent layers in duplicate. All cells used in this study were subjected to a period of two hours serum starvation prior to any treatment. One set of cell lines was treated with HGF 40ng/ml for 60 minutes in serum free medium while the other set was treated with serum free medium alone. Cells were washed with phosphate buffered saline and scrapped. Cells were pelleted, washed and then lysed in HCMF buffer. This buffer contained 1% Triton, 0.2% SDS and 100 mg/ml PMSF, and lysed the cells for 45 min at 4°C. This was followed by centrifugation at 13,000g for 10 min and the resulting protein lysates were collected. Following protein quantification, the samples were adjusted to equal concentrations with sample buffer and then boiled at 100°C for 5 min. Equal amounts of protein from each cell line (20 µg/lane) were resolved on an 8% polyacrylamide gel by electrophoresis. These separated protein samples were then electroblotted onto a nitrocellulose membrane,

before blocking in 10% skimmed milk for 60 min. The membranes were probed with selection of antibodies (paxillin, FAK, ezrin, radixin and moesin), followed by a peroxidase conjugated secondary antibody (1:800) (Sigma-Aldrich Co. Ltd., Poole, Dorset, UK). Protein bands were visualised using an enhanced chemiluminescence (ECL) system (Kirkegaard and Perry Laboratories, Maryland), while the protein band size was determined using a pre-stained molecular weight marker.

6.2.3: Immunoprecipitation:

Sub-confluent PC-3 cells (PC-3^{WT}, PC-3^{pEF} and PC-$3^{WAVE\text{-}3KD}$) were cultured in duplicate. One set were treated with serum-free DMEM medium for 1 h and other set was treated with HGF (40 ng/ml) for 60 minutes. Following this, the cells were washed with phosphate buffered saline, then scraped off and lysed as above (SDS free lysis buffer). Tyrosine phosphorylation was detected following immunoprecipitation with the PY20 antibody (1:500) (Santa Cruz Biotechnology, Calne, Wiltshire, UK). This antibody is specific for tyrosine in its phosphorylated form, was incubated at 4°C for 1 h, followed by the addition of 5 ml of protein A/G agarose (Santa Cruz Biotechnology, Calne, Wiltshire, UK). After overnight binding at 4°C the antigen antibody complexes were pelleted by centrifugation, washed three times in lysis buffer and then solubilized with sample buffer. The immunoprecipitates were separated by SDS–PAGE (10% gel), electroblotted onto a nitrocellulose membrane, and probed with specific antibodies (see Western blotting of total protein for details, chapter:3, 3.4.1). Proteins that reacted with the antibody were detected using the ECL system as above. Densitometry was

performed using Image J software, following the instruction available on line (imagej.nih.gov/ij/). Values were normalized against the loading control or housekeeping gene expression i.e. GAPDH. The data obtained from these methods was analyzed statistically using Student's *t* test (Excel software).

6.2.4: Immunofluorescent staining (IFC)

PC-3 cells (PC-3^{WT}, PC-3^{pEF} and PC-$3^{WAVE\text{-}3KD}$) were seeded in chamber slides (Nunc, Denmark), at a density of 20,000 cells/well, and incubated for 60 minutes with and without HGF (40 ng/ml). Following the incubation period the cells were washed with BSS, fixed with 4% formalin for 20 min and then permeabilised with Triton X-100 (0.1%) for 15 min. The cells were washed again with BSS and then blocked with 10% horse serum for 40 min. Cells were then treated with a primary antibodies (paxillin, phophorylated paxillin, FAK, ezrin, radixin and moesin) for 60 min, washed in 3% horse serum in BSS, and then the secondary antibody (anti-mouse or anti-goat IgG TRITC/FITC conjugate, 1:400 dilution), was added for a further 40 min. Following 3 washes with 3% horse serum and BSS the slides were mounted with Fluosave and allowed to dry (Fluosave, Calbiochem, Nottingham, UK), prior to examination under a fluorescent microscope and acquisition of pictures.

6.3: Results:

6.3.1: Expression and phosphorylation status of different cytoskeletal proteins:

Following documentation of the well defined role for WAVE-3 in cellular movement, we tried to investigate the underlying mechanism involving different proteins required in the spatial orientation of cellular movement. The role of paxillin acting as a nexus for co-ordination of different proteins has been studied before and tyrosine phosphorylation has been observed as an important step in HGF induced cellular changes in prostate cancer cells (Parr et al. 2001). We analyzed the expression of paxillin and its tyrosine phosphorylation following elimination of WAVE-3 and response to addition of HGF.

Expression and tyrosine phosphorylation of ezrin, radixin, moesin, FAK and paxillin were detected by immunoprecipitation and subsequent western blotting with protein specific antibodies. In our experiment, all cell lines revealed good expression of paxillin along with the control sample. There were no changes in the expression of paxillin in three cell lines (Fig: 6.1 and Graph: 6.1). However levels of phosphorylated paxillin after WAVE-3 knock down were reduced. When cells were treated with HGF (40ng/ml for 60 minutes), there was a significant increase in the levels of phosphorylated paxillin (Fig: 6.2 and Graph 6.2) in PC-3^{WT} and PC-3^{pEF} cell lines but PC-$3^{WAVE\text{-}3KD}$ failed to show such a response.

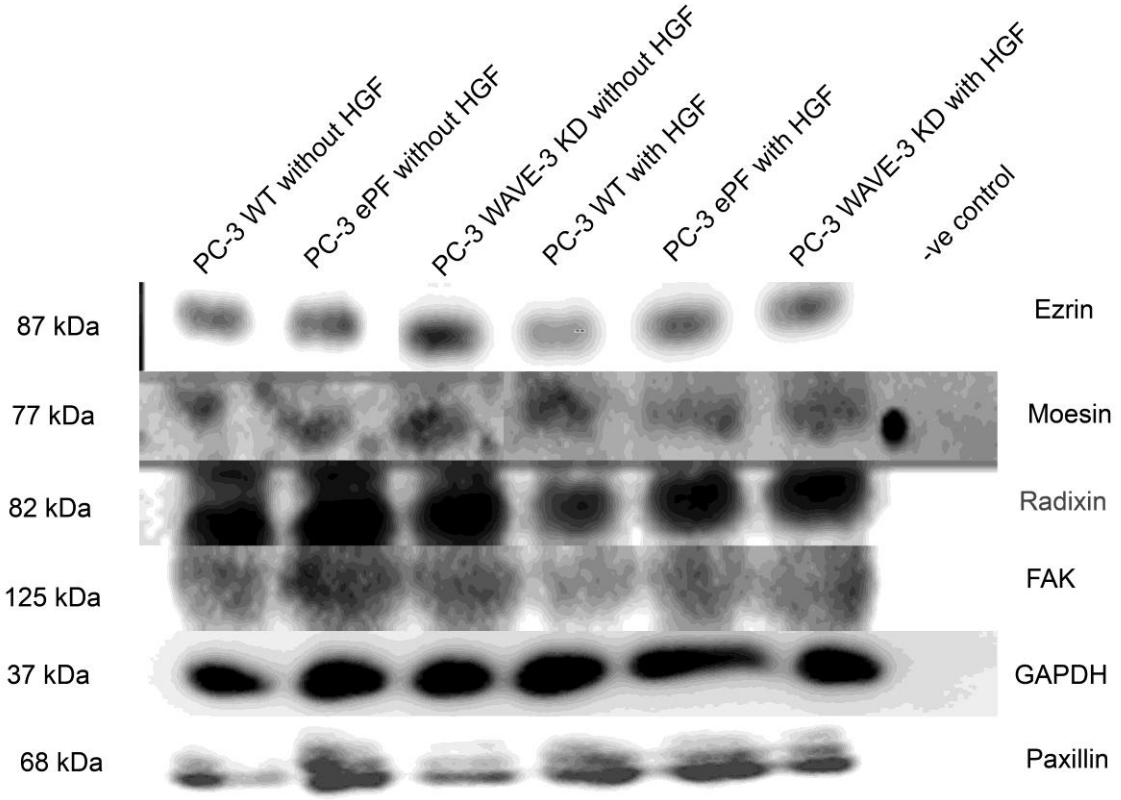

Fig 6.1: Western blotting showing expression of ezrin, moesin, radixin, FAK, paxillin and GAPDH in three cell lines without any treatment and following treatment with HGF. Expression of these proteins did not show any gross difference in expression.

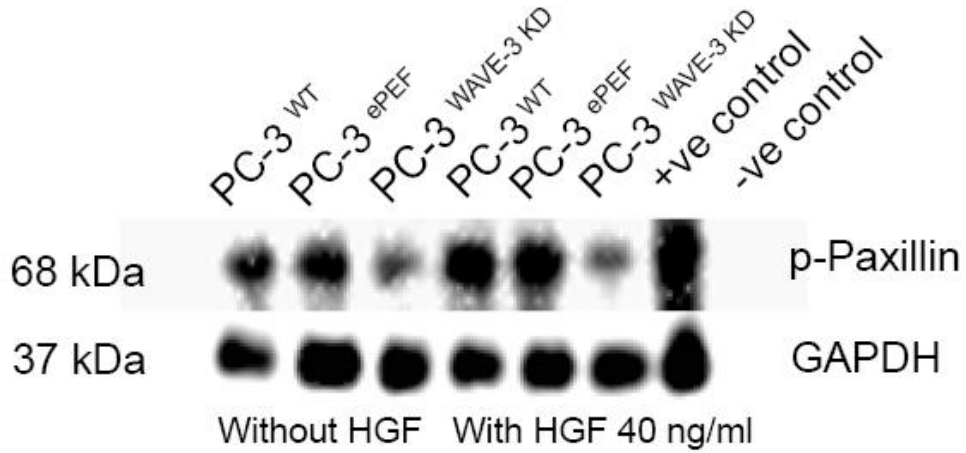

Fig 6.2: Western blotting showing expression of phosphorylated paxillin and GAPDH in three cell lines without and following treatment with HGF. This figure illustrates the reduced band density for p-paxillin in PC-$3^{WAVE\text{-}3KD}$ cell line as compared to PC-3^{WT} and PC-3^{ePEF} cell lines. Reduced level of phosphorylated paxillin was demonstrated following treatment of cells with HGF in PC-$3^{WAVE\text{-}3KD}$ cell line. In contrast PC-3^{WT} and PC-3^{ePEF} cell lines showed increased expression of phosphorylated paxillin following treatment with HGF.

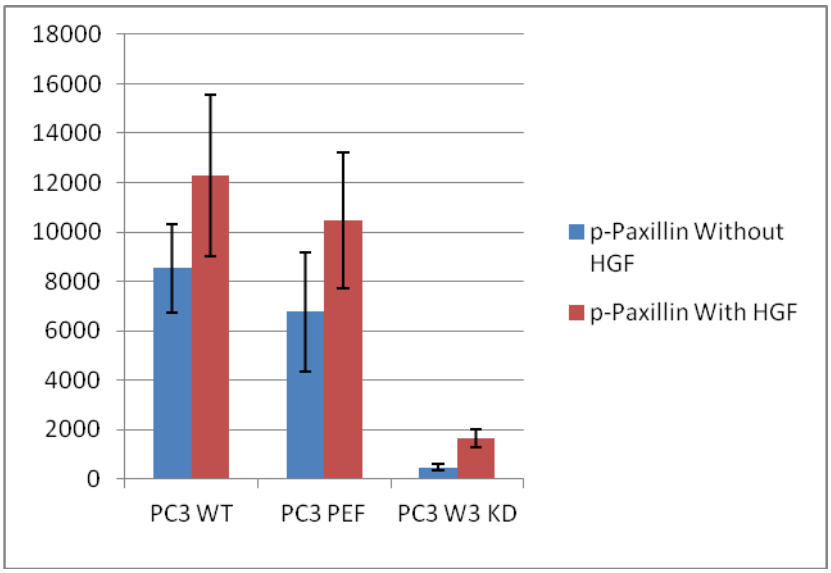

Graph 6.1: Quantification of phosphorylated paxillin bands from western blotting (pixels) in three transgenic cell lines with and without HGF treatment. Experiment was repeated twice in duplicate fashion.

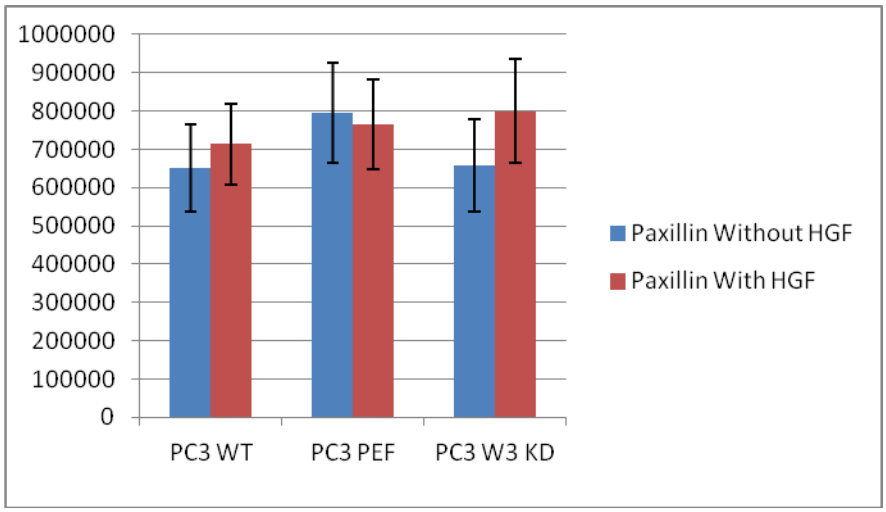

Graph 6.2: Quantification of paxillin bands from western blotting (pixels) in three transgenic cell lines with and without HGF treatment. Experiment was repeated twice in duplicate fashion.

6.3.2: Immunofluorescent detection of paxillin and ERM protiens:

All PC-3 cell lines (PC-3^{WT}, PC-3^{pEF} and PC-$3^{WAVE\text{-}3KD}$) demonstrated good levels of staining for paxillin that was localised to the focal adhesion plaques. However, the level of staining in the PC-$3^{WAVE\text{-}3KD}$ cell line was remarkably lower than PC-3^{WT}, PC-3^{pEF} cell lines. Upon addition of HGF the number of focal adhesions was increased and degree of paxillin staining concentrated in the focal adhesions was greatly enhanced in PC-3^{WT}, PC-3^{pEF} cell lines, with more prominent peripheral location. Furthermore, these cells also displayed membrane ruffling and extensive spreading. The PC-$3^{WAVE\text{-}3KD}$ cell line failed to exhibit these enhanced changes (Fig: 6.3). No obvious difference was seen in the immunofluorescent staining of FAK, ezrin, radixin and moesin, whilst a more enhanced staining was seen in the WAVE3 knockdown cells on exposure to HGF (Fig: 6.4, 6.5, 6.6 & 6.7).

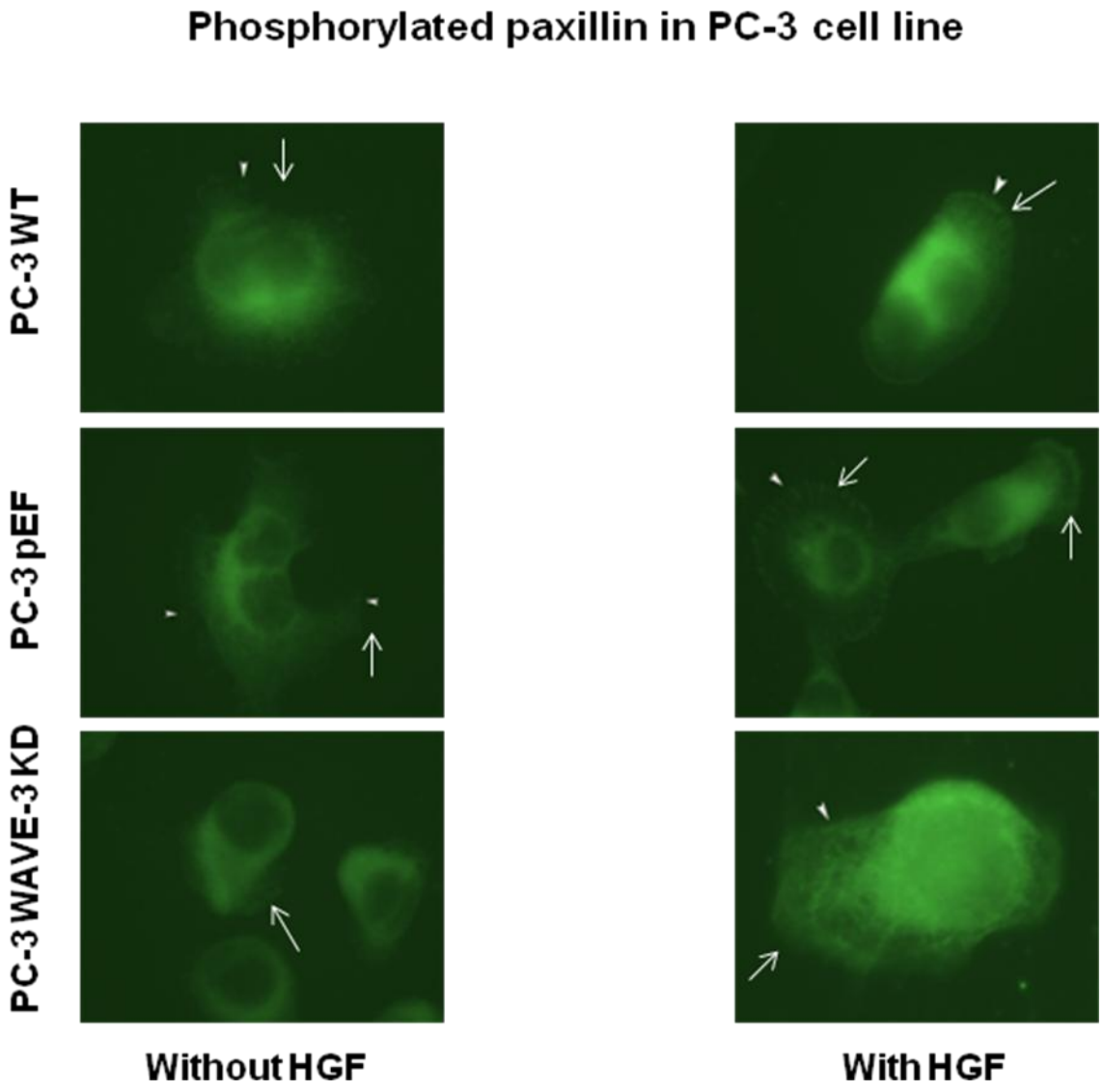

Figure 6.3: Immunoflourescent cytology for p-paxillin in different PC-3 cell lines (FITC). Arrows pointing to the prominent areas of immunoflourescent antibody, indicating the presence of p-paxillin mainly in the periphery of cells.

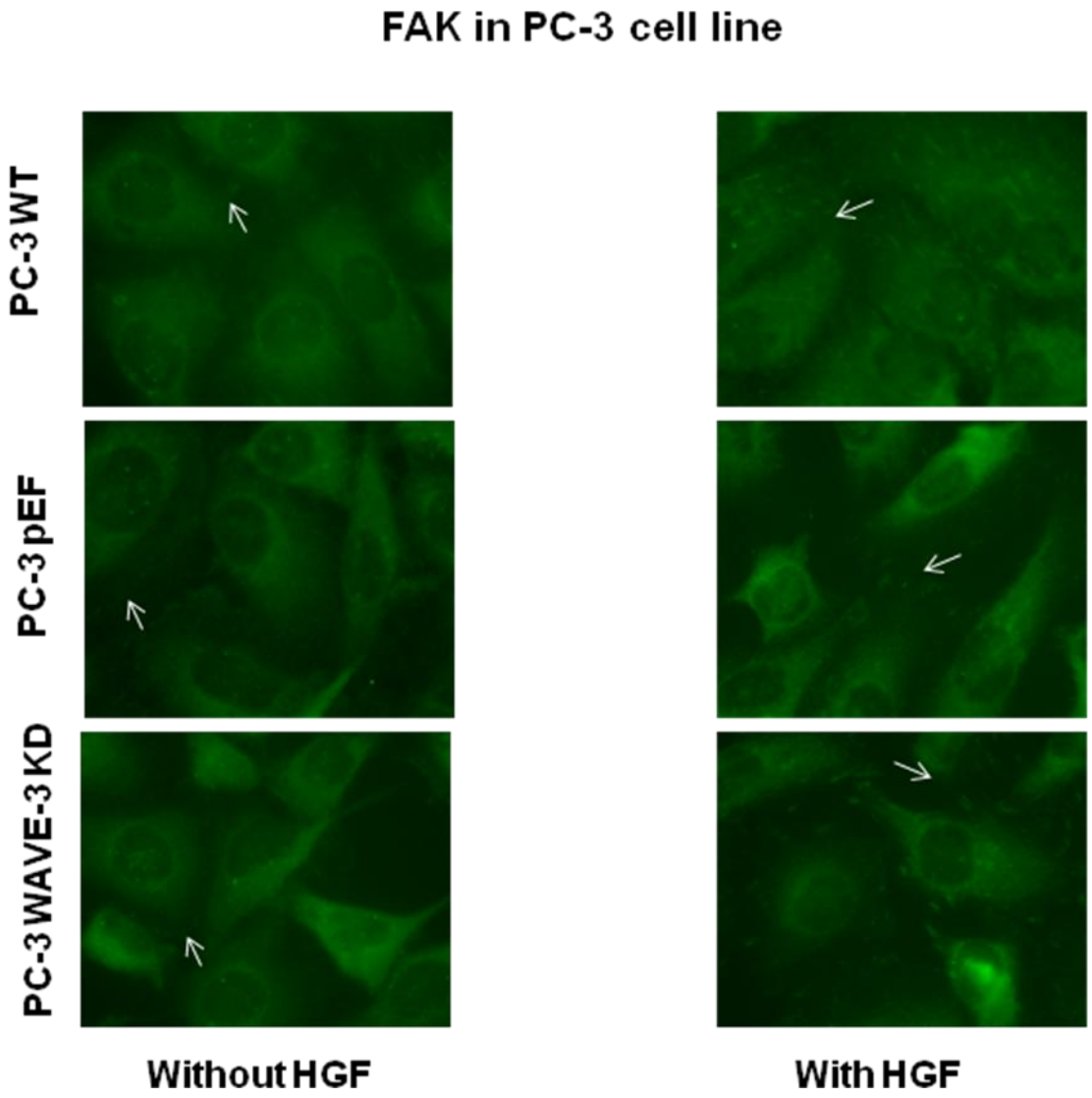

Figure 6.4: Immunoflourescent cytology for FAK in different PC-3 cell lines (FITC). Arrows pointing to the prominent areas of iImmunoflourescent antibody, indicating the presence of FAK.

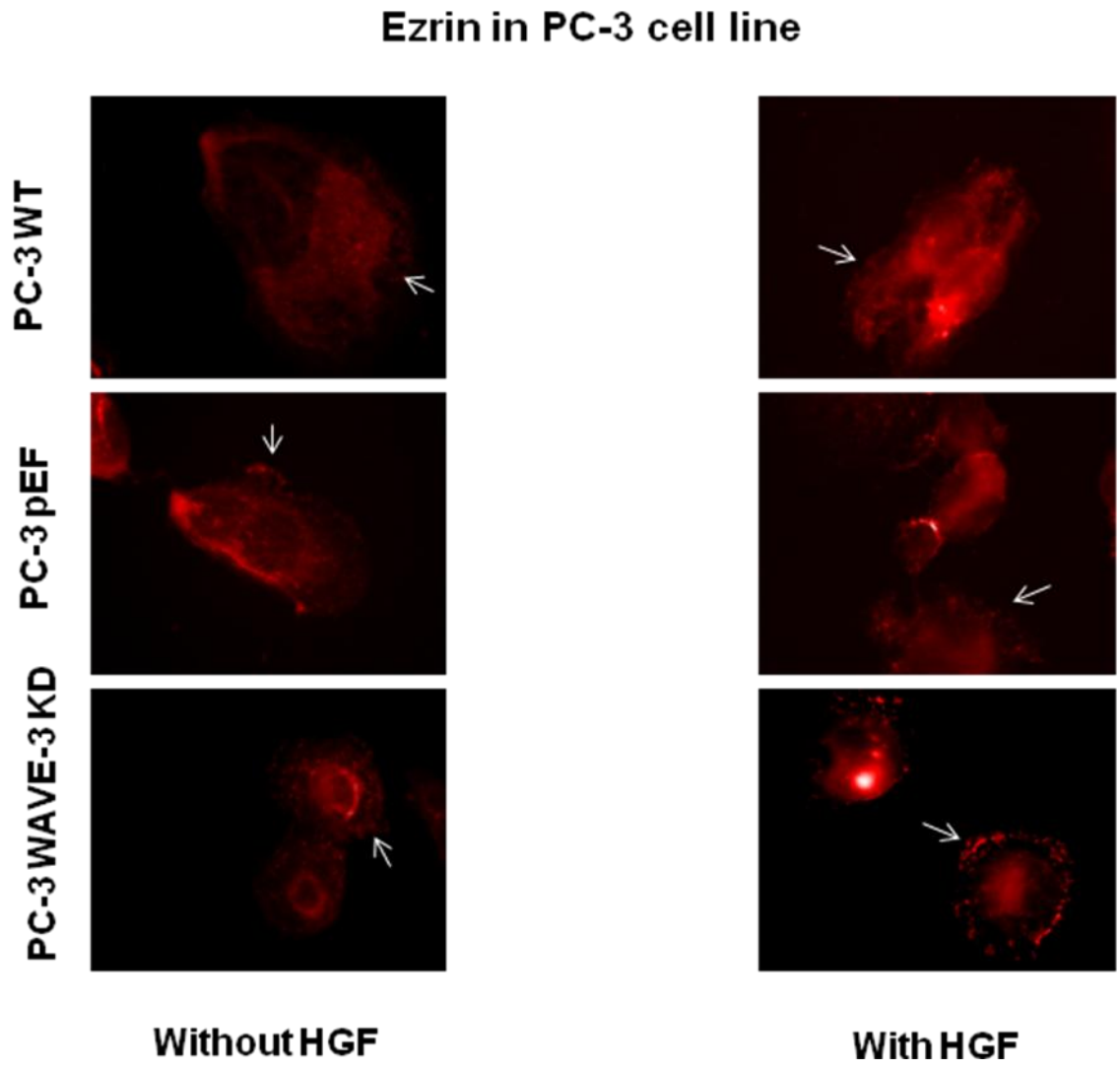

Figure 6.5: Immunoflourescent cytology for ezrin in different PC-3 cell lines (TRITC). Arrows pointing to the prominent areas of immunoflourescent antibody, indicating the presence of ezrin.

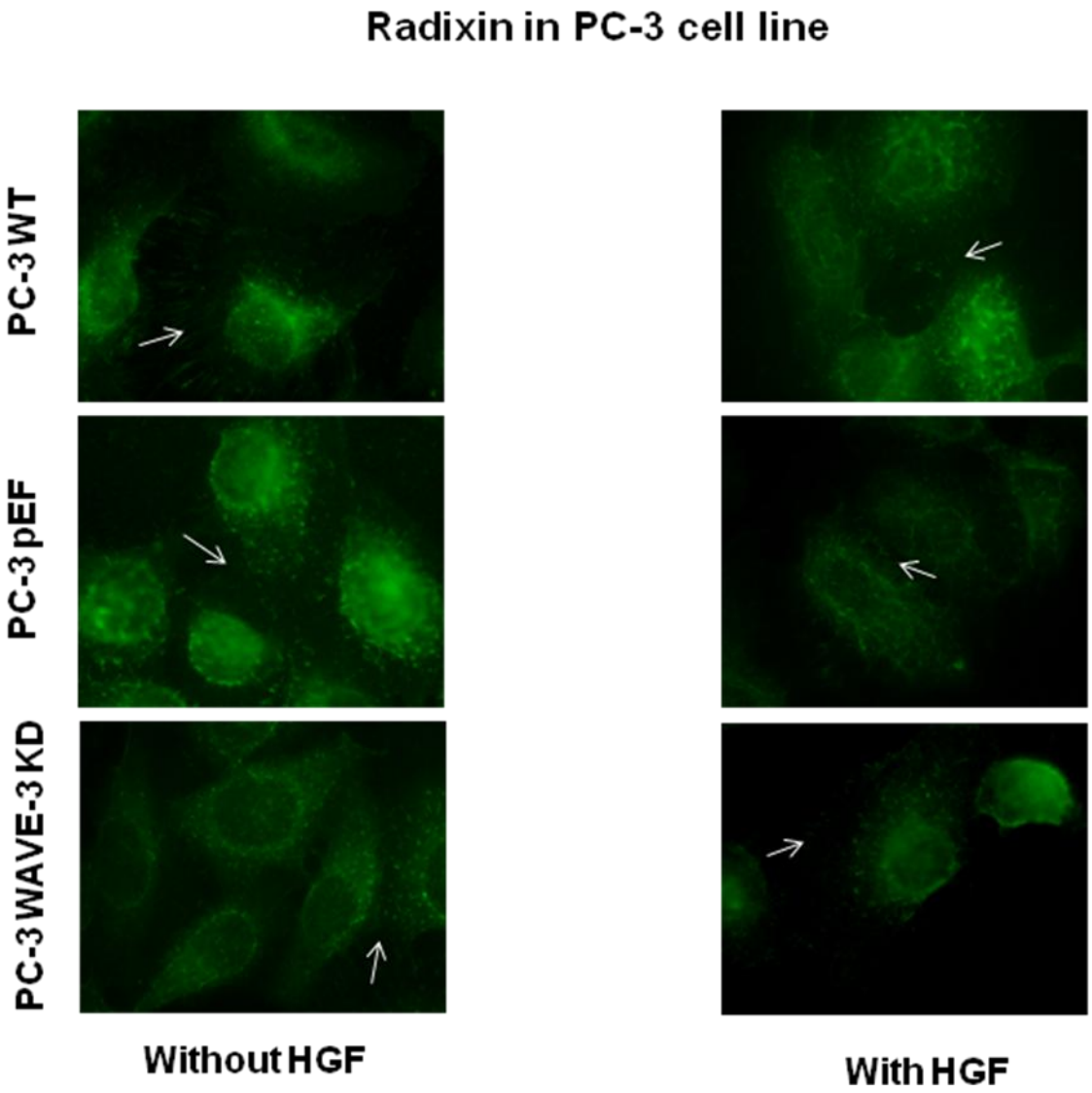

Figure 6.6: Immunoflourescent cytology for radixin in different PC-3 cell lines (FITC). Arrows pointing to the prominent areas of immunoflourescent antibody, indicating the presence of radixin.

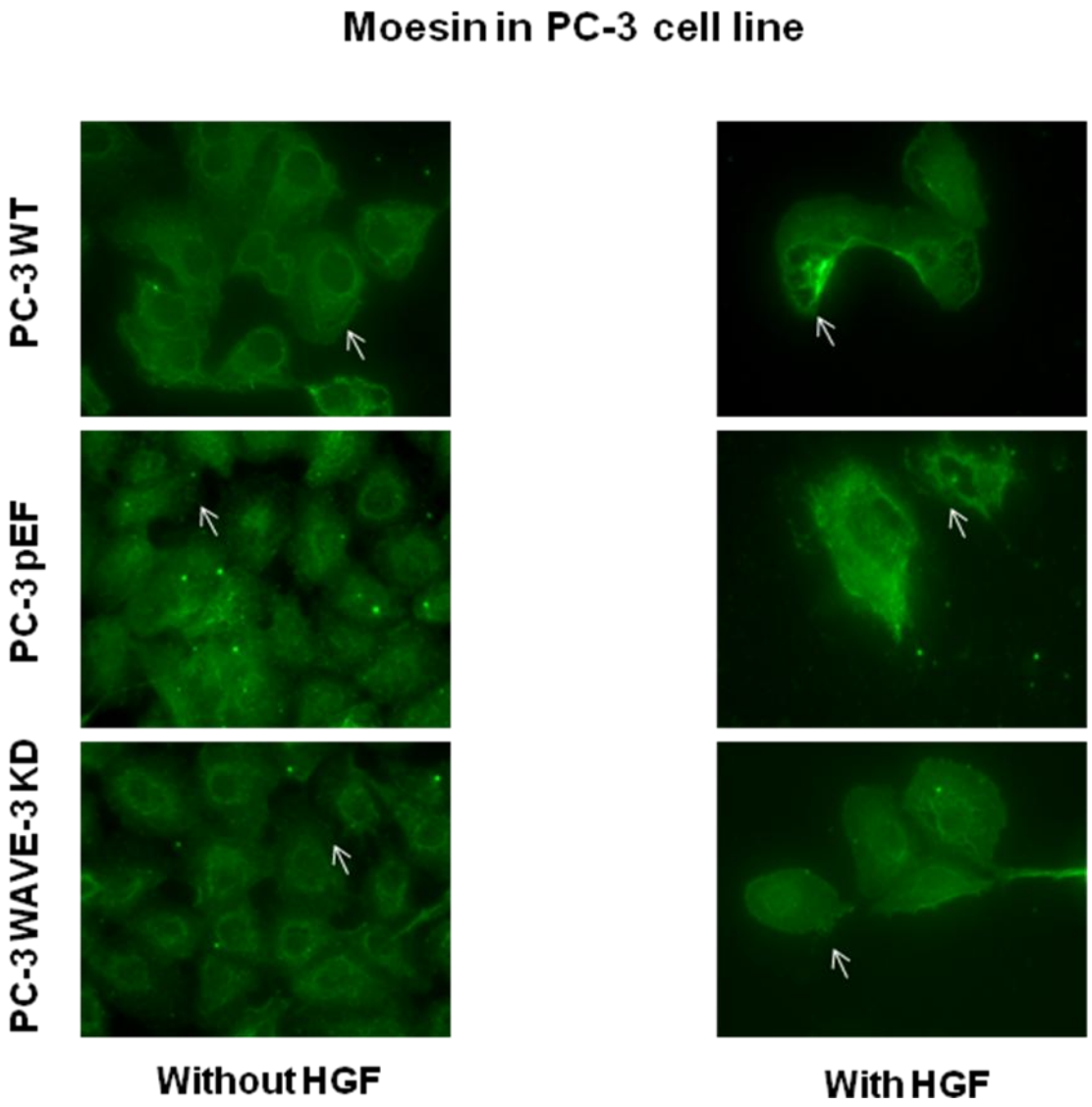

Figure 6.7: Immunoflourescent cytology for moesin in different PC-3 cell lines (FITC). Arrows pointing to the prominent areas of immunoflourescent antibody, indicating the presence of moesin.

6.4: Discussion:

Tumour stage at the time of diagnosis has a major impact on the subsequent treatment and future prognosis of prostate cancer patients. From a therapeutic point of view, prevention of metastasis would have an important role in improving survival of the patient. The metastatic process is a complex of multiple successive procedures and involves a multitude of molecules being expressed at appropriate time intervals. Adhesion of tumor cells to the matrix and coherant interactions are critical for the metastatic process. This interaction relies heavily on the formation of complexes known as focal adhesion complexes. These complexes not only provide cells with anchorage to the ECM, but also transmit signals from the environment to the actin cytoskeleton. During formation of these focal adhesions, integrin clustering occurs along with stimulation of different kinases associated with these molecules. Paxillin is a cytoskeletal docking protein which localizes to these complexes (Jiang et al. 1996) and its active phosphorylated state has been associated with increased metastatic ability of cells (Rodina et al. 1999).

Extensive research has been performed to investigate the key steps in this procedure and the different factors controlling cell migration. The role of the actin cytoskeleton in this process has been well documented and newer research is being carried out to investigate the molecules involved in the regulation of actin dynamics. The actin cytoskeleton is dynamically remodeled during cell migration and this reorganization

produces the force necessary for cell migration. Actin-related protein (ARP) 2/3 complex-dependent actin polymerization and its regulation are of particular interest in cancer cell metastasis. WASP family proteins play an important role by triggering the activation the actin-related protein (Arp) 2/3 complex in response to external stimuli like HGF, via the Rho family of peptides (RhoA, Rac, and Cdc42) (Hall et al. 1998). WAVE-1, 2, and 3 are members of the WASP family along with N-WASP and WASP. Various studies have shown the functions of WAVE-3 through genetic silencing in different cancer cell lines like breast and prostate. In our prior laboratory work we have documented that WAVE-3 knock down results in reduced cellular motility and invasion. Another important aspect of these results was the absence of increased motility and invasion following addition of HGF to the cellular environment. It is important to note that HGF has emerged as an important factor in prostate cancer dynamics and is known to be clinically associated with more aggressive phenotypes of prostate cancer and is well documented to induce aggressive changes in prostate cancer cell lines. A previous study has reported the localization of paxillin to the actin stress fibre associated ends in the focal adhesions (Norman et al. 1998).

HGF is known to enhance tumor matrix adhesion and interactions (Jiang et al. 1996). This study examined the effects of hepatocyte growth factor (HGF) on adhesion of HT115 (human colon cancer) and MDA-MB-231 (human breast cancer) tumor cells to the extracellular matrix. It was exclusively associated with the tyrosine phosphorylation of focal adhesion kinase (FAK) and paxillin located to the focal adhesion area. HGF was also associated with increased tyrosine phosphorylation of FAK and paxillin and increased formation of focal adhesion complexes as well. Our

results revealed that HGF enhanced the phosphorylation and peripheral localization of paxillin, in the control cells. However this response was very limited in the cell line with loss of WAVE-3. This situation resulted in reduced cell migration and reduced metastatic potential in these cells. These observed effects can be potentially considered in the future for therapeutic values.

Parr et al demonstrated that HGF was able to induce paxillin phosphorylation in PC-3 prostate cancer cells with increased cellular motility. These effects were blocked by NK40 along with reduced paxillin in the focal adhesion complexes (Parr et al. 2001). Reduced appearance of phosphorylated paxillin following WAVE-3 knock down may reflect reduced cellular interaction with the extracellular matrix contributing to the changes in phenotype of these cells. HGF was also not able to induce paxillin associated changes in this cell line. In summary this study has demonstrated an important role of paxillin in cell movement and its activity is considerably reduced following WAVE-3 knock down which potentially reflect its important role in WAVE-3 mediated cell adhesion and movement.

Chapter 7
Role of MMPs in the impaired prostate cancer invasion by WAVE-3 knockdown.

7.1: Introduction:

Prostate cancer is the most common male cancer and second highest cause of cancer related mortality in the Western population. It represents a complex of heterogeneous disease which may run an indolent course and therefore does not need any clinical intervention. On the other end of spectrum it may be invasive and metastatic to lymph nodes and bones. The differences in clinical behavior of prostate cancer in these clinical scenarios are still poorly understood. Such an understanding will facilitate advances in diagnostic and therapeutic treatment options. A key step in cancer progression and establishment of metastasis is the degradation of the extracellular matrix. This is achieved through expression of a range of proteases including matrix metalloproteinases (MMPs).

During the metastatic process, prostate cancer cells have to pass through the collagen containing barriers such as the basement membrane and interstitial stroma. This process is facilitated by expression of specific proteins which cleave constituents of extracellular matrix and help the physical passage of metastatic cells through these barriers (Jiang et al. 1994; DeClerck, 2000). During this process, proteolysis also influences tumour growth through the release of different growth factors and chemoattractant molecules. MMPs, plasminogen activators, proteases of collagen system and proteins such as Cathepsin B are some representations of these proteolytic proteins (Hiraoka et al. 1998).

The MMP family comprises more than 16 structurally related proteins which are further subdivided into groups based on extracellular matrix proteins substrates (MacDougall et al. 1995). There are three major subgroups of MMPs: collagenases degrade fibrillar collagen, stromelysins prefer proteoglycans and glycoproteins as substrates, and gelatinases are particularly potent in degradation of nonfibrillar and denatured collagens (gelatin). They share a catalytic domain with the HEXGH motif responsible for ligating zinc, which is essential for catalytic function. MMPs are also characterized by a distinctive PRCGVPD sequence in the domain, responsible for maintaining latency in the zymogen form (Birkedal-Hansen et al. 1993). MMP activity is regulated at multiple levels including mRNA and protein expression. In general once produced these proteins are rapidly secreted from the cells and require activation through the enzyme cascades for different members of the MMP family. Once activated, these proteins can be inhibited by general protease inhibitor like α2-macroglobulin or specific inhibitors known as tissue inhibitors of MMPs (TIMPs). These inhibitors do not distinguish effectively between individual family members (Birkedal-Hansen et al. 1993; Egeblad and Werb, 2002).

Changes in expression of MMPs in the prostate are related to normal physiological functions and pathological problems such as prostate cancer. MMP-2 is expressed during organ development of the prostate in rats and similar changes are observed during castration induced repression of the prostate (Wilson et al. 1991 & 1992). In human prostate MMP-2 is up regulated in BPH as compared to normal epithelial cells (Luo et al. 2002). High grade PIN usually shows this activity limited to the basal layer of cells (Montironi et al. 1996). It is interesting to observe that MMP-2 immunoreactivity is

observed in high-grade solid and cribriform prostate cancers exhibiting heterogeneous intensity and location (Bodey et al. 2001). Increased expression of MMP-2, the ratio of MMP-2:TIMMP-2 and particularly the active form of MMP-2 correlate with increasing Gleason score (Still et al. 2000; Bodey et al. 2001). Increased MMP-2 polymorhism is shown to be associated with more aggressive and higher Gleason score prostate cancer (dos Reis et al. 2010).

There are a few discrepancies regarding the expression of MMP-9 in prostate cancer. Its expression has been detected in macrophages present in areas of prostatic inflammation and at the invasive edge of high Gleason score prostate cancers (Knox et al. 1996). The expression of MMP-9 in high-grade prostate cancers may indicate the process of epithelial to mesenchymal transformation which occurs during cancer progression (Behnsawy et al. 2013). The amount and proportion of active and pro-enzyme form of MMP-9, varies among different prostate cancers and does not appear to correlate with increasing Gleason grade (Knox et al. 1996). There are a few studies indicating the presence of immunoreactivity for MMP-3 and MMP-11 in prostate cancer but it appears to be concentrated around the blood vessels in the stroma rather than prostate cancer epithelial cells (Bodey et al. 2001).

Prior studies have documented that the PC-3 prostate cancer cell line strongly expresses MMP-2 & MMP-9 (Roomi et al. 2011). Considering the important role of MMPs in prostate cancer invasion and metastasis, we tried to establish the role of these proteins in reduced invasion of PC-3 prostate cancer cells, following WAVE-3 knock down.

7.2: Materials and methods:

7.2.1: Cell lines:

In this study we used already established PC-3 prostate cancer cell lines which have been previously used in our projects. Human prostate cancer cell lines PC-3^{WT}, PC-3^{ePEF}, and PC-$3^{WAVE\text{-}3KD}$ were grown in DMEM medium supplemented with 10% FCS, penicillin (100 units/ml) and streptomycin (100µg/ml) in tissue culture flasks. The cells were plated at a density $5x10^5$ cells/ml and grown to confluency in a humidified atmosphere at 5% CO^2 at 37˚C. Serum-supplemented medium was removed and the cell monolayer was washed once with PBS and with the DMEM serum-free medium. Cells were incubated with 1ml of serum free media at 37˚C in a tissue culture incubator equilibrated with 95% air and 5% CO^2 for 24 hours. The conditioned media were collected separately, pooled, and centrifuged for 10min at 3000rpm to remove cells and cell debris. Media samples were stored at -4ºC until used.

7.2.2: RNA isolation and PCR:

RNA was isolated from selected cells using total RNA isolation reagent (ABgene, Surrey, UK). Following quantification, this RNA was used to construct complimentary DNA using the Dura Script reverse transcriptase-polymerase chain reaction (RT-PCR) kit (Invitrogen, Paisley, UK). The DNA was used for PCR to detect expression of RNA for different MMPs in the cell lines described above.

7.2.3: Sodium dodecyl sulfate-polyacrylamide gel electrophoresis (SDS-PAGE) and western blot:

Equal amounts of proteins were quantified from the cell lysate using the DC Protein Assay kit (Bio-Rad Laboratories, Hemel Hempstead, UK). These proteins were separated using sodium dodecyl sulfate-polyacrylamide gel electrophoresis (SDS-PAGE) and blotted on to nitrocellulose membrane. The membrane was treated with milk to block non-specific proteins prior to probing with anti-MMP primary antibodies, followed by peroxidise conjugated secondary antibodies. Protein bands were visualized and analysed using the Supersignal West Dura system and documented using a gel documentation system (UVITech, Cambridge, United Kingdom).

7.2.4: Zymography:

Gelatinase zymography was performed in 8% SDS polyacrylamide gel (Invitrogen Corp.) in the presence of 0.1% gelatin under non-reducing conditions. Culture media (40µL) were mixed with sample buffer and loaded for SDS-PAGE with Tris glycine SDS buffer. Samples were not boiled before electrophoresis. Following electrophoresis the gels were washed twice in 2.5% Triton X-100 for 30min at room temperature to remove SDS. The gels were then incubated at 37˚C overnight in substrate buffer containing 50mM Tris-HCl and 10mM $CaCl_2$ at pH8.0 and stained with 0.5% Coomassie Blue in 50% methanol and 10% glacial acetic acid for 30min and destained gradually until clear bands appeared. Upon renaturation of the enzyme, the gelatinases digest the gelatin in the gel and give clear bands against an intensely stained background. Pre-stained

protein standards were run concurrently and approximate molecular weights were determined by plotting the relative motilities of known proteins. Gels were subsequently scanned on a digital scanner and digital images were saved for subsequent analysis.

7.2.5: Immunocytochemistry (ICC):

PC-3 cells (PC-3^{WT}, PC-3^{pEF} and PC-$3^{WAVE\text{-}3KD}$) were seeded in chamber slides (Nunc, Denmark), at a density of 20,000 cells/well. Cell culture medium was removed by aspiration and washed twice with TBS buffer to remove culture medium proteins. Buffered formalin (4%) was added and incubated at RT for 10 minutes. Fixative was aspirated and cells washed twice with TBS buffer. Permeabilization buffer mixture (0.1% Triton in TBS buffer) was added and incubated for 10 min. The cells were washed twice with washing buffer following aspiration of permeabilization buffer.

Non specific protein block was performed with diluted horse serum for 20 minutes (1 drop to 5 ml washing buffer). Chambers were washed again in washing-buffer 4 times. Cells were incubated with diluted primary antibody (anti-MMP diluted 1:100 in blocking buffer) at 37˚C, for 1 hour. The cells were washed again in washing buffer 4 times to remove any unbound primary antibodies. Secondary antibodies were added (anti-mouse, rabbit or goat depending upon the origin of primary antibodies, with a dilution of 1:250 in blocking buffer) and incubated for 30 minutes at room temperature. The cells were washed again in washing buffer 4 times to remove any unbound antibodies. ABC

complex was added and incubated for 30 minutes at RT. DAB chromogen was added for 5 minutes in a dark area after washing again four times (covered by a tray). Excess chromogen was removed by washing with water for 2 minutes. Cells were counterstained with Mayer's Haematoxylin for 1 minute. Finally they were washed in water for 5 minutes to remove excess Haematoxylin.

7.3: Results:

7.3.1: Expression of MMPs in PC-3 cell lines:

We analyzed three prostate cancer cell lines which have been previously used in our experiments. These included PC-3^{WT}, PC-3^{ePF}, PC-3$^{WAVE\text{-}3\ KD}$. We screened these cell lines for expression of MMP-1, MMP-2, MMP-7, MMP-9, and MMP-11. There was no significant difference in expression of the different MMPs in three different cell lines except MMP-2. Messenger RNA levels of MMP-1, MMP-2, MMP-7, MMP-9 and MMP-11 in the three different cell lines are illustrated in figure (Figure: 7.1). MMP-2 was expressed at a relatively low level in PC-3 $^{WAVE\text{-}3\ KD}$ cell line as compared to PC-3 ^{WT} and control PC-3 ^{ePF} cell lines. Considering the role of gelatinases in prostate cancer invasion, we also analysed the expression of MMP-2 by western blotting in these cell lines which did not show any significant difference among different cell lines (Figure: 7.2). Concordant with this, ICC staining revealed no significant difference in the staining intensity of MMP-2 in different cell lines (Fig: 7.3). It was interesting to observe that western blotting of conditioned medium from PC-3 $^{WAVE\text{-}3\ KD}$ revealed reduced expression of MMP-2 (Fig: 7.2).

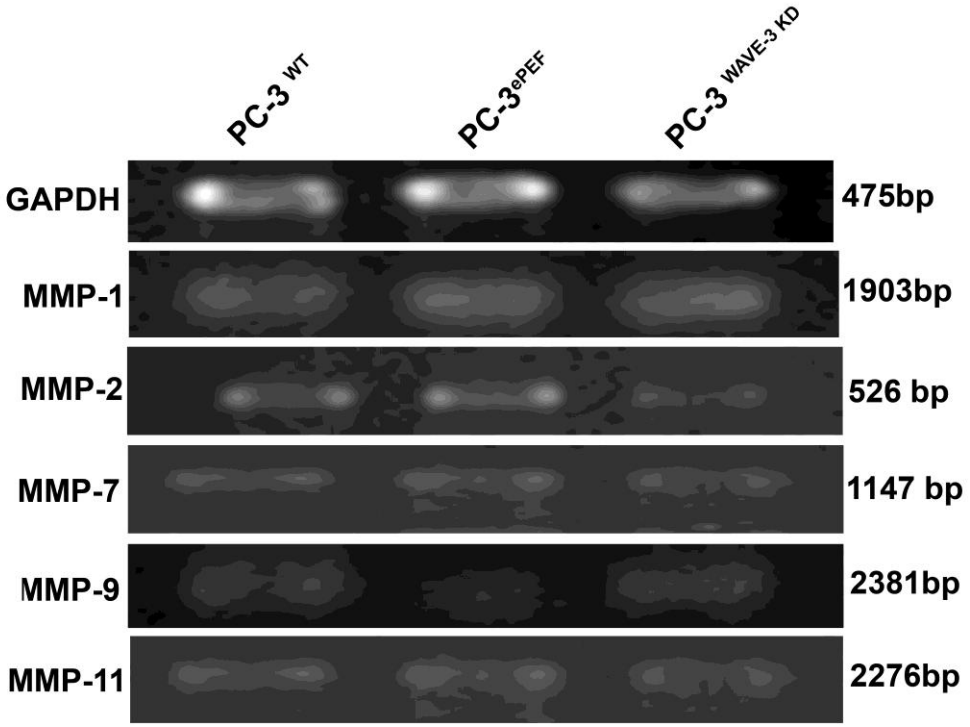

Figure 7.1: RT-PCR picture showing the expression of different MMPs in three different cell lines.

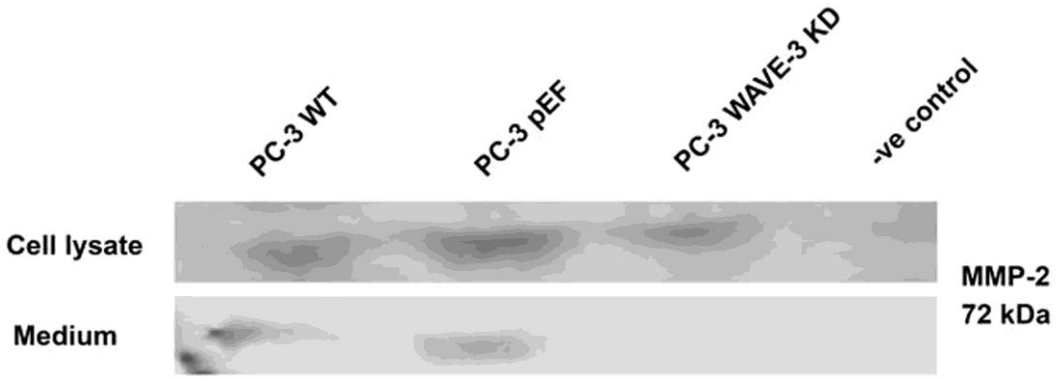

Fig 7.2: Western blotting showing the expression of MMP-2 in cell lysate and conditioned cell medium extracted from three different cell lines. There is good expression of MMP-2 in cell lysate (PC-3 WAVE-3^{KD}) but minimal expression is demonstated in cell medium (PC-3 WAVE-3^{KD}).

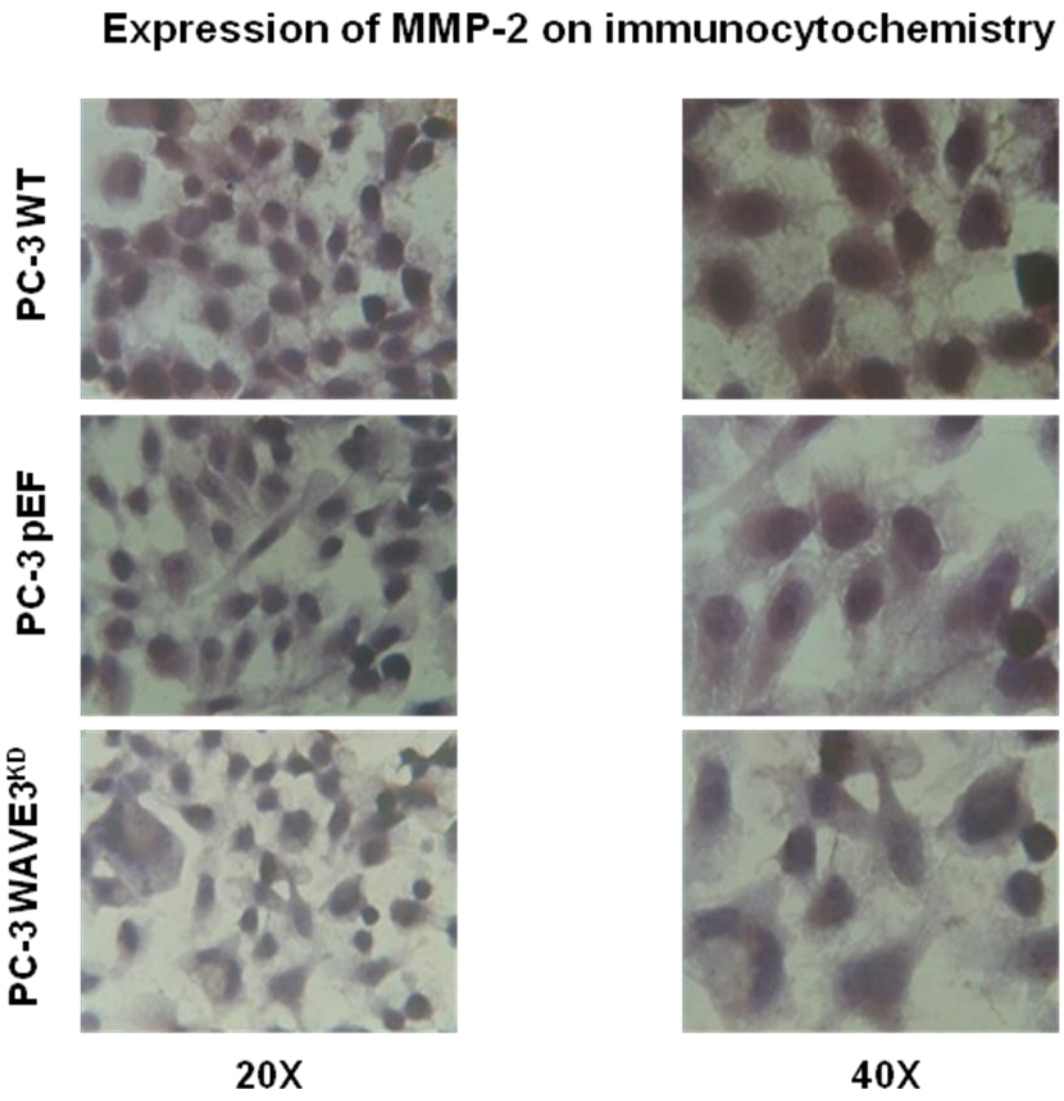

Fig 7.3: Immunocytochemistry for expression of MMP-2 in three different transgenic cell lines**.**

7.3.2: Reduced MMP-2 activity on gelatin zymography:

Gelatin zymography is a simple but powerful method to detect proteolytic enzymes capable of degrading gelatin from various biological sources. It is particularly useful for the assessment of two key members of the matrix metalloproteinase family, MMP-2 (gelatinase A) and MMP-9 (gelatinase B), due to their potent gelatin-degrading activity. This polyacrylamide gel electrophoresis-based method can provide a reliable assessment of the type of gelatinase, relative amount, and activation status (latent, compared with active enzyme forms) in cultured cells, tissues, and biological fluids. We used this method to detect the presence of gelatinases activity in the conditioned cell culture medium. It was very interesting to note that MMP-2 activity was significantly reduced in the medium extracted from PC-3 $^{\text{WAVE-3 KD}}$ cell line as compared to PC-3 $^{\text{WT}}$ and control PC-3 $^{\text{ePEF}}$ cell lines (Figure:7.4). No significant MMP-9 activity was observed in all three cell lines.

It was very interesting to note that zymographic analysis of conditioned medium duplicated the results of earlier study involving western blotting. MMP-2 expression was demonstrated exclusively in the cell lysate among all three cell lines. However western blotting did not show any significant expression of MMP-2 in medium extracted from cells deficient in WAVE-3. This may potentially indicate towards the failure of mechanism to deliver the MMP-2, in to the medium.

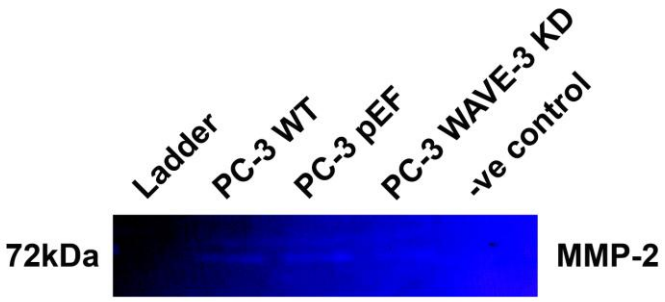

Figure 7.4: Zymograpy for expression of MMP-2 and MMP-9 in conditioned medium from three different cell lines. There was reduced MMP-2 (72kDa) activity in PC-3$^{WAVE\text{-}3KD\ cell}$ line as compared to control cell lines. No expression of MMP-9 was observed on zymography.

7.4: Discussion:

Tumour metastasis is a multistep process including new vessel formation, changes in cell attachment and adhesion, invasion, migrational properties and cell proliferation. These events are regulated by multiple complex pathways with involvement and cross talk of different cellular components. Specific agents aimed to prevent metastasis are not available yet but will be a critical achievement in cancer treatment.

Evidence from our prior research suggested that genetic silencing of WAVE-3 in prostate cancer cells results in reduced migratory and invasive potential without any significant effect on the cellular growth and adhesion. This effect persisted even with the addition of the stimulatory molecule, hepatocyte growth factor (HGF). Subsequent studies at the molecular level indicated the important role of paxillin for possible mediation of these changes. In the present study we investigated the possible role of different MMPs in reducing the invasive potential of prostate cancer cells at different levels, including transcriptional, translational and functional levels. Overall our results in this study suggested decreased activity of MMP-2 in the extracellular medium on zymography, which may reflect reduced activity or reduced availability. There was no significant change in the expression of this important gelatinase in all cell lines.

Numerous studies have shown that inhibition of MMPs activity or expression can be a potential target for prevention of metastasis (Coussens et al. 1996; Chakraborti et al. 2003). MMP-2 and MMP-9 belong to the gelatinase group of MMPs and their role has been extensively studied in prostate cancer (Zhang et al. 2004). Expression of most MMPs is normally low in tissues, and only induced when remodelling of the extracellular

matrix is required. MMP expression is primarily regulated at the transcriptional level, although stabilization of MMP transcripts in response to growth factors, as well as the influence of cytokines, also plays a role in the regulation of MMP activity (Sasaki et al. 2000; Reunanen et al. 2002).

The possible involvement of WAVE proteins in the regulation of MMPs was initially reported by Suetsugu et al., who showed that down regulation of WAVE-1, but not WAVE-2, affected MMP-2 activity (Suetsugu et al. 2003). In this study, they pharmacologically inhibited MMPs with GM6001, which blocks the activities of a wide range of MMPs including MMP-2. Migration of WAVE-1 deficient cells dependent on MMPs through the ECM was inhibited by GM6001. In contrast, migration of wild-type and WAVE-2 deficient cells was reduced only to 70%–80% by GM6001. The levels of secreted MMP-2 were also decreased on zymographic studies of conditioned medium in the WAVE-1 deficient cell line, although the amount of MMP-2 contained in cells did not change significantly. On immunohistochemistry, MMP-2 was co-localized with WAVE-1 at dorsal ruffles formed after treatment with PDGF, supporting the relationship between WAVE-1 and MMP-2 (Suetsugu et al. 2003).

Conversely, Sossey-Alaoui et al., while investigating the functional consequences of the loss of WAVE-3 using RNA interference (RNAi), identified a MAPK signaling axis, where WAVE-3 was essential for regulation of the expression of different MMPs, in human neuroblastoma cell lines (Sossey-Alaoui et al. 2005). They showed that knockdown of WAVE-3 expression affects the activity of the p38 MAPK pathway, but not that of AKT or ERK1/2 pathways. WAVE-3 mediated down regulation of p38 activity was found to be

independent of both WAVE-1 and WAVE-2 expression, as WAVE-3 knockdown did not alter the transcription levels of either WAVE-1 or WAVE-2. Loss of WAVE-3 resulted in a significant decrease in expression levels of MMP-1, MMP-3, and MMP-9. However no significant effect on expression of MMP-2 was noted. The inhibition of these MMPs as a result of WAVE-3 loss led to a dramatic inhibition of cell migration and invasion using both the *in vitro* wound closure and matrigel assays in human neuroblastoma cells (Sossey-Alaoui et al. 2005). In our study, expression of MMP-1 and MMP-9 was not significantly affected. Expression of MMP-2 was reduced as compared to MMP-9 and zymography showed significantly reduced activity in WAVE-3 deficient cells. It is also important to note that the Sossey-Alaoui et al. study lacks any data on zymography which may have added additional information on this matter.

Paxillin is an important molecule in integrin-mediated adhesion signals and is localized in dorsal ruffles, at the leading edge of cellular movement (Pixley et al. 2001). Cortactin, dynamin and ARP2/3 complex are localized in the dorsal ruffles and podosomes which may represent the invading edge of the cell as well (Kruege et al. 2003). It is not clear how the WAVE family is involved in MMP secretion and MMP-dependent migration. Suetsugu et al. demonstrated that WAVE-1 dependant cell migration is remarkably sensitive to the absence of MMP-2 as compared to WAVE-2 dependant cell migration, which is partially affected. It is well documented that integrins generate adhesion and induce MMP-mediated ECM degradation (Friedl et al. 2003). Integrin-mediated adhesion simultaneously activates Rac (Bishop et al. 2000) and a paxillin-associated kinase, FAK (Schlaepfer et al. 1999). Both Rac and FAK enhance secretion and activation of MMP-2 (Sein et al. 2000; Zhuge et al. 2000; Hauck et al. 2002). The actin

cytoskeleton itself is involved in regulation of MMPs. Treatment of fibroblasts with cytochalasins increased expression, secretion, and activation of MMP-2 (Harris et al. 1975; Tomasek et al. 1997). Our prior studies regarding the role of paxillin showed markedly reduced levels of phosphorylated paxillin which may indicate crosstalk between these molecules and WAVEs and suggest the differential effects on the MMP-2 and hence on invasion as well.

He et al. studied the role of WAVE-1 in leukaemia cell line invasion. K562 cells, deficient in WAVE-1 were found to lose their invasive potential along with reduced MMP-2 expression, as compared to control cells. At the same time forced expression of WAVE-1 using pcDNA increased the expression of MMP-2. The invasion ability of K562 cells was enhanced after transfected with pcDNA3 as well. Immunoflourescence studies showed co-localization of WAVE-1 and MMP-2, indicating the close relationship and involvement of both in the invasive potential of these cells (He et al. 2009).

MMP-2 is also expressed by prostate cancer stromal cells. Yu et al. determined that estradiol treatment of prostate cancer stromal cells enhanced the production of MMP-2 in these cells. Subsequent use of conditioned medium showed increased invasion in a matrigel invasion assay with prostate cancer cells. Conditioned medium treated with an anti-MMP2 antibody lost its stimulatory effect on invasion of prostate cancer cells. However, mechanistic studies showed that oestradiol up-regulated MMP2 in an indirect manner. It was revealed that estradiol induced TGFβ1 expression via oestrogen receptor (ERα); TGFβ1 stimulated MMP2 expression in prostate stromal cells and the

invasion of prostate cancer cells was stimulated by elevated MMP2 expression induced by estradiol in a paracrine manner (Yu et al. 2011).

Reduction in the activity of MMP-2 has been attributed to reduced invasive potential in different cancer cell lines but multiple associated changes and proposed possible underlying mechanisms have been described in different studies. For example Li et al investigated the underlying mechanism of β-human chorionic gonadotropin (β-hCG) in promoting motility and invasion in human glioblastoma U87MG cells. Through western blot and gelatine zymography studies, it was concluded that β-hCG increased phosphorylation of ERK1/2 and up-regulated MMP-2 expression in a dose and time-dependent manner, whereas ERK1/2 blocker, PD98059 (25 μM) significantly decreased both ERK1/2 and MMP-2 expression and activity, indicating a possible role for ERK1/2 in controlling the activity of MMP-2 (Li et al. 2012).

Kwiatkowska et al investigated the molecular mechanisms underlying the inhibitory effect of Cyclosporin-A on the migration/invasion of human glioblastoma cells with different alterations of the PI3K/AKT signalling pathway. This study demonstrated that Cyclosporin-A impairs Akt and FAK signaling which results in the reduction of motility and invasion of glioblastoma cells. Cyclosporin-A, as a pharmacological and genetic inhibitor of PI3K/AKT signaling, reduced invasion and MMP-2 proteolytic activity likely by two mechanisms: by rapid impairment of MT1-MMP shuttling to lamellipodia and delayed downregulation of NFκB-dependent MMP expression. These findings showed for the first time, the anti-invasive action of Cyclosporin-A and defined a complex

involvement of AKT signaling into the regulation of cellular motility and invasion (Kwiatkowska et al. 2011).

Reduced activity of MMP2 following WAVE-3 knockdown may be the sequel of imbalance between the level of MMP-2 and its tissue inhibitors. TIMP1 has been shown to regulate MMP2 activity and numerous pieces of evidence have indicated a correlation between elevated TIMP1 levels and diminished MMP-2 activity and invasiveness (Khokha et al. 1992; Ramer et al. 2008).

Results of our current study clearly suggest the active role of MMP-2 in the reduction of cell motility and invasion following WAVE-3 elimination. It provides part of a larger puzzle underpinning the process of metastasis which needs to be further investigated for the role of pathways such as ERK1/2 and MAPK/p53.

Chapter 8
General discussion

Prostate cancer is the 4th most common cause of cancer deaths in the UK, accounting for approximately 7% of all cancer related deaths. Survival from prostate cancer is strongly related to the stage of the disease at the time of diagnosis. For organ confined prostate cancer, five year survival in England in 1999-2002 was more than 90%. In contrast, the presence of metastatic disease at the time of presentation produces five year relative survival of around 30%. Since the introduction of PSA testing, the incidence of local-regional disease has increased, whereas the incidence of metastatic disease has decreased (Newcomer et al. 1997).

In spite of all advanced treatment options available for prostate cancer, management of metastatic disease remains a major challenge. Prevention of the development of metastatic disease would be a significant breakthrough in the management of any cancer like prostate cancer, which is responsible for a high rate of morbidity and mortality in the UK. Morbidity and mortality arising from metastatic disease can result from direct organ damage by the enlarging lesions, paraneoplastic syndromes, or from the complications of treatment.

The major problem during the treatment of metastasis is the biological heterogeneity of the cells in the primary and metastatic sites. This heterogeneity is exhibited in the form of specific biological characteristics such as expression of cell receptors, enzymes, growth properties and growth factors. Manipulation of these essential pathways and different members of participating cellular molecules can potentially inhibit this process and thus halt the metastatic cascade.

8.1: WAVEs and cell motility in cancer and cancer metastasis

Cellular movement is an integral part of metastasis and has attracted a lot of attention from researchers as a potential target to prevent or inhibit the process of metastasis. Cellular movement is primarily controlled by polymerisation and depolymerisation of actin. In addition to cellular movement, the actin cytoskeleton also plays an important role in cell shape changes, cell proliferation and membrane transport of essential molecules. Considering these vital functions, the dynamics of actin polymerization and organization is of critical importance. Defects in actin polymerization results in human diseases like Wiskott-Aldrich syndrome (Sullivan et al. 1994) but at the same time it can be manipulated to modify and stop the metastatic cascade. There are multiple genes involved in controlling actin polymerization including genes encoding for the WASP/WAVE family of proteins. This family comprises 5 members including WASP, N-WASP, WAVE-1, WAVE-2, and WAVE-3. Both WASP and WAVE subfamilies activate the Arp2/3 complex, leading to the stimulation of actin polymerization and assembly of actin filaments.

The WASP/WAVE proteins are downstream effectors of Rho GTPases (Takenawa et al. 2001). These small GTPases are responsible for controlling vital functions such as cellular motility and proliferation. The activity of WASP and WAVE proteins are regulated through different mechanisms. Cdc42 is responsible for activation and regulation of WASP and N-WASP (Rohatgi et al. 1999) while activity of WAVEs is regulated by a multi-protein complex downstream of Rac (Millard et al. 2004).

8.2: Genetic silence of WAVE-3 using constructed ribozyme

Cellular cloning in this project involved silencing the specific gene of interest (WAVE-3) which is normally expressed in these cell lines. Specific gene expression can be modified at transcriptional and post-transcriptional levels. Transcriptional genetic silencing involves histone modifications through creation of an environment of heterochromatin around the gene, resulting in the gene being inaccessible to cellular machinery such as RNA polymerase and other transcriptional factors (Perry et al. 2010). Post-transcriptional modification involves the mRNA of a specific gene being destroyed through introduction of specific agents targeted against the gene of interest. A common mechanism is the introduction of small interfering RNAs (siRNA) which prevent the translation of a specific gene mRNA. This concept has been used successfully in therapeutic treatment of diseases such as cancer and has shown promising results. Major targets of this therapy include silencing of genes involved in the process of angiogenesis, metastasis, apoptosis and resistance to chemotherapy (Ramachandran et al. 2012).

The hammerhead ribozyme is a small RNA motif consisting of three helices that intersect at a conserved core. They were first discovered as self-cleaving domains in the RNA genome of different plant viroids and virusoids (Forster et al. 1987). Soon thereafter, it was demonstrated that the hammerhead motif could be incorporated into short synthetic oligonucleotides and transformed into a true, multiple turnover catalyst, suitable for cleaving a variety of RNA targets (Uhlenbeck et al. 1987; Haseloff et al. 1988). Their role in research and therapeutic options for cancer has been studied

extensively (Takagi et al. 2002). This method of gene silencing has been previously used successfully at our host research facility (Jiang et al. 2001; Jiang et al. 2005). The secondary structure of WAVE-3 mRNA was predicted using the Zuker's RNA Mfold software (Zuker, 2003). This software is designed to predict the stem and loop structure of RNA under optimal conditions, enabling the identification of a suitable GUC codon. The resulting ribozyme targets this specific codon. Following synthesis these ribozyme transgenes were cloned in to pEF6 plasmids in the cloning reaction and successfully used to transform the PC-3 prostate cancer cell line. The specific plasmid (pEF6) used in our experiments, also carries a genetic sequence for resistance to blasticidine antibiotic. This characteristic enabled us to select the cell populations with expression of plasmid while inhibiting the growth of cells lacking the plasmid. Knock down of WAVE-3 expression was maintained successfully during culture of progressive cell populations. It is also important to note that expression of WAVE-1 and WAVE-2 was not changed (Q-PCR, chapter: 4, page: 119). Similar results have been reported in MDA-MB-231 cells using siRNAs (Sossey-Alaoui et al. 2005).

The WAVE family of proteins play a critical role in actin polymerization, downstream of Rac which leads to cell migration (Takenawa et al. 2001). The exact and definitive roles of each family member is not known; however gene silencing studies of each member has provided a few glimpses of their function in the regulation of actin polymerization. In the present study we were able to demonstrate the stable knock down of WAVE-3 through ribozyme transgene introduction into the PC-3 prostate cancer cell line. Inhibition of WAVE-3 in this cell line did not affect cellular proliferation at 72 hours. There was no statistically different change in the number of adherent cells to an artificial

basement membrane among the three different cell lines (WT, ePEF and WAVE-3^{KD}). The most striking and important phenotypic change following WAVE-3 knock down was a change in the motility and invasive potential of these cells. Elimination of WAVE-3 resulted in reduced cell motility which was evident on the Cytodex-2® beads assay and wounding assay. At the same time, the number of invading cells through the artificial matrigel basement membrane was reduced quite significantly. Considering there was no change in the expression of WAVE-1 and WAVE-2, this finding potentially points towards the significant role of WAVE-3 in these processes. Similar data has been previously reported (Fernando et al. 2007; Teng et al. 2010).

8.3: WAVE-3 and HGF induced motility of prostate cancer cells

Hepatocyte growth factor/scatter factor (HGF/SF) has attracted much attention in recent years for its potential role in progression of prostate cancer. HGF is known to play an important role in the metastatic process through its effects on proliferation, dissociation, migration and invasion (Tajima et al. 1991; Sugawara et al. 1997; Gmyrek et al. 2001). HGF/SF derived from prostate stroma promotes proliferation, differentiation, motility, and invasion of malignant epithelial cells indicating possible involvement in the progression of prostate cancer (Gmyrek et al. 2001). Serum levels of HGF and PSA are found to be significantly increased in prostate cancer patients compared to a control group (Maha Hashem et al. 2005). Higher plasma levels of SF/HGF in men with hormone-refractory prostate cancer are associated with decreased patient survival

(Humphrey et al. 2006). Considering a possible significant role of HGF in prostate cancer progression and metastasis, the role of WAVE-3 in HGF mediated increased cellular motility, proliferation, adhesion and invasion was studied. HGF imparts its effects through its receptor c-MET. Various factors downstream of c-Met have been well characterised, including the extracellular signal-regulated kinases (ERKs). Radtke et al. showed that ERK 1 & 2 play an important role in c-MET mediated cell migration through its effect on paxillin. Important findings from this study in non small cell lung carcinoma cell lines, demonstrated that paxillin phosphorylation could be blocked by inhibition of ERK 1 & 2 (Radtke et al. 2013). Similar findings were reported by Liu et al. in their study using mIMCD-3 epithelial cells. They studied the effect of HGF on the focal adhesion proteins, focal adhesion kinase (FAK) and paxillin and their associated proteins. HGF was found to increase the tyrosine phosphorylation of paxillin and to a lesser degree FAK. Interestingly paxillin phosphorylation could be inhibited by the ERK inhibitor U0126. Their data suggest that HGF can induce serine/threonine phosphorylation of paxillin most probably mediated directly by ERK, resulting in the recruitment and activation of FAK and subsequent enhancement of cell spreading and adhesion (Liu et al. 2002). In the present study WAVE-3 knock-down resulted in reduced phosphorylation of paxillin and this change persisted following treatment with HGF. Considering the findings from the above two studies, pathways involving ERK1&2 appear to play an important role in induction of these changes in prostate cancer cell lines. The exact machinery of this effect orchestrated by ERK, WAVE and paxillin downstream of HGF/MET pathway requires further investigation.

The ERM (Ezrin, Radixin, and Moesin) proteins are a group of highly conserved and related proteins which provide a regulated linkage between the membrane and the underlying actin cytoskeleton.

Chuan et al. demonstrated that forced expression of c-Myc in the mouse prostate and in normal human prostate epithelial cells results in tumour transformation with an invasive phenotype. C-Myc induces cell invasion and anchorage-independent growth by regulating ezrin protein expression in the presence of androgens (Chuan et al, 2010). Valdman et al. and Musial et al. demonstrated significant inverse correlation between ezrin expression and the degree of prostate cancer differentiation (Valdman et al. 2005; Musiał et al. 2007). Valderrama et al. investigated the role of ERM in prostate cancer cells. This study showed that radixin is required for migration of PC-3 prostate cancer cells. Radixin depletion by RNA interference increases the cell spread area and cell-cell adhesion mediated by adherens junctions. Radixin depletion also alters actin organization, and distribution of active phosphorylated ezrin and moesin (Valderrama et al. 2012). Bartholow et al. reported expression profiles of radixin and moesin in prostatic adenocarcinoma. There was a statistically significant difference observed between high grade prostatic intraepithelial neoplasia (HGPIN) and prostate cancer in terms of radixin but no difference was observed in expression of moesin (Bartholow et al. 2011). Phosphorylation of a threonine residue (T558 in moesin, T567 in ezrin, T564 in radixin) within the C-terminal actin-binding domain of ERM proteins is considered a hallmark of ERM activation (Nakamura et al. 1995; Gautreau et al. 1995; Brown et al. 2003). It has

also been shown that PIP_2 is a key factor for the activation of ERM proteins *in vivo* (Matsui et al. 1999).

In our studies we investigated the expression and phosphorylation status of ERM proteins in prostate cancer cells following WAVE-3 knock down, in order to investigate their potential role in the reduced cellular motility and invasion. Expression of these proteins was detected through immunoblotting of pre-quantified protein samples while phosphorylation status was detected through immunoprecipitation studies.

Ezrin has been previously documented as an effector of HGF mediated migration and morphogenesis in epithelial cells. Crepaldi et al. reported that ezrin is crucial to morhogenesis in polarized kidney derived epithelial cells. HGF produced enrichment of ezrin recovered in the detergent insoluble fraction of the cytoskeleton protein fraction. Overproduction of ezrin through stable transfection in these cells, enhances cell migration and tubule formation induced by HGF. It has also been suggested that site directed mutagenesis of ezrin codonY145 and Y353 to phenylalanine does not affect ezrin localization but reduced motility and morphological changes induced by HGF (Crepaldi et al. 1997). In the present study there were no significant changes in the expression and phosphorylation of ezrin following WAVE-3 knock down. Addition of HGF to three prostate transgenic cell lines showed cell spreading and peripheral localization of these proteins on immunoflourescence studies. However, this effect was limited in the cell line lacking the presence of WAVE-3. Similar findings were noted in case of the radixin and moesin as well.

8.4: WAVE-3 and MMPs in the invasiveness of prostate cancer cells

Numerous studies have shown that inhibition of MMPs activity or expression can be a potential target for prevention of metastasis (Coussens et al. 1996; Chakraborti et al. 2003). MMP-2 and MMP-9 belong to the gelatinase group of MMPs and their role has been extensively studied in prostate cancer (Zhang et al. 2004). MMP-2 polymorphism has been associated with locally advanced or metastatic disease (dos Reis et al. 2010). Emerging evidence has shown that the tumour microenvironment plays a crucial role in prostate cancer development and progression. Gravina et al. performed phenotypic characterisation of human prostatic stromal cells in primary cultures derived from human tissue samples. They used cultures from stromal cells obtained from BPH (15 cases) and prostate cancer patients (30 cases). This study analyzed the expression of matrix metalloproteinase MMP-2, MMP-9 and tissue inhibitors of MMPs (TIMPs). MMP-2 was secreted by all primary cultures; whereas MMP-9 secretion was observed in only a few prostate cancer derived stromal cells (Gravina et al. 2013). Murray et al. performed an immunocytochemical study of MMP-2 expression in circulating prostate cells (CPCs), disseminated tumour cells (DTCs), and micro metastases (mM) in the bone marrow of men with prostate cancer. Tumour cells were identified with anti-PSA immunocytochemistry. PSA positive samples were processed with anti-MMP-2 antibody along with its expression compared with Gleason score, concordance of expression, and metastatic and non-metastatic disease. Out of 215

men that participated in the study, circulating prostate cells were detected in 62.7%, disseminated tumour cells in 62.2%, and micro metastases in 71.4% with non-metastatic cancer. All patients with clinically metastatic prostate cancer had CPCs, DTCs, and mM detected. All CPCs and DTCs expressed MMP-2. In micro metastases, MMP-2 expression was positively associated with increasing Gleason score (Murray et al. 2012). This study highlighted the early expression and importance of MMP-2 in the prostate cancer metastatic process.

Overall our results suggested decreased activity of MMP-2 in the extracellular medium on zymography, which may reflect reduced activity or reduced availability of MMP-2 in the medium. There was no significant change in the expression of this important gelatinase in all cell lines. In general, activity of MMPs is controlled through expression at the transcriptional level (Sasaki et al. 2000). However in the present study there was no significant difference in the expression of MMP-2 at mRNA and protein levels in different cell lines. Immunoblotting studies of MMP-2 in cell lysates and conditioned medium from different cell lines showed markedly reduced MMP-2 in the medium, following WAVE-3 knock down. At the same time there was significantly reduced activity of MMP-2 in the medium on zymography studies.

The possible involvement of WAVE proteins in the regulation of MMPs was initially reported by Suetsugu et al who showed that down regulation of WAVE-1, but not WAVE-2, affected MMP-2 activity (Suetsugu et al. 2003). It is not clear how the WAVE family is involved in MMP secretion and MMP-dependent migration. Both Rac and FAK enhance secretion and activation of MMP-2 (Sein et al. 2000; Zhuge et al. 2001; Hauck

et al. 2002). FAK is a paxillin associated kinase which plays important role in regulation of the actin cytoskeleton.

When cells invade the ECM, cell-ECM adhesion through integrins coupled with degradation of ECM by proteases, as well as leading edge formation by actin polymerization are important. The integrins generate adhesion and induce MMP-mediated ECM degradation. Integrin-mediated adhesion simultaneously activates Rac and paxillin-associated kinases like FAK. Both Rac and FAK enhance secretion and activation of MMP-2. Collectively, the findings of the present study indicate that WAVE-3 regulates the activation of paxillin and consequently affect the function of MMP-2 and eventually coordinate the invasiveness of prostate cancer cells, particularly HGF enhanced motility and metastasis.

8.5: Prospects of future study:

This study examined the role of the WAVE-3 in prostate cancer cell motility and also demonstrated its role in the HGF mediated changes in prostate cancer cells. In addition the underlying pathways, including role of paxillin and MMP-2 to reduce the cellular motility and invasive potential were investigated. There is little doubt about the fact that WAVE-3 and HGF expression represent aggressive properties of prostate cancer and they can be used as important prognostic markers for the risk stratification including clinical studies. The exact mechanisms underlying phenotypic changes following WAVE-3 knock-down, still remain unclear and require further investigations. Moreover, WAVE-3 being tumour promoter gene, further studies using *in vivo* tumour model are

necessary to elucidate the implication of WAVE-3 in prevention and treatment of prostate primary tumour and development of corresponding secondary tumour.

The interaction and influence of intermediate molecules such as paxillin and their interaction with WAVEs family needs further investigations. Reduced levels of phosphorylated paxillin following WAVE-3 knock down may be attributed to possible loss of positive feedback effect from WAVE-3, which facilitates the activation of paxillin through its phosphorylation. This possible interaction should be further investigated through co-localization studies involving paxillin and WAVE-3 in resting phase and during cellular stimulation like addition of HGF, which may be able to explain the close relationship of these molecules. Paxillin plays an important role in the dynamics of focal adhesion complexes as well and further studies can potentially investigate the changes in these vital structures, following WAVE-3 knock down. Indirectly, these changes involving focal adhesions may further explain the role of focal adhesions in reducing cellular motility and invasion with loss of WAVE-3.

MMP-2 appears to play an important role in reduction of invasion following loss of WAVE-3. Its expression appears to be stable following WAVE-3 knock-down but reduced availability in the medium indicates a possible influence on the secretion into the medium. Previous studies have suggested co-localization of WAVE-1 and MMP-2 on the leading edge of motile cells. Similarly, WAVE-3 warrants further investigation such as co-localisation with MMP-2 during cell invasion and motility. N-WASP have also been implicated in the promotion of membrane associated MMP (MT1-MMP) trafficking in to invadopodia of invasive breast cancer cells. Reduced availability in the medium following WAVE-3 loss may result from interference with transport mechanisms such as

the movement of storage vesicles, which is also affected by cell movement through actin polymerization. Considering the important role of MMP-2 in prostate cancer invasion, further studies are required to elucidate the underlying mechanism for this effect. Further investigations involving the possible role of pathways such as ERK1/2 and MAPK/p53 may also be helpful to explain this phenomenon in prostate cancer cell line. Reduced activity of MMP-2 following WAVE-3 knockdown may be the sequel of imbalance between the level of MMP-2 and its tissue inhibitors such as TIMP-1, which has been shown to regulate MMP-2 activity.

Bibliography

Abécassis, I. et al (2003). "RhoA induces MMP-9 expression at CD44 lamellipodial focal complexes and promotes HMEC-1 cell invasion." *Exp Cell Res* 291(2): 363-376.

Abercrombie, M. (1980). "The crawling movement of metazoan cells." *Proc. R. Soc. London B Biol.Sci*. 207: 129–147.

Aguirre Ghiso J. et al (1999). "Tumor dormancy induced by downregulation of urokinase receptor in human carcinoma involves integrin and MAPK signaling." *J Cell Biol* 147(1): 89-104.

Aleksandar, A. et al (2004). "Ezrin/radixin/moesin proteins and Rho GTPase signalling in leucocytes." *Immunology* 112(2): 165–176.

Altman, S. (1995). "RNase P in research and therapy." *Biotechnology* 13(4): 327-329.

Aprikian, A. et al (1997). "Bombesin stimulates the motility of human prostate-carcinoma cells through tyrosine phosphorylation of focal adhesion kinase and of integrin-associated proteins." *Int J Cancer* 72(3): 498-504.

Azuma, K. et al (2005). "Tyrosine phosphorylation of paxillin affects the metastatic potential of human osteosarcoma." *Oncogene* 24(30): 4754-4764.

Bartholow, T. et al (2011). "Immunohistochemical staining of radixin and moesin in prostatic adenocarcinoma." *BMC Clin Pathol* 14(11): Published online 2011 January 2014. doi: 2010.1186/1472-6890-2011-2011.

Bartsch, G. et al (2001). Tyrol prostate cancer screening group. Prostate cancer mortality after introduction of prostate specific antigen mass screening in the Federal State of Tyrol, Austria. *Urology* 58(3):417-24.

Bear, J. et al (1998). "SCAR, a WASP-related protein, isolated as a suppressor of receptor defects in late Dictyostelium development." *J. Cell. Biol* 142(5): 1325–1335.

Ben-Yosef, Y. et al (2005). "Hypoxia of endothelial cells leads to MMP-2-dependent survival and death." *Am J Physiol Cell Physiol* 289(5): 1321-1331.

Bergers, G. et al (2000). "Matrix metalloproteinase-9 triggers the angiogenic switch during carcinogenesis." *Nat Cell Biol* 2(10): 737-744.

Berrier, A. and Yamada, K. (2007). "Cell matrix adhesion." *J Cell Physiol* 213(3): 565–573.

Bertrand, E. et al (1994). "Can hammerhead ribozymes be efficient tools to inactivate gene function?" *Nucleic Acids Res* 22(3): 292-300.

Birkedal-Hansen, H. et al (1993). "Matrix metalloproteinases: a review." *Crit Rev Oral Biol Med* 4(2): 197-250.

Bishop, A. and Hall, A. (2000). "Rho GTPases and their effector proteins." *Biochem J* 1(348 Pt 2): 241-255.

Bodden, M. et al (1994). "Functional domains of human TIMP-1 (tissue inhibitor of metalloproteinases)." *J Biol Chem* 269(29): 18943-18952.

Bodey, B. et al (2001). "Immunocytochemical detection of matrix metalloproteinase expression in prostate cancer." *In Vivo* 15(1): 65-70.

Brown, M. and Turner, C. (2002). "Roles for the tubulin- and PTP-PEST-binding paxillin LIM domains in cell adhesion and motility." *Int J Biochem Cell Biol* 34(7): 855-863.

Brown, M. et al (2003). "Chemokine stimulation of human peripheral blood T lymphocytes induces rapid dephosphorylation of ERM proteins, which facilitates loss of microvilli and polarization." *Blood* 102(12): 3890-3899.

Cech, T. (1990). "Nobel lecture. Self-splicing and enzymatic activity of an intervening sequence RNA from Tetrahymena." *Biosci Rep* 10(3): 239-261.

Chakraborti, S. et al (2003). "Regulation of matrix metalloproteinases: an overview." *Mol Cell Biochem* 253(1-2): 269-285.

Chen, W. and Wang, J. (1999). "Specialized surface protrusions of invasive cells, invadopodia and lamellipodia, have differential MT1-MMP, MMP-2, and TIMP-2 localization." *Ann N Y Acad Sci* 30(878): 361-371.

Cheng, X. et al (2008). "Advances in assays of matrix metalloproteinases (MMPs) and their inhibitors." *J Enzyme Inhib Med Chem* 23(2): 154-167.

Chuan, Y. et al (2010). "Ezrin mediates c-Myc actions in prostate cancer cell invasion." *Oncogene* 29(10): 1531-1542.

Condeelis, J. et al (2005). "The great escape: when cancer cells hijack the genes for chemotaxis and motility." *Ann Rev Cell Dev Biol* 21: 695–718.

Coussens, L. and Werb. Z (1996). "Matrix metalloproteinases and the development of cancer." *Chem Biol* 3(11): 895-904.

Coussens, L. et al (1999). "Inflammatory mast cells up-regulate angiogenesis during squamous epithelial carcinogenesis." *Genes Dev* 13(11): 1382-1397.

Coussens, L. et al (2000). "MMP-9 supplied by bone marrow-derived cells contributes to skin carcinogenesis." *Cell* 103(3): 481-490.

Crepaldi, T. et al (1997). "Ezrin is an effector of hepatocyte growth factor-mediated migration and morphogenesis in epithelial cells." *J Cell Biol* 138(2): 423-434.

Czekay, R. et al (2003). "Plasminogen activator inhibitor-1 detaches cells from extracellular matrices by inactivating integrins." *J Cell Biol* 160(5): 781-791.

DeClerck, Y. (2000). "Interactions between tumour cells and stromal cells and proteolytic modification of the extracellular matrix by metalloproteinases in cancer." *Eur J Cancer* 36(10): 1258-1268.

Dennis, L. and Dawson, D. (2002). "Meta-analysis of measures of sexual activity and prostate cancer." *Epidemiology* 13(1): 72-79.

Dennis, L. et al (2002). "Vasectomy and the risk of prostate cancer: a meta-analysis examining vasectomy status, age at vasectomy, and time since vasectomy." *Prostate Cancer Prostatic Dis* 5(3): 193-203.

Derry, J. et al (1994). "Isolation of a novel gene mutated in Wiskott-Aldrich syndrome." *Cell* 78(4): 635–644.

Djavan, D. et al (2000). Optimal predictors of prostate cancer on repeat prostate biopsy: A prospective study of 1,051 men. *J Urol* 163(4):1144-1148.

Dolo, V. et al (1999). "Matrix-degrading proteinases are shed in membrane vesicles by ovarian cancer cells in vivo and in vitro." *Clin Exp Metastasis* 17(2): 131-140.

dos Reis, S. et al (2010). "Matrix metalloproteinase-2 polymorphism is associated with prognosis in prostate cancer." *Urol Oncol* 28(6): 624-627.

Dumin, J. et al (2001). "Pro-collagenase-1 (matrix metalloproteinase-1) binds the alpha(2)beta(1) integrin upon release from keratinocytes migrating on type I collagen." *J Biol Chem* 276(31): 29368-29374.

Eble, J. et al (2002). "Rhodocetin antagonizes stromal tumor invasion in vitro and other alpha2beta1 integrin-mediated cell functions." *Matrix Biol* 21(7): 547–558.

Egeblad, M. and Werb, Z. (2002). "New functions for the matrix metalloproteinases in cancer progression." *Nat Rev Cancer* 2(3): 161-174.

Fernando, H. et al (2007). "Expression of the WASP verprolin-homologues (WAVE members) in human breast cancer." *Oncology* 73(5-6): 376-383.

Fernando, H. et al (2010). "WAVE3 is associated with invasiveness in prostate cancer cells." *Urol Oncol* 28(3): 320-327.

Fini, M. et al (1998). *Regulation of matrix metalloproteinase gene expression in Matrix Metalloproteinases.* Academic Press, San Diego, CA.

Fiore, E. et al (2002). "Matrix metalloproteinase 9 (MMP-9/gelatinase B) proteolytically cleaves ICAM-1 and participates in tumor cell resistance to natural killer cell-mediated cytotoxicity." *Oncogene* 21(34):5213-23.

Forster, A. et al (1987). "Self-cleavage of plus and minus RNAs of a virusoid and a structural model for the active sites." *Cell* 49(2): 211-220.

Friedl, P. and Wolf, K. (2003). "Tumour-cell invasion and migration: diversity and escape mechanisms." *Nat Rev Cancer* 3(5): 362-374.

Friedl, P. (2004). "Prespecification and plasticity: shifting mechanisms of cell migration." *Curr Opin Cell Biol* 16(1): 14–23.

Gautreau, A. et al (2000). "Morphogenic effects of ezrin require a phosphorylation-induced transition from oligomers to monomers at the plasma membrane." *J Cell Biol* 150(1): 193-203.

Giannelli, G. et al (1997). "Induction of cell migration by matrix metalloprotease-2 cleavage of laminin-5." *Science* 277(5323): 225-228.

Ginestra, A. et al. (1997). "Urokinase plasminogen activator and gelatinases are associated with membrane vesicles shed by human HT1080 fibrosarcoma cells." *J Biol Chem* 272(27): 17216-17222.

Goldberg, G. et al (1992). "Interaction of 92-kDa type IV collagenase with the tissue inhibitor of metalloproteinases prevents dimerization, complex formation with interstitial collagenase, and activation of the proenzyme with stromelysin." *J Biol Chem* 267(7): 4583-4591.

Gomez, D. et al (1997). "Tissue inhibitors of metalloproteinases: structure, regulation and biological functions." *Eur J Cell Biol* 74(2): 111-122.

Gravina, G. et al (2013). "Phenotypic characterization of human prostatic stromal cells in primary cultures derived from human tissue samples." *Int J Oncol* 42(6): 2116-2122.

Grimm P, B. et al. (2012). "Comparative analysis of prostate-specific antigen free survival outcomes for patients with low, intermediate and high risk prostate cancer treatment by radical therapy. Results from the Prostate Cancer Results Study Group." *BJU Int* 109(Suppl: 1):22-29.

Grimsley, C. et al (2004). "Dock180 and ELMO1 proteins cooperate to promote evolutionarily conserved Rac-dependent cell migration." *J. Biol. Chem* 279(7): 6087-6097.

Gross, J. and Lapiere, C. (1962). "Collagenolytic activity in amphibian tissues: a tissue culture assay." *Proc Natl Acad Sci* 15(48): 1014-1022.

Gum, R. et al (1996). "Stimulation of 92-kDa gelatinase B promoter activity by ras is mitogen-activated protein kinase kinase 1-independent and requires multiple transcription factor binding sites including closely spaced PEA3/ets and AP-1 sequences." *J Biol Chem* 271(18): 10672-10680.

Guo, H. et al (2000). "EMMPRIN (CD147), an inducer of matrix metalloproteinase synthesis, also binds interstitial collagenase to the tumor cell surface." *Cancer Res* 60(4): 888-891.

Gupta, A. et al (2008). "Predictive value of plasma hepatocyte growth factor/scatter factor levels in patients with clinically localized prostate cancer." *Clin Cancer Res* 14(22): 7385-7390.

Gupta, G. and Massague, J. (2006). "Cancer metastasis: building a framework." *Cell* 127(4): 679–695.

Hall, A. (1998). "Rho GTPases and the actin cytoskeleton." *Science* 279(5350): 509–514.

Hangai, M. et al (2002). "Matrix metalloproteinase-9-dependent exposure of a cryptic migratory control site in collagen is required before retinal angiogenesis." *Am J Pathol* 161(4): 1429-1437.

Harris, E. et al (1975). "Cytochalasin B increases collagenase production by cells in vitro." *Nature* 18(257): 243-244.

Haseloff, J. et al (1988). "Simple RNA enzymes with new and highly specific endoribonuclease activities." *Nature* 334(6183): 585-591.

Hauck, C. et al (2002). "FRNK blocks v-Src-stimulated invasion and experimental metastases without effects on cell motility or growth." *EMBO J* 21(23): 6289-6302.

He, Y. et al (2009). "Role of WAVE1 in K562 leukemia cells invasion and its mechanism." *Zhonghua Xue Ye Xue Za Zhi* 30(4): 237-241.

Hipps, D. et al (1991). "Purification and characterization of human 72-kDa gelatinase (type IV collagenase). Use of immunolocalisation to demonstrate the noncoordinate regulation of the 72-kDa and 95-kDa gelatinases by human fibroblasts." *Biol Chem Hoppe Seyler* 372(4): 287-296.

Hiraoka, N. et al (1998). "Matrix metalloproteinases regulate neovascularization by acting as pericellular fibrinolysins." *Cell* 95(3): 365-377.

Hiroaki Miki, S. et al (1998). "WAVE, a novel WASP-family protein involved in actin reorganization induced by Rac." *The EMBO Journal* 17(23): 6932-6941.

Ho, A. et al (2001). "MMP inhibitors augment fibroblast adhesion through stabilization of focal adhesion contacts and up-regulation of cadherin function." *J Biol Chem* 276(43): 40215-40224.

Hoivels, A. et al (2008). "The diagnostic accuracy of CT and MRI in the staging of pelvic lymph nodes in patients with prostate cancer: a meta-analysis." *Clinical Radiology* 63(4): 387-395.

Horoszewicz, J. et al (1980). The LNCaP cell line-a new model for studies on human prostatic carcinoma. New York, AlanR. Liss, Inc.

Hsia, D. et al (2003). "Differential regulation of cell motility and invasion by FAK." *J Cell Biol* 160(5): 753-767.

Imamov, O. et al (2004). "Estrogen receptor beta regulates epithelial cellular differentiation in the mouse ventral prostate." *Proc Natl Acad Sci* 101(25): 9375-9380.

Insall, L. et al (1998). "Scar1 and the related Wiskott–Aldrich syndrome protein, WASP, regulate the actin cytoskeleton through the Arp2/3 complex." *Curr Biol* (8): 1347–1356.

Irani, J. et al. (2008). "Association for Research in Urological Oncology. Continuous versus six months a year maximal androgen blockade in the management of prostate cancer: a randomized study." *Eur Urol* 54(2): 382-391.

Itoh, T. et al (1998). "Reduced angiogenesis and tumor progression in gelatinase A-deficient mice." *Cancer Res* 58(5): 1048-1051.

Iwaya, K. et al (2007). "Correlation between liver metastasis of the colocalization of actin-related protein 2 and 3 complex and WAVE2 in colorectal carcinoma." *Cancer Sci* 98(7): 992-999.

Jaffe, A. and Hall, A. (2005). "Rho GTPases: biochemistry and biology." *Annu Rev Cell Dev Biol* 21: 247–269.

Jewett H (1956). "Significance of the palpable prostatic nodule." *JAMA* 160(10): 838.

Jhaveri, F. et al (1999). "Declining rates of extracapsular extension after radical prostatectomy: Evidence for continued stage migration." *J Clin Oncol* 17(10): 3167-3172.

Jiang, W. et al (1994). "Molecular and cellular basis of cancer invasion and metastasis: implications for treatment." *Br J Surg* 81(11): 1576-1590.

Jiang, W. et al (1996). "Hepatocyte growth factor induces tyrosine phosphorylation of focal adhesion kinase (FAK) andpaxillin and enhances cell-matrix interactions." *Oncol Rep* 3(5): 819-823.

Jiang, W. et al (1999). "Antagonistic effect of NK4, a novel hepatocyte growth factor variant, on in vitro angiogenesis of human vascular endothelial cells." *Clin Cancer Res* 5(11): 3695-3703.

Jiang, W. et al (2001). "A hammerhead ribozyme suppresses expression of hepatocyte growth factor/scatter factor receptor c-MET and reduces migration and invasiveness of breast cancer cells." *Clin Cancer Res* 7(8): 2555-2562.

Jiang, W. et al (2005). "Targeting matrilysin and its impact on tumor growth in vivo: the potential implications in breast cancer therapy." *Clin Cancer Res* 11(16): 6012-6019.

Jiang, W. et al (2005). "Expression of Com-1/p8 in human breast cancer, and its relevance to clinical outcome and ER status." *Int J Cancer* 117(5): 730–737.

Kaighn, M. et al (1979). "Establishment and characterization of a human prostatic carcinoma cell line (PC-3)." *Invest Urol* 17(1): 16-23.

Kaverina, I. et al. (2002). "Regulation of substrate adhesion dynamics during cell motility." *Int J of Biochem & Cell Bio* 34(7): 746–761.

Kazuhiro, K. et al (2004). "N-WASP and WAVE2 acting downstream of phosphatidylinositol 3-kinase are required for myogenic cell migration induced by hepatocyte growth factor." *J Bio Chem* 279(24): 54862–54871.

Kheradmand, F. et al. (1998). "Role of Rac1 and oxygen radicals in collagenase-1 expression induced by cell shape change." *Science* 280(5365): 898-902.

Khokha, R. et al (1992). "Suppression of invasion by inducible expression of tissue inhibitor of metalloproteinase-1 (TIMP-1) in B16-F10 melanoma cells." *J Natl Cancer Inst* 84(13): 1017-1022.

Kim, A. (2000). "Autoinhibition and activation mechanisms of the Wiskott–Aldrich syndrome protein." *Nature* 404(6774): 151–158.

Kim, M. et al (2011). "Absence of paxillin gene mutation in lung cancer and other common solid cancers." *Tumori* 97(2): 211-213.

Kleiner, D. et al (1994). "Quantitative zymography: detection of picogram quantities of gelatinases." *Anal Biochem* 218(2): 325-329.

Knäuper, V. et al (1996). "Cellular mechanisms for human procollagenase-3 (MMP-13) activation. Evidence that MT1-MMP (MMP-14) and gelatinase a (MMP-2) are able to generate active enzyme." *J Biol Chem* 271(29): 17124-17131.

Knox, J. et al (1996). "Matrilysin expression in human prostate carcinoma." *Mol Carcinog* 15(1): 57-63.

Kolkenbrock, H. et al (1995). "Generation and activity of the ternary gelatinase B/TIMP-1/LMW-stromelysin-1 complex." *Biol Chem* 376(8): 495-500.

Krueger, E. et al (2003). "A dynamin-cortactin-Arp2/3 complex mediates actin reorganization in growth factor-stimulated cells." *Mol Biol Cell* 14(3): 1085-1096.

Kryczka, J. et al (2012). "Matrix metalloproteinase-2 cleavage of the β1 integrin ectodomain facilitates colon cancer cell motility." *J Biol Chem* 287(43): 36556-36566.

Kuban, D. et al (2011). "Long-term failure patterns and survival in a randomized dose-escalation trial for prostate cancer. Who dies of disease?" *Int J Radiat Oncol Biol Phys* 79(5): 1310-1317.

Kupferman, M. et al (2000). "Matrix metalloproteinase 9 promoter activity is induced coincident with invasion during tumor progression." *Am J Pathol* 157(6): 1777-1783.

Kurisu, S. et al (2005). "Rac-WAVE2 signalling is involved in the invasive and metastatic phenotypes of murine melanoma cells." *Oncogene* 24(8): 1309-1319

Kwiatkowska, A. et al (2011). "Downregulation of Akt and FAK phosphorylation reduces invasion of glioblastoma cells by impairment of MT1-MMP shuttling to lamellipodia and downregulates MMPs expression." *Biochimica et Biophysica Acta* 1813(5): 655–667.

Landis, S. et al (1999). Cancer statistics, 1999. *CA Cancer J Clin* 49:8-31.

Larjava, H. et al (1993). "Anti-integrin antibodies induce type IV collagenase expression in keratinocytes." *J Cell Physiol* 157(1): 190-200.

Lauffenburger, D. and Horwitz, A. (1996). "Cell migration: a physically integrated molecular process." *Cell* 84(3): 359–369.

Li Z, D. et al (2012). "Human chorionic gonadotropin β induces cell motility via ERK1/2 and MMP-2 activation in human glioblastoma U87MG cells." *J Neurooncol*.111(3): 237-244.

Liu, T. et al (2002). "Induction of RECK by nonsteroidal anti-inflammatory drugs in lung cancer cells." *Oncogene* 21(54): 8347-8350.

Liu, Y. et al (1997). "Preparation and characterization of recombinant tissue inhibitor of metalloproteinase 4 (TIMP-4)." *J Biol Chem* 272(33): 20479-20483.

Liu, Z. et al (2002). "Hepatocyte growth factor induces ERK-dependent paxillin phosphorylation and regulates paxillin-focal adhesion kinase association." *J Biol Chem* 277(12): 10452-10458.

Luo, J. et al (2002). "Gene expression signature of benign prostatic hyperplasia revealed by cDNA microarray analysis." *Prostate* 51(3): 189-200.

Machesky, L. et al (1994). "Purification of a cortical complex containing two unconventional actins from Acanthamoeba by affinity chromatography on profilin-agarose." *Journal of Cell Biology* 127(1): 107–115.

Machesky, L. et al (1999). "Scar, a WASp-related protein, activates nucleation of actin filaments by the Arp2/3 complex." *Proc Natl Acad Sci* 96(7): 3739-3744.

Mackay, D. et al (1997). "Rho- and rac-dependent assembly of focal adhesion complexes and actin filaments in permeabilized fibroblasts: an essential role for ezrin/radixin/moesin proteins." *J Cell Biol* 138(4): 927-938.

Marchand, J. (2001). "Interaction of WASP/Scar proteins with actin and vertebrate Arp2/3 complex." *Nat. Cell Biol* 3(1): 76–82.

Martinez-Quiles, N. et al (2001). "WIP regulates N-WASP-mediated actin polymerization and filopodium formation." *Nat Cell Biol* 3(5): 484–491.

Matsui, T. et al (1999). "Activation of ERM proteins in vivo by Rho involves phosphatidyl-inositol 4-phosphate 5-kinase and not ROCK kinases." *Curr Biol* 9(21): 1259-1262.

Mattern, R. et al (2005). "Glioma cell integrin expression and their interactions with integrin antagonists." *Cancer Ther* 3A: 325–340.

MacDougall, J. et al (1995). "Contributions of tumor and stromal matrix metalloproteinases to tumor progression, invasion and metastasis." *Cancer Metastasis Rev* 14(4): 351-362.

McQuibban, G. et al (2002). "Matrix metalloproteinase processing of monocyte chemoattractant proteins generates chemokine receptor antagonists with anti-inflammatory properties in vivo." *Blood* 100(4): 1160-1167.

Mignatti, P. and Rifkin, D. (1996). "Plasminogen activators and matrix metalloproteinases in angiogenesis." *Enzyme Protein* 49(1-3): 117-137.

Miki, H. (1996). "N-WASP, a novel actin-depolymerizing protein, regulates the cortical cytoskeletal rearrangement in a PIP2-dependent manner downstream of tyrosine kinases." *EMBO J* 15(19): 5326–5335.

Miki, H. (1998). "WAVE, a novel WASP-family protein involved in actin reorganization induced by Rac." *EMBO J* 17(23): 6932–6941.

Miki, H. et al (1998). "Direct binding of the verprolin-homology domain in N-WASP to actin is essential for cytoskeletal reorganization." *Biochem Biophys Res Commun* 243(1): 73-78.

Mikolajczyk, S. et al (2001). A truncated precursor form of prostate-specific antigen is a more specific serum marker of prostate cancer. *Cancer Res* 61(18):6958-6963.

Millard, T. et al (2004). "Signalling to actin assembly via the WASP (Wiskott-Aldrich syndrome protein)-family proteins and the Arp2/3 complex." *Biochem J* 15(380): 1-17.

Moissoglu, K. and Schwartz M (2006). "Integrin signaling in directed cell migration." *Biol Cell* 98(9): 547–555.

Montironi, R. et al (1996). "Immunohistochemical evaluation of type IV collagenase (72-kd metalloproteinase) in prostatic intraepithelial neoplasia." *Anticancer Res* 16(4): 2057-2062.

Moore, B. et al (1998). "CXC chemokines mechanism of action in regulating tumor angiogenesis." *Angiogenesis* 2(2): 123-134.

Muir, C. et al (1991). The epidemiology of prostatic cancer. Geographical distribution and time-trends. *Acta Oncol* 30(2):133-140.

Mullins, R. et al (1998). "The interaction of Arp2/3 complex with actin: nucleation, high affinity pointed end capping, and formation of branching networks of filaments." *Proc of Nat Acad of Sci* 95(11): 6181–6186.

Murphy-Ullrich, J. (2001). "The de-adhesive activity of matricellular proteins: is intermediate cell adhesion an adaptive state?" *J Clin Invest* 107(7): 785-790.

Murray, N. et al (2012). "Differential expression of matrix metalloproteinase-2 expression in disseminated tumor cells and micrometastasis in bone marrow of patients with nonmetastatic and metastatic prostate cancer: theoretical considerations and clinical implications-an immunocytochemical study." *Bone Marrow Res*. 259351. doi: 10.1155/2012/259351. Epub 2012 Nov 26.

Musiał, J. et al (2007). "Prognostic significance of E-cadherin and ezrin immunohistochemical expression in prostate cancer." *Pol J Pathol* 58(4): 235-243.

Naba, A. et al (2008). "Spatial recruitment and activation of the Fes kinase by ezrin promotes HGF-induced cell scattering." *EMBO J* 27(1): 38-50.

Nagase, H. (1997). "Activation mechanisms of matrix metalloproteinases." *Biol Chem* 378(3-4): 151-160.

Nagase, T. et al (1996). "Prediction of the Coding Sequences of Unidentified Human Genes. VI. The Coding Sequences of 80 New Genes (KIAA0201-KIAA0280) Deduced by Analysis of cDNA Clones from Cell Line KG-1 and Brain." *DNA Res* 3(5): 321–329.

Nakamura, F. et al (1995). "Phosphorylation of threonine 558 in the carboxyl-terminal actin-binding domain of moesin by thrombin activation of human platelets." *J Biol Chem* 270(52): 31377-31385.

Naslund, M. et al (1988). "The role of androgens and estrogens in the pathogenesis of experimental nonbacterial prostatitis." *J Urol* 140(5): 1049-1053.

Nelson, A. et al (2000). "Matrix metalloproteinases: biologic activity and clinical implications." *J Clin Oncol* 18(5): 1135-1149.

Nurmikko, P. et al (2000). Production and characterization of novel anti-prostate-specific antigen (PSA) monoclonal antibodies that do not detect internally cleaved Lys145-Lys146 inactive PSA. *Clin Chem* 46(10):1610-1618.

Oda, A. et al (2005). "WAVE/Scars in platelets." *Blood* 105(8): 3141-3148.

Oikawa, T. et al (2004). "PtdIns (3,4,5)P3 binding is necessary for WAVE2-induced formation of lamellipodia." *Nat Cell Biol* 6(5): 420-426.

Owens, L. et al (1995). "Overexpression of the focal adhesion kinase (p125FAK) in invasive human tumors." *Cancer Res* 55(13): 2752-2755.

Pacheco, M. et al (1998). "Expression of gelatinases A and B, stromelysin-3 and matrilysin genes in breast carcinomas: clinico-pathological correlations." *Clin Exp Metastasis* 16(7): 577-585.

Panchal, S. (2003). "A conserved amphipathic helix in WASP/Scar proteins is essential for activation of Arp2/3 complex." *Nat. Struct. Biol* 10(8): 591–598.

Parolini, O. et al (1997). "Expression of Wiskott-Aldrich syndrome protein (WASP) gene during hematopoietic differentiation." *Blood* 90(1): 70-75.

Parr, C. et al (2001). "The HGF/SF-induced phosphorylation of paxillin, matrix adhesion, and invasion of prostate cancer cells were suppressed by NK4, an HGF/SF variant." *Biochem Biophys Res Commun* 285(5): 1330-1337.

Parsons, J. et al (2000). "Focal adhesion kinase: a regulator of focal adhesion dynamics and cell movement." *Oncogene* 19(49): 5606-5613.

Partin, A. et al (2003). Complexed prostate specific antigen improves specificity for prostate cancer detection: Results of a prospective multicenter clinical trial. *J Urol.* 170(5):1787-1791.

Perry, A. et al (2010). "The epigenome as a therapeutic target in prostate cancer." *Nat Rev Urol* 7(12): 668-680.

Pilpel, Y. and Segal, M. (2005). "Rapid WAVE dynamics in dendritic spines of cultured hippocampal neurons is mediated by actin polymerization." *J. Neurochem* 95(5): 1401–1410.

Pinsky, P. et al (2012). "Prostate cancer specific survival in the Prostate, Lung, Colorectal, and Ovarian (PLCO) cancer screening trial." *Cancer Epidemiol* 36(6):401-6.

Pixley, F. et al (2001). "Protein tyrosine phosphatase phi regulates paxillin tyrosine phosphorylation and mediates colony-stimulating factor 1-induced morphological changes in macrophages." *Mol Cell Biol* 21(5): 1795-1809.

Pollard, T. and Borisy, G. (2003). "Cellular motility driven by assembly and disassembly of actin filaments." *Cell* 112(4): 453-465.

Radtke, S. et al (2013). "ERK2 but not ERK1 mediates HGF-induced motility in non small cell lung carcinoma cell lines." *J Cell Sci* 126(Pt 11):2381-91

Ramachandran, P. and Ignacimuthu, S. (2012). "RNA interference as a plausible anticancer therapeutic tool." *Asian Pac J Cancer Prev* 13(6): 2445-2452.

Ramer, R. and Hinz, B. (2008). "Inhibition of cancer cell invasion by cannabinoids via increased expression of tissue inhibitor of matrix metalloproteinases-1." *J Natl Cancer Inst* 100(1): 59-69.

Ray, J. and Stetler-Stevenson, W. (1995). "Gelatinase A activity directly modulates melanoma cell adhesion and spreading." *EMBO J* 14(5): 908-917.

Rebbeck, T. (2000). "More about: modification of clinical presentation of prostate tumors by a novel genetic variant in CYP3A4." *J Natl Cancer Inst* 92(1): 76-82.

Reunanen, N. et al (2002). "Activation of p38 alpha MAPK enhances collagenase-1 (matrix metalloproteinase (MMP)-1) and stromelysin-1 (MMP-3) expression by mRNA stabilization." *J Biol Chem* 277(35): 32360-32368.

Richardson, A. et al (1997). "Inhibition of cell spreading by expression of the C-terminal domain of focal adhesion kinase (FAK) is rescued by coexpression of src or catalytically inactive FAK: A role for paxillin tyrosine phosphorylation." *Mol Cell Biol* 17(12): 6906-6914.

Riento, K. and Ridley, A. (2003). "Rocks: multifunctional kinases in cell behavior." Nat Rev Mol Cell Biol 4(6): 446–456.

Riikonen, T. et al (1995). "Integrin alpha 2 beta 1 is a positive regulator of collagenase (MMP-1) and collagen alpha 1(I) gene expression." *J Biol Chem* 270(22): 13548-13552.

Rodina, A. et al (1999). "Phosphorylation of p125FAK and paxillin focal adhesion proteins in src-transformed cells with different metastatic ability." *FEBS Lett* 455(1-2): 145–151.

Rohatgi, R. et al (1999). "The interaction between N-WASP and the Arp2/3 complex links Cdc42-dependent signals to actin assembly." *Cell* 97(2): 221-231.

Roomi, M. et al (2011). "Down-regulation of urokinase plasminogen activator and matrix metalloproteinases and up-regulation of their inhibitors by a novel nutrient mixture in human prostate cancer cell lines PC-3 and DU-145." *Oncol Rep* 26(6): 1407-1413.

Rosenthal, E. et al (1998). "Role of the plasminogen activator and matrix metalloproteinase systems in epidermal growth factor- and scatter factor-stimulated invasion of carcinoma cells." *Cancer Res* 58(22): 5221-5230.

Sasaki, M. et al (2000). "Differential regulation of metalloproteinase production, proliferation and chemotaxis of human lung fibroblasts by PDGF, interleukin-1beta and TNF-alpha." *Mediators Inflamm* 9(3-4): 155-160.

Schenk, S. and Quaranta, V. (2003). "Tales from the cryptic sites of the extracellular matrix." *Trends Cell Biol* 13(7): 366-375.

Schlaepfer, D. et al (1999). "Signaling through focal adhesion kinase." *Prog Biophys Mol Biol* 71(3-4): 435-478.

Schroder, F. et al (2012). "Landmarks in prostate cancer screening." *BJU Int* 110(1):3-7.

Schnaper, H. et al (1993). "Type IV collagenase(s) and TIMPs modulate endothelial cell morphogenesis in vitro." *J Cell Physiol* 156(2): 235-246.

Scorilas, A. et al (2001). "Overexpression of matrixmetalloproteinase-9 in human breast cancer: a potential favourable indicator in node-negative patients." *Br J Cancer* 84(11): 1488-1496.

Seftor, R. et al (2001). "Cooperative interactions of laminin 5 gamma2 chain, matrix metalloproteinase-2, and membrane type-1-matrix/metalloproteinase are required for mimicry of embryonic vasculogenesis by aggressive melanoma." *Cancer Res* 61(17): 6322-6327.

Sein, T. et al (2000). "A role for FAK in the Concanavalin A-dependent secretion of matrix metalloproteinase-2 and -9." *Oncogene* 19(48): 5539-5542.

Shofuda, T. et al (2004). "Cleavage of focal adhesion kinase in vascular smooth muscle cells overexpressing membrane-type matrix metalloproteinases." *Arterioscler Thromb Vasc Biol* 24(5): 839-844.

Sloane, J. and Vartanian, T. (2007). "WAVE1 and regulation of actin nucleation in myelination." *Neuroscientist* 13(5): 486-491.

Small, J. (1994). "Lamellipodia architecture: actin filament turnover and the lateral flow of actin filaments during motility." *Semin in Cell Bio* 5(3): 157–163.

Small, J. et al (1999). "Functional design in the actin cytoskeleton." *Cur Op Cell Bio* 11(1): 54–60.

Snoek-van Beurden, P. et al (2005). "Zymographic techniques for the analysis of matrix metalloproteinases and their inhibitors." *Biotechniques* 38(1): 73-83.

Sossey-Alaoui, K. et al (2002). "WAVE3, an actin-polymerization gene, is truncated and inactivated as a result of a constitutional t(1;13)(q21;q12) chromosome translocation in a patient with ganglioneuroblastoma." *Oncogene* 21(38): 5967–5974.

Sossey-Alaoui, K. et al (2005). "WAVE3 promotes cell motility and invasion throughthe regulation of MMP-1, MMP-3, and MMP-9 expression." *Exp Cell Res* 308(1): 135–145.

Sossey-Alaoui, K. et al (2005). "WAVE3-mediated cell migration and lamellipodia formation are regulated downstream of phosphatidylinositol 3-kinase." *J. Biol.Chem* 280(23): 21748–21755.

Sossey-Alaoui, K. et al (2007). "Down-regulation of WAVE3, a metastasis promoter gene, inhibits invasion and metastasis of breast cancer cells." *Am. J. Pathol* 170(6): 2112–2121.

Stam, J. et al (1998). "Invasion of T-lymphoma cells: cooperation between Rho family GTPases and lysophospholipid receptor signaling." *EMBO J* 17(14): 4066-4074.

Sternlicht, M. and Werb, Z. (1999). ECM proteinases. In *Guidebook to the Extracellular Matrix, Anchor and Adhesion Proteins*, Oxford Univ. Press, Oxford, UK.

Still, K. et al (2000). "Localization and quantification of mRNA for matrix metalloproteinase-2 (MMP-2) and tissue inhibitor of matrix metalloproteinase-2 (TIMP-2) in human benign and malignant prostatic tissue." *Prostate* 42(1): 18-25.

Suetsugu, S. et al (1999). "Identification of two human WAVE/SCAR homologues as general actin regulatory molecules which associate with the Arp2/3 complex." *Biochem. Biophys. Res Commun* 260(1): 296–302.

Suetsugu, S. et al (2003). "Differential roles of WAVE1 and WAVE2 in dorsal and peripheral ruffle formation for fibroblast cell migration." *Dev Cell* 5(4): 595–609.

Sullivan, K. et al (1994). "A multiinstitutional survey of the Wiskott-Aldrich syndrome." *J Pediatrics* 125(1): 876–885.

Sung, J. et al (2008). "WAVE1 controls neuronal activity-induced mitochondrial distribution in dendritic spines." *Proc Natl Acad Sci* 105(8): 3112-3116.

Svitkina, T. and Borisy, G. (1999). "Arp2/3 complex and actin depolymerizing factor/cofilin in dendritic organization and treadmilling of actin filament array in lamellipodia." *Journal of Cell Biology* 145(5): 1009–1026.

Takagi, Y. et al (2002). "Mechanism of action of hammerhead ribozymes and their applications in vivo: rapid identification of functional genes in the post-genome era by novel hybrid ribozyme libraries." *Biochem Soc Trans* 30(6): 1145-1149.

Takeha, S. et al (1997). "Stromal expression of MMP-9 and urokinase receptor is inversely associated with liver metastasis and with infiltrating growth in human colorectal cancer: a novel approach from immune/inflammatory aspect." *Jpn J Cancer Res* 88(1): 72-81.

Takenawa, T. and Miki, H. (2001). "WASP and WAVE family proteins: key molecules for rapid rearrangement of cortical actin filaments and cell movement." *J Cell Sci* 114(10): 1801-1809.

Takenawa, T. and Suetsugu, S. (2007). "The WASP–WAVE protein network: connecting the membrane to the cytoskeleton." *Mol Cell Bio* 8(1): 37-48.

Tang, C. et al (1998). "ErbB-4 ribozyme abolish neuregulin-induced mitogenesis" *Cancer Res* 58(15): 3415-3422.

Taraboletti, G. et al (2002). "Shedding of the matrix metalloproteinases MMP-2, MMP-9, and MT1-MMP as membrane vesicle-associated components by endothelial cells." *Am J Pathol* 160(2): 673-680.

Teng, Y. et al (2010). "Inactivation of the WASF3 gene in prostate cancer cells leads to suppression of tumorigenicity and metastases." *Br J Cancer* 103(7): 1066-1075.

Tomasek, J. et al (1997). "Gelatinase A activation is regulated by the organization of the polymerized actin cytoskeleton." *J Biol Chem* 14(272): 7482-7487.

Tremblay, L. et al (1996). "Focal adhesion kinase (pp125FAK) expression, activation and association with paxillin and p50CSK in human metastatic prostate carcinoma." *Int J Cancer* 68(2): 164-171.

Uhlenbeck, O. (1987). "A small catalytic oligoribonucleotide." *Nature* 328(6131): 596-600.

Valderrama, F. et al (2012). "Radixin regulates cell migration and cell-cell adhesion through Rac1." *J Cell Sci* 15(125): 3310-3319.

Valdman, A. et al (2005). "Ezrin expression in prostate cancer and benign prostatic tissue." *Eur Urol* 48(5): 852-857.

Van den Oord, J. et al (1997). "Expression of gelatinase B and the extracellular matrix metalloproteinase inducer EMMPRIN in benign and malignant pigment cell lesions of the skin." *Am J Pathol* 151(3): 665-670.

Van Wart, H. and Birkedal-Hansen, H. (1990). "The cysteine switch: a principle of regulation of metalloproteinase activity with potential applicability to the entire matrix metalloproteinase gene family." *Proc Natl Acad Sci* 87(14): 5578-5582.

Vogel, W. et al (1997). "The discoidin domain receptor tyrosine kinases are activated by collagen." *Mol Cell* 1(1): 13-23.

Vu, T. et al (1998). "MMP-9/gelatinase B is a key regulator of growth plate angiogenesis and apoptosis of hypertrophic chondrocytes." *Cell* 93(3): 411-422.

Vu, T. and Werb, Z. (2000). "Matrix metalloproteinases: effectors of development and normal physiology." *Genes Dev* 14(17): 2123-2133.

Wang, Y. (1985). "Exchange of actin subunits at the leading edge of living fibroblasts: possible role of treadmilling." *J. Cell Biol* 101(2): 597-602.

Wang, Z. et al (2008). "Expression of WAVE1 in childhood acute lymphocytic leukemia and in the apoptosis of Jurkat cells induced by adriamycin." *Zhongguo Dang Dai Er Ke Za Zhi* 10(5): 620-624.

Weaver, A. et al (2002). "Interaction of cortactin and N-WASp with Arp2/3 complex." *Current Biology* 12(15): 1270–1278.

Weisberg, E. et al. "Role of focal adhesion proteins in signal transduction and oncogenesis." *Crit Rev Oncog* 8(4): 343-358.

Werb, Z. et al (1989). "Signal transduction through the fibronectin receptor induces collagenase and stromelysin gene expression." *J Cell Biol* 109(2): 877-889.

Westermarck, J. and Kahari, V. (1999). "Regulation of matrix metalloproteinase expression in tumor invasion." *FASEB J* 13(8): 781-792.

Westermarck, J. et al (1997). "Differential regulation of interstitial collagenase (MMP-1) gene expression by ETS transcription factors." *Oncogene* 14(22): 2651-2660.

Williams, C. et al (1999). "The role of cyclooxygenases in inflammation, cancer, and development." *Oncogene* 18(55): 7908-7916.

Wilson, M. et al (1992). "Metalloprotease activities expressed during development and maturation of the rat prostatic complex and seminal vesicles." *Biol Reprod* 47(5): 683-691.

Wilson, M. et al (1991). "Calcium-dependent, independent gelatinolytic proteinase activities of the rat ventral prostate, its secretion: Characterization, effects of castration, testosterone treatment." *Biol Reprod* 44(5): 776-785.

Wize, J. et al (1998). "Ligation of selectin L and integrin CD11b/CD18 (Mac-1) induces release of gelatinase B (MMP-9) from human neutrophils." *Inflamm Res* 47(8): 325-327.

Xu, J. et al (2001). "Proteolytic exposure of a cryptic site within collagen type IV is required for angiogenesis and tumor growth in vivo." *J Cell Biol* 154(5): 1069-1079.

Yamaguchi, H. (2000). "Two tandem verprolin homology domains are necessary for a strong activation of Arp2/3 complex-induced actin polymerization and induction of microspike formation by N-WASP." *Proc. Natl. Acad. Sci* 97(23): 12631–12636.

Yamaguchi, H. (2002). "Two verprolin homology domains increase the Arp2/3 complex-mediated actin polymerization activities of N-WASP and WAVE1 C-terminal regions." *Biochem. Biophys. Res. Commun* 297(2): 214–219.

Yamazaki, D. et al (2003). "WAVE2 is required for directed cell migration and cardiovascular development." *Nature* 424(6947): 452-456.

Yamazaki, D. et al (2005). "A novel function of WAVE in amellipodia: WAVE1 is required for stabilization of lamellipodial protrusions during cell spreading." *Genes Cells* 10(5): 381–392.

Yan, C. et al (2003). "WAVE2 deficiency reveals distinct roles in embryogenesis and Rac-mediated actin-based motility." *EMBO J* 22(14): 3602-3612.

Yang, L. et al (2006). "Increased expression of Wiskott-Aldrich Syndrome protein family verprolin-homologous protein 2 correlated with poor prognosis of hepatocellular carcinoma." *Clin Cancer* 12(19): 5673-5679.

Yu, L. et al (2011). "Estrogens promote invasion of prostate cancer cells in a paracrine manner through up-regulation of matrix metalloproteinase 2 in prostatic stromal cells." *Endocrinology* 152(3): 773-781.

Yu, Q. and Stamenkovic, I. (2000). "Cell surface-localized matrix metalloproteinase-9 proteolytically activates TGF-beta and promotes tumor invasion and angiogenesis." *Genes Dev* 14(2): 163-176.

Zalevsky, J. (2001). "Different WASP family proteins stimulate different Arp2/3 complex-dependent actin-nucleating activities." *Curr. Biol* 11(24): 1903–1913.

Zamir, E. and Geiger, B. (2001). "Molecular complexity and dynamics of cellmatrix adhesions." *J Cell Sci* 114(20): 3583-3590.

Zeng, Z. et al (1996). "Prediction of colorectal cancer relapse and survival via tissue RNA levels of matrix metalloproteinase-9." *J Clin Oncol* 14(12): 3133-3140.

Zhang, L. et al (2004). "Type IV collagenase (matrix metalloproteinase-2 and -9) in prostate cancer." *Prostate Cancer Prostatic Dis* 7(4): 327-332.

Zhuge, Y. and Xu, J. (2001). "Rac1 mediates type I collagen-dependent MMP-2 activation. role in cell invasion across collagen barrier." *J Biol Chem* 276(19): 16248-16256.

Zietman, A. et al (2010). "Randomized trial comparing conventional-dose with highdose conformal radiation therapy in early-stage adenocarcinoma of the prostate: long-term results from proton radiation oncology group/american college of radiology." *J Clin Oncol* 28(7): 1106-1111.

Zigmond, S. (1993). "Recent quantitative studies of actin filament turnover during cell locomotion." *Cell Motility and the Cytoskeleton* 25(4): 309–316.

Zuker, M. (2003). "Mfold web server for nucleic acid folding and hybridization prediction." *Nucleic Acids Res* 31(13): 3406-3415.

Appendices

Appendix: 1. Suppliers of materials and reagents as detailed in this thesis.

Material & Reagent	Supplier
10% foetal calf serum (FCS)	PAA Laboratories, Coelbe, Germany
A/G protein agarose beads	Santa-Cruz Biotechnology, Santa-Cruz, CA, USA
Acetic acid	Fisher Scientific, Leicestershire, UK
Acrylamide mix (30%)	Sigma-Aldrich Co, Poole, Dorset, UK
Agarose	Melford Laboratories Ltd, Suffolk, UK
Ammonium persulfate (APS)	Sigma-Aldrich Co, Poole, Dorset, UK
Bio-Rad DC Protein Colourimic Assay	Bio-Rad Laboratories, Hercules, CA, USA
Boric acid	Duchefa Biochemie, Haarlem, Netherlands
Bromophenol Blue	Sigma-Aldrich Co, Poole, Dorset, UK
CaCl2	Sigma-Aldrich Co, Poole, Dorset, UK
Chloroform	Sigma-Aldrich Co, Poole, Dorset, UK
Commasine Blue	Sigma-Aldrich Co, Poole, Dorset, UK
DAB Chromogen	Vector Laboratories Inc, Burlingame, CA, USA
DEPC (Diethylpyrocarbonate)	Sigma-Aldrich Co, Poole, Dorset, UK
Dimethylsulphoxide (DMSO)	Fisons Scientific Equipment, Loughborough, UK
DMEM/Ham's F12 with L-Glutamine medium	PAA Laboratories, Coelbe, Germany
EDTA (Ethylenediaminetetraacetic acid)	Duchefa Biochemie, Haarlem, Netherlands
Ethanol	Fisher Scientific, Leicestershire, UK
Ethidium bromide	Sigma-Aldrich Co, Poole, Dorset, UK
FITC conjugated rabbit anti-goat IgG	Santa-Cruz Biotechnology, Santa-Cruz, CA, USA
FITC conjugated sheep anti-mouse IgG	Santa-Cruz Biotechnology, Santa-Cruz, CA,

	USA
Fluorescence mounting medium	CalBiochem, Nottingham, UK
Glycine	Melford Laboratories Ltd, Suffolk, UK
HCL	Sigma-Aldrich Co, Poole, Dorset, UK
Horse Serum	Sigma-Aldrich Co, Poole, Dorset, UK
Isopropanol	Sigma-Aldrich Co, Poole, Dorset, UK
KCl	Fisons Scientific Equipment, Loughborough, UK
KH2PO4	BDH Chemicals Ltd, Poole, England, UK
Mayers Htx	Sigma-Aldrich Co, Poole, Dorset, UK
Methanol	Fisher Scientific, Leicestershire, UK
NaCl	Sigma-Aldrich Co, Poole, Dorset, UK
Na2HPO4	BDH Chemicals Ltd., Poole, Dorset, UK
NaN3	Sigma-Aldrich Co, Poole, Dorset, UK
NaOH	Sigma-Aldrich Co, Poole, Dorset, UK
Nitrocellulose membrane	Amersham, Cardiff, UK
Penicillin	Sigma-Aldrich Co, Poole, Dorset, UK
Peroxidase conjugated goat anti-rabbit IgG	Sigma-Aldrich Co, Poole, Dorset, UK
Peroxidase conjugated rabbit anti-goat IgG	Sigma-Aldrich Co, Poole, Dorset, UK
Peroxidase conjugated rabbit anti-mouse IgG	Sigma-Aldrich Co, Poole, Dorset, UK
Ponceau S Stain	Sigma-Aldrich Co, Poole, Dorset, UK
Precision qScriptTM RT PCR kit	Primerdesign LTD, Southampton, UK
REDTaqTM ReadyMix PCR reaction mix	Sigma-Aldrich Co, Poole, Dorset, UK
RNA extraction buffer	Advanced Biotechnologies Ltd, Epsom, Surrey, UK
SDS (Sodium dodecyl sulphate)	Melford Laboratories Ltd, Suffolk, UK

Bovine albumin	Sigma-Aldrich Co, Poole, Dorset, UK
Streptomycin	Sigma-Aldrich Co, Poole, Dorset, UK
Sucrose	Fisons Scientific Equipment, Loughborough, UK
Supersignal™ West Dura system	Pierce Biotechnology Inc., Rockford, IL, USA
Tetramethylethylenediamine (TEMED)	Sigma-Aldrich Co, Poole, Dorset, UK
TRI Reagent	Sigma-Aldrich Co, Poole, Dorset, UK
Tris-Cl	Melford Laboratories Ltd, Suffolk, UK
TRITC conjugated goat anti-rabbit IgG	Sigma-Aldrich Co, Poole, Dorset, UK
Trion	Sigma-Aldrich Co, Poole, Dorset, UK
Trypsin	Sigma-Aldrich Co, Poole, Dorset, UK
Tween 20	Melford Laboratories Ltd, Suffolk, UK
Vectastain Universal ABC kit	Vector Laboratories Inc, Burlingame, CA, USA
ZnCl	Sigma-Aldrich Co, Poole, Dorset, UK

Appendix: 2. Suppliers of hardware and software as detailed in this thesis.

Hardware/Software	Supplier
16-well chamber slide (for Immunohistochemistry)	Nalge NUNC International, Rochester, NY
25cm2 and 75cm2 culture flasks	Cell Star, Germany
Cytodex 2 beads®	Sigma-Aldrich Co, Poole, Dorset, UK
Electroporation cuvette	Euro Gentech, Southampton, UK
Fluorescent microscope	Olympus, Lake Success, NY, USA
iCycler iQt system	Bio Rad, Hercules, CA, USA
Image J	Public Domain
Lecia DM IRB microscope	Lecia Microsystems GmbH, Wetzlar, Germany
Microscope heated plate	Lecia Microsystems GmbH, Wetzlar, Germany
Microsoft Excel	Microsoft In., Redmond, WA, USA
Neubauer haemocytometer counting chamber	Reichert, Austria
Nitrocellulose membrane	Hybond C, Ammersham, Cardiff
Protein spectrophotometer	BIO-TEK, Wolf Laboratories, York, UK
RNA spectrophotometer	BIO-TEK, Wolf Laboratories, York, UK
UVI-doc system	UVITech, Inc., Cambridge, England, UK
UVITech imager	UVITech, Inc., Cambridge, England, UK